Ph.D. degree in System Medicine (curriculum in Molecular Oncology)

European School of Molecular Medicine (SEMM)

University of Milan and University of Naples "Federico II"

Faculty of Medicine (MED/04)

The role of quiescence in Acute Myeloid Leukemia growth

Cecilia Restelli

European Institute of Oncology (IEO), Milan

Student ID: R12080

Supervisor: Prof. Pier Giuseppe Pelicci

Added Supervisor: Prof.ssa Emanuela Colombo

Academic year 2020-2021

A chi c'è, c'è stato, ci sarà.
Alle mie innumerevoli famiglie, sparse in ogni dove.
A tutto ciò a cui appartengo, ma che non possiedo.

"**Science itself, however precise and objective, is a human activity**. It's a way of wondering as well as a way of knowing. It's a process, not a body of facts or laws. Like music, like poetry, like baseball, like grandmaster chess, it's something gloriously imperfect that people do. **The smudgy fingerprints of our humanness are all over it.**"

The Tangled Tree: A Radical New History of Life, David Quammen (2018)

"Why are you searching for dark matter?" (…) "**To further our knowledge**, (…) **and to give life meaning. If we're not exploring, we're not doing anything. We're just waiting**."

"**Science is full** (…) **of happenstance and stumbles and getting knackered and crazy in the field or the lab**. It's so weird to me how science always presents its knowledge as *clean*. (…) I have this plan, (…) that for each formal scientific paper I ever publish I will also write its dark twin, its underground mirror-piece – the true story of how the data for that cool, tidy hypothesis-evidence-proof paper actually got acquired. I want to write about the happenstance and the shaved bumblebees and the pissing monkeys and the drunken conversations and the fuck-ups that actually bring science into being. This is the frothy, mad network that underlies and interconnects all scientific knowledge – but about which we so rarely say anything."

Underland: A Deep Time Journey, Robert Macfarlane (2019)

"«Quando penso che la birra è fatta di atomi, mi passa la voglia di bere». Ecco, questa frase riassume il disagio diffuso nei confronti della scienza (…). Eppure, dopo tanto tempo ho capito alla fine che la birra non perde la sua qualità magica neanche a raccontarla così. Anzi, tutto il mondo è fatto di atomi e viene voglia di viverlo, di esplorarlo e parlarne, e di conoscere persone. **L'idea che si possa razionalizzare l'incanto è un fastidio, ma è solo un effetto collaterale della vertigine della conoscenza**".

Medusa, storie dalla fine del mondo (per come lo conosciamo), Matteo De Giuli e Nicolò Porcelluzzi (2021)

"…**Quella strana attitudine che è la pazienza amorosa nella ricerca, la pazienza ardente, l'intensa padronanza dell'attenzione, sarebbe un'ancestralità animale depositata in noi.** Un'eredità della fase del nostro passato di primati, che risale a circa due milioni di anni fa, quando, da raccoglitori frugivori, siamo diventati tracciatori parzialmente carnivori. È con la pazienza della pantera che seguiamo le tracce della pantera. E non è una metafora, è un'ancestralità animale condivisa."

"Immaginate, in un passato immemorabile, una banda di ominidi indistinti dotati di un protolinguaggio che ci sfugge, mentre isolano una pista sulla sabbia. Si fermano all'altezza dell'ultima impronta, nel punto in cui perdono la pista. Uno di loro punta la sua lancia verso ponente, mentre un altro punta la sua lancia verso levante: ha visto altro nell'enigma del suolo -**questo visibile che obbliga a vedere l'invisibile, a immaginare e a pensare**. A quel punto si riuniscono in circolo e si lanciano in gesti, frasi, in un conciliabolo che ci sfugge, per mettere alla prova dell'intelligenza altrui la versione di ognuno, e determinare insieme dove andremo."

Sulla pista animale, Baptiste Morizot, traduzione di Alessandro Nucera e Alessandro Palmieri (2020)

Table of Contents

Figures Index

Tables Index

List of Abbreviations

aHSCs	active HSCs
ALDH	aldehyde dehydrogenase
AML	acute myeloid leukemia
AMPK-FIS1	AMP-dependent kinase-mitochondrial fission 1
Ang1	angiopoietin 1
APL	acute promyelocytic leukemia
ARCH	age-related clonal hematopoiesis
ATF4	activating transcription factor 4
ATO	arsenic trioxide
ATRA	*all-trans* retinoic acid
BCL2	B-cell lymphoma 2
BM	bone marrow
BMSCs	bone marrow mesenchymal stromal/stem cells
c-Myc	c-Myelocytomatosis viral oncogene homolog
CAR	chimeric antigen receptor
CDKs	cyclin-dependent kinases
cDNA	complementary DNA
CKIs	CDK inhibitors
CML	chronic myeloid leukemia
CRT	calreticulin
CSF-1	colony stimulating factor 1
CTLA4	cytotoxic T-lymphocyte associated protein 4
CXCL12/4	CXC motif chemokine ligand 12/4
CXCR2/4/7	CXC motif chemokine receptor 2/4/7
DAMPs	damage associated molecular patterns
dHSCs	dormant HSCs
DOT1L	disruptor of telomeric silencing 1-like
DTCs	disseminated tumor cells
ECM	extracellular matrix
eIF2α	eukaryotic initiation factor 2 α
ELN	European Leukemia Net
ER	endoplasmic reticulum
EV	empty vector
FACS	fluorescence-activated cell sorting
FBS	fetal bovine serum
FLT3	FMS-like tyrosine kinase 3
FLT3-ITD	internal tandem duplication in FLT3
Fox	forkhead box (family)
G-CSF	granulocyte colony-stimulating factor
GEMs	gel bead-in-emulsions
Gfi1	growth factor independent 1
GM-CSF	granulocyte-macrophage colony-stimulating factor
GSEA	gene set enrichment analysis
H3K79	histone 3 lysine 79 (methyltransferase)
HH	hedgehog proteins

HMA	hypomethylating agents
HMGB	high-mobility group box (proteins)
HSCs	hematopoietic stem cells
HSCT	hematopoietic stem cell transplantation
HSP	heat-shock protein
HSPCs	hematopoietic stem progenitor cells
i.p.	intraperitoneally
i.v.	intravenously
ICD	immunogenic cell death
IFNs	interferons
IL1RAP	IL-1 receptor accessory protein
IL3/6	interleukin 3/6
IMDM	Iscove's modified Dulbecco's medium
IRE-1	inositol-requiring enzyme 1
IRF1	interferon regulatory factor 1
Irgm1	immunity-related GTPase family M protein
ISR	integrated stress response
ISRIB	integrated stress response inhibitor
ITH	intratumoral heterogeneity
JAK	Janus Kinases
KD	knock-down
KI	knock-in
KO	knock-out
LAG3	lymphocyte activation gene 3
LGALS9	galectin 9
LSCs	leukemia stem cells
LT-HSCs	long-term HSCs
Luc	luciferase
MA9	MLL-AF9
MC	methylcellulose
MCL1	myeloid cell leukemia 1
MDS	myelodysplastic syndrome
MHC I	major histocompatibility complex 1
miR126/300	micro RNA 126/300
MKs	megakaryocytes
MLL(r)	(rearranged) mixed-lineage leukemia
MPL	myeloproliferative leukemia virus protooncogene
MPN	myeloproliferative neoplasm
NES	nuclear export signal
NGS	next generation sequencing
NK cells	natural killer cells
NK-AML	normal karyotype acute myeloid leukemia
NLS	nuclear localization signal
NPM1	nucleophosmin 1
NPMc^{+}	cytoplasmic nucleophosmin 1
NPY	neuropeptide Y
NSG	NOD-scid IL2Rgamma^{null}
OPN	osteopontin

OXPHOS	oxidative phosphorylation
PARP1	poly-ADP-ribose polymerase 1
PB	peripheral blood
PBS	phosphate-buffered saline
PD1	programmed cell death protein 1
PDL1	programmed cell death ligand 1
PERK	protein kinase R-like ER kinase
PGE_2	prostaglandin E2
PML-RARα	promyelocytic leukemia retinoic acid receptor α
PTEN	phosphatase and tensin homologue
PuroR	puromycin resistance
qPCR	quantitative polymerase chain reactions
Rb	retinoblastoma (proteins)
RBCs	red blood cells
ROS	reactive oxygen species
RTK	receptor tyrosine kinase
SCF	stem cell factor
scRNAseq	single cell RNA sequencing
SDF1α	stromal-derived factor 1α
shRNA	short hairpin RNA
Socs2	suppressor of cytokine signaling 2
ST-HSCs	short-term HSCs
STAT	signal transducer and activator of transcription (family)
Sytl4	synaptotagmin-like protein 4
TagRFP	red fluorescent protein
TGFß	transforming growth factor ß
TIGIT	T cell immune receptor with Ig and ITIM domains
Tim-3	T cell immunoglobulin and mucin domain 3
TNF	tumor necrosis factor
TNSRs	TNF receptors
TPO	thrombopoietin
Tregs	regulatory T cells
tSNE	t-distributed stochastic neighbor embedding
TU	transducing units
UMAP	uniform manifold approximation and projection
UPR	unfolded protein response
VCAM-1	vascular cell adhesion molecule 1
VISTA	V-domain Ig suppressor of T cell activation
WBCs	white blood cells
WHO	World Health Organization
WT	wild-type

Abstract

Acute myeloid leukemia (AML) is the most common leukemia in adults and its prognosis is usually poor. The main culprit of therapy failure and leukemia relapse is the genomic and biological heterogeneity of the tumor. At biological level, AML is hierarchical organized with leukemia stem cells (LSCs) at the apex. LSCs are a rare cell population able to initiate and sustain leukemia growth and share many features with hematopoietic stem cells (HSCs), including self-renewal capacity and quiescence. Traditional therapies have limited effects on LSCs, mainly due to their quiescent state.

Preliminary data in our group have shown that different leukemia-initiating oncogenes (NPMc^{+}, PML-RARα and MLL-AF9) share the property of enforcing quiescence in HSCs, and that this is critical for the progression and maintenance of the leukemia clone. Underlying molecular mechanisms, however, are unknown.

To this end, we performed an *in vivo* genetic screening to identify quiescence-related genes that are fundamental for leukemia growth. Among the identified hits, *Socs2*, *Stat1* and *Sytl4* silencing prevented AML outgrowth *in vivo*. Notably, *Socs2* and *Stat1* interference increased proliferation while preventing the progressive accumulation of quiescent blasts in the growing leukemia.

Interestingly, *Socs2* and *Stat1* silencing *in vitro* significantly decreased the clonogenic activity of AML blasts, while having no effects on proliferation, cell cycle distribution or survival, suggesting that the effects of *Socs2* and *Stat1* were largely dependent on the *in vivo* leukemia context. scRNAseq analysis of *Socs2*-interfered blasts showed marked downregulation of genes characterizing the dormant status of quiescent HSCs, suggesting that loss of quiescence in *Socs2*-interfered blasts may be linked to the loss of their regenerative potential. Since prolonged stress signals are responsible for the disruption of dormancy and self-renewal potential in HSCs, scRNAseq data were analyzed for the activation of the integrated stress response (ISR). Strikingly, we found that ATF4, UPR and autophagic transcriptional programs were increasingly expressed in proliferating blasts, while they were aberrantly activated in both proliferating and cell cycle restricted *Socs2*-interfered cells. Elevated levels of UPR may act as danger signals, favoring an immune-mediated clearance. Consistently, *Socs2*-silenced blasts markedly downregulated specific immune check-point molecules, including CD24a, galectin 9 and VISTA, which are

involved in the regulation of B cells, T cells, NK cells and macrophages. Notably, activation of the ISR and immune check-point molecules in MA9 blasts resembled the adaptive response of HSCs to oncogene-induced hyperproliferation. Based on these findings, we hypothesized that *Socs2* regulates the resolution of the ISR response in hyperproliferating MA9 blasts by allowing cells with activated ISR to enter quiescence and trigger further pathways of ISR resolution, including upregulation of immune check-point molecules. In the absence of *Socs2*-mediated quiescence, cells maintain a sustained activation of the ISR, downregulate immune check-point molecules and activate immune-mediated cell death.

To preliminarily test this hypothesis, the growth potential of *Socs2*-interfered blasts was evaluated in immunocompromised mice, where a significant attenuation of the anti-leukemic effect of *Socs2* interference was observed. As well, macrophage depletion prolonged disease latency of immunocompetent mice transplanted with *Socs2*-interfered blasts.

These findings provide preliminary evidence of the existence, in AML blasts, of an adaptive response to hyperproliferation that involves ISR activation, induction of quiescence and immune evasion. Targeting this adaptive response, as by *Socs2* interference, may activate potent mechanisms of AML immune clearance.

Chapter 1: Introduction

1.1 Acute Myeloid Leukemia

Acute myeloid leukemia (AML) is a heterogeneous group of aggressive hematological diseases characterized by a malignant proliferation of hematopoietic myeloid progenitor cells in the peripheral blood (PB), in the bone marrow (BM) and/or in other tissues.[1–3] These abnormally or poorly differentiated cells, called leukemic blasts, infiltrate the BM lowering the number of normal terminally differentiated blood cells (hematopoietic failure) with consequent anemia, neutropenia, lymphocytopenia and thrombocytopenia: this is the major culprit of the clinical manifestations of the disease (weakness, lethargy, fatigue, hemorrhages, infections…).[4] If AML remains untreated, it ends up in a rapid fatal outcome.[4]

In terms of prevalence, AML is the most common leukemia in adults, with increasing incidence in patients aged 65 years or older.[5,6] In the United States, AML occurrence ranges between 3-5 cases per 100,000 population. In 2020, as reported by the American Cancer Society, about 20,000 new cases of AML were described, and more than 10,000 patients died.[6] Despite the initial response to chemotherapy and the improvement in the therapeutic regimens for some AML subtypes, around the 40-50% of younger patients and the majority of the elderly ones relapse and succumb to the disease within 5 years from diagnosis.[7] Affected individuals, in fact, die because of both leukemia- and therapy-associated complications.[8]

The standard therapeutic approach to AML, used since the 1970s', is known as "*7 + 3 regimen*" and consists in 7 days of cytarabine infusion followed by 3 days of anthracycline-based chemotherapy (e.g. doxorubicine).[3,9] In addition, consolidation chemotherapy and/or allogeneic hematopoietic stem cell transplantation (HSCT) can be used in patients with higher risk of relapse.[8,9] However, some patients (around 25%) do not respond to the induction therapy (refractory AML) and almost half of them experience a relapse after an initial and transient remission.[7,8] In addition, although effective, these approaches may be poorly tolerated in patients with comorbidities and/or advanced age.[9] In recent years, the Food and Drug Administration approved new drugs to treat both newly diagnosed (midostaurin, gemtuzumab ozogamicin, CPX-351, venetoclax, and glasdegib) and refractory/relapsed AML (gilterninb, a *FLT3* inhibitor, and ivosidenib and enasidenib, *IHD 1* and *2* inhibitors). Even if these new drugs may be crucial in AML treatment, more clinical

research and biomarker analysis/identification are needed to understand which patients are eligible and to explore the possibility of combination therapies.[9]

In this scenario, since AML is considered as a "*heterogeneous group of diseases*", an accurate classification of AML pathophysiological, clinical, cytogenetic and molecular profiles is fundamental for a proper diagnosis, risk classification and choice of the best therapeutic approach. The World Health Organization (WHO) and the European Leukemia Net (ELN) recently published an updated classification of myeloid neoplasms and acute leukemias, attempting to integrate clinical, morphological, immunophenotypic and cytogenetic features with molecular genetic alterations.[10,11]

The WHO classification, dated 2016, starts from the anamnestic data of patients, including both previous cytotoxic therapies ("therapy-related myeloid neoplasms") and/or a history of myelodysplastic syndrome (MDS) or myeloproliferative neoplasms ("AML with myelodysplasia-related changes"). Then, it investigates the presence of genetic rearrangements or mutations ("AML with recurrent genetic abnormalities"). From a cytogenetic point of view, the detection of balanced or unbalanced aberrations associated with MDS and/or morphological multilineage dysplasia define AML "with recurrent genetic abnormalities". In case the disease cannot be classified in the aforementioned categories, it is defined as "AML, not otherwise specified" and subclassified based on the morphological examination of the PB and the BM (**Table 1.1**).[10]

Table 1.1 WHO classification of acute myeloid leukaemia.[10]

Types	Genetic abnormalities
AML with recurrent genetic abnormalities	AML with t(8;21)(q22;q22.1); RUNX1-RUNX1T1
	AML with inv(16)(p13.1q22) or t(16;16)(p13.1;q22);CBFB-MYH11
	APL with PML-RARA
	AML with t(9;11) (p21.3;q23.3); MLLT3-KMT2A
	AML with t(6;9)(p23;q34.1); DEK-NUP214
	AML with inv(3)(q21.3q26.2) or t(3;3)(q21.3;q26.2);GATA2, MECOM
	AML (megakaryoblastic) with t(1;22)(p13.3;q13.3); RBM15-MKL1
	AML with mutated NPM1
	AML with biallelic mutations of *CEBPA*
	Provisional entity: AML with BCR-ABL1
	Provisional entity: AML with mutated RUNX1
AML with myelodysplasia-related changes	
Therapy-related myeloid neoplasms	
AML, not otherwise specified (NOS)	AML with minimal differentiation
	AML without maturation
	AML with maturation

	Acute myelomonocytic leukemia
	Acute monoblastic/monocytic leukemia
	Acute megakaryoblastic leukemia
	Acute basophilic leukemia
	Acute panmyelosis with myelofibrosis Pure erythroid leukemia
Myeloid sarcoma	
Myeloid proliferations related to Down syndrome	Transient abnormal myelopoiesis (TAM)
	Myeloid leukemia associated with Down syndrome

However, since this classification does not take into account the impact on prognosis of the multiple genetic abnormalities that accumulate in leukemic blasts, the ELN developed the first genetic-based stratification system for AML in 2010, revising it in 2017.[10,12] Based on both karyotype assessment and presence of mutations, this system allows for the allocation of patients into three prognostic subgroups: favorable, intermediate and adverse (**Table 1.2**).[10,12] In this classification the prognostic impact of a mutation is highly context-dependent, subordinated to the presence/absence of other co-occurring mutations. The translocations t(8;21) and t(15;17), which are responsible for the expression of the AML1-ETO and PML-RARα fusion proteins respectively, are indicative of favorable prognosis, while complex and/or monosomal karyotype are usually associated with a higher probability of therapy failure. Moreover, since about half of all the cases of AML lack cytogenetic abnormalities (NK-AML, normal-karyotype AML), recurrent gene mutations are often indicative for the risk stratification. In particular, mutations in *CEBPA* or *NPM1*, in the absence of *FLT3* mutation, are good prognostic indicators, while mutated *KMT2A*, *DNMT3A* or *FLT3* itself are associated with worse prognosis.[11,12] Lastly, it is important to underline that this patient stratification, in line with the modern personalized medicine approaches, can be applied also to refractory or relapsed AML. [12]

The recent advances in the next-generation sequencing (NGS) and single-cell technologies have revealed the complex mutational landscape of AML: over 200 recurrent mutations, many of which co-existing in a single patient (80% of the patients have three or more recurrent mutations) and associated with different transcriptional and epigenetic features. [13–15] AML is indeed a complex and heterogeneous ecosystem of genetic clones and subclones that evolves over time under natural or therapeutic selection,[13,15] providing the biological basis for the frequent therapy failure and relapse. Indeed, the major obstacle in AML eradication is represented by the extensive genomic and biological inter- and intra-tumoral heterogeneity.[14,16,17]

Table 1.2 Risk stratification of AML, based on genetic and cytogenetic profile.[12]

Risk category	Genetic abnormality
Favorable	t(8;21)(q22;q22.1); *RUNX1-RUNX1T1*
	inv(16)(p13.1q22) or t(16;16)(p13.1;q22); *CBFB-MYH11*
	Mutated *NPM1* without *FLT3-ITD* or with *FLT3-ITD^{low}* [a]
	Biallelic mutated *CEBPA*
Intermediate	Mutated *NPM1* and *FLT3-ITD^{high}* [a]
	Wild-type *NPM1* without *FLT3-ITD* or with *FLT3-ITD^{low}* [a] (without adverse-risk genetic lesions)
	t(9;11)(p21.3;q23.3); *MLLT3-KMT2A* [b]
	Cytogenetic abnormalities not classified as favorable or adverse
Adverse	t(6;9)(p23;q34.1); *DEK-NUP214*
	t(v;11q23.3); *KMT2A*-rearranged
	t(9;22)(q34.1;q11.2); *BCR-ABL1*
	inv(3)(q21.3q26.2) or t(3;3)(q21.3;q26.2); *GATA2,MECOM(EVI1)*
	−5 or del(5q); −7; −17/abn(17p)
	Complex karyotype,[c] monosomal karyotype[d]
	Wild-type *NPM1* and *FLT3-ITD^{high}* [a]
	Mutated *RUNX1*[e]
	Mutated *ASXL1*[e]
	Mutated *TP53*[f]

[a]Low, low allelic ratio (<0.5); high, high allelic ratio (≥0.5).
[b]The presence of t(9;11)(p21.3;q23.3) takes precedence over rare, concurrent adverse-risk gene mutations.
[c]Three or more unrelated chromosome abnormalities in the absence of one of the WHO-designated recurring translocations or inversions, that is, t(8;21), inv(16) or t(16;16), t(9;11), t(v;11)(v;q23.3), t(6;9), inv(3) or t(3;3); AML with *BCR-ABL*.
[d]Defined by the presence of 1 single monosomy (excluding loss of X or Y) in association with at least 1 additional monosomy or structural chromosome abnormality (excluding core-binding factor AML).
[e]These markers should not be used as an adverse prognostic marker if they co-occur with favorable-risk AML subtypes.
[f]*TP53* mutations are significantly associated with complex and monosomal karyotype AML.

1.2 Hematopoiesis and Hematopoietic Stem Cells

Every day hundreds of billions of blood and immune cells are generated in the BM, which is the primary tissue responsible for blood cell production.[18] There, self-renewing and multipotent hematopoietic stem cells (HSCs) give rise to mature blood cell types of the lymphoid, myeloid, megakaryocytic and erythroid lineages through a process called hematopoiesis. Normal hematopoiesis has been considered for a long time as a stepwise process that proceeds from pluripotent to mature blood cells passing through several different intermediate stages (namely multipotent, oligopotent and unipotent progenitors).[18–21] In this classical hierarchical tree-like model, the first branch of lymphoid progenitors early segregates from all the other lineages, followed by further branching steps corresponding to increasingly lineage-committed progenitor states (**Figure 1.1, A**). Later, the introduction of additional surface markers suggested some modifications to this first model, as depicted in

the **Figure 1.1, B**.[22] However, these models, with their graphical representation as single, rigid, branching trees, miss all the transition states, since they have been generated analyzing a series of population purified by fluorescence-activated cell sorting (FACS), and fail to fully capture the heterogeneity of the HSCs pool.[19–21]

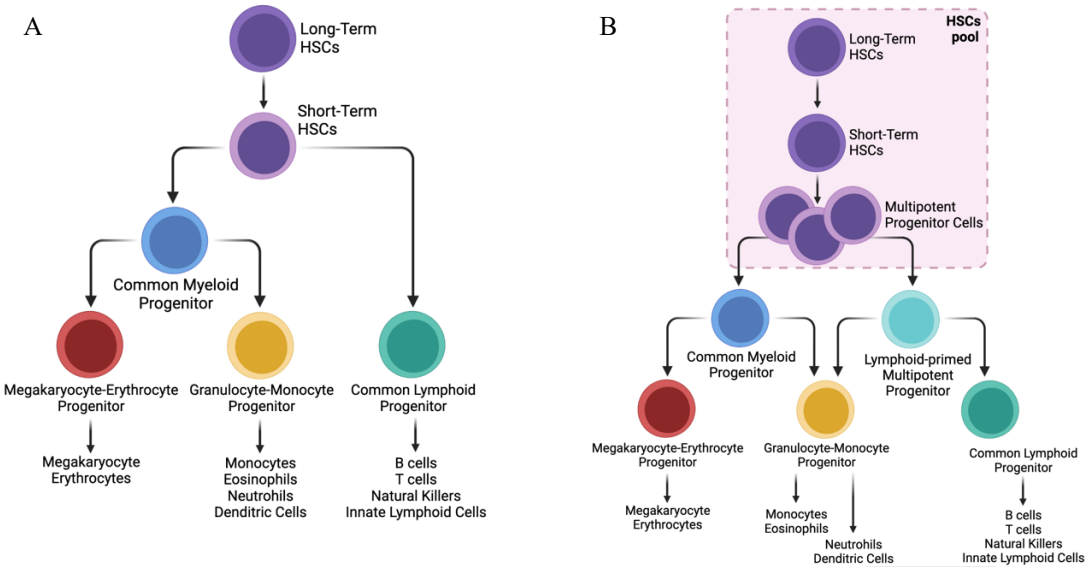

Figure 1.1 Stepwise hierarchical models of hematopoiesis. **A**. HSCs are represented as a homogeneous population giving rise, at the first branching point, to common myeloid and lymphoid progenitor populations. **B**. The HSCs pool is a heterogenous population, both in terms of self-renewal and differentiation; the lymphoid and myeloid progenitors are associated until further down in the hierarchy and the granulocyte-monocyte progenitor compartment is fairly heterogeneous (adapted from Laurenti and Göttgens, Nature 2018).[19]

Recently, the employment of single cell RNA-sequencing (scRNAseq) allowed to demonstrate that hematopoiesis cannot be considered anymore as a discrete stepwise process, but rather a continuous one.[18,20,21] Still, inconsistency persists among the most recent studies. Velten *et al*. proposed the presence of a cellular continuum of undifferentiated hematopoietic stem progenitor cells (HSPCs), containing both myeloid and lymphoid multipotent progenitors, giving rise directly to distinct independent lineage trajectories (**Figure 1.2, A**).[20] Tusi *et al*. suggested a continuum of transcriptional cell states, branching towards seven hierarchically organized fates (erythroid, megakaryocytic, basophilic/mast cells, granulocytic neutrophils, lymphocytic, monocytic and dendritic) (**Figure 1.2, B**).[21] In the most recent study, Qin *et al*., while confirming the continuum state of the hematopoietic process, have identified a tree-like structure in which HSCs form the root, with the seven lineages gradually emerging with a hierarchical structure slightly different from the previous

reports (**Figure 1.2, C**).[18] Globally, these studies depict the hematopoietic system as the result of a dynamic equilibrium between a wide number of transitional states and cells, able to mutually convert into each other (hematopoietic reprogramming) through the conversion into other cell lineages (transdifferentiation) or the acquisition of stemness (dedifferentiation). Noteworthy, the cell fate is not predefined but gradually determined during the differentiation process.[18,20,23,24]

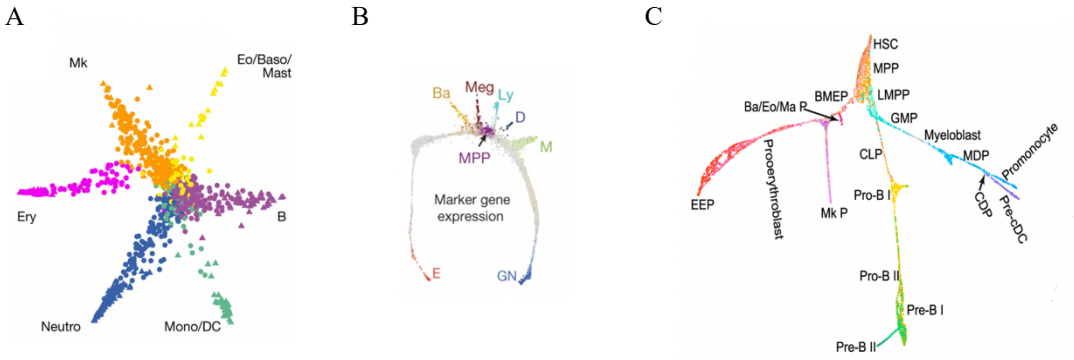

Figure 1.2 Hierarchically continuous transition models for hematopoiesis. A. In the model proposed by Velten *et al*. the HSPCs directly give rise to distinct independent lineage trajectories.[20] **B**. Tusi *et al*. suggested a continuous hierarchical model for hematopoiesis.[21] **C**. Continuous transition model from HSCs to seven hematopoietic lineages proposed by Qin *et al*.[18]

Nevertheless, whatever model is considered, HSCs are localized at the starting point of the hematopoietic process. HSCs are a rare cell population constituted by self-renewing, blood-forming stem cells, able either to self-renew and maintain themselves or to differentiate into downstream multipotent and more lineage-committed progenitors.[19,23,25] Two are the major HSCs populations that have been identified: long-term (LT) and short-term (ST) HSCs. While ST-HSCs maintain the hematopoiesis in short periods of time (14 days), LT-HSCs are the main responsible for life long multilineage reconstitution. Moreover, their ability to preserve life lasting self-renewal potential relies on the fact that they are maintained in the G0 phase of the cell cycle, a reversible absence of cycling also referred to as quiescence.[23,25–28] Emerging evidence shows that HSCs quiescence prevents organelle injury and programmed cell death that can occur because of replication errors, genotoxic insults from reactive oxygen species (ROS) and DNA damage checkpoint-dependent apoptosis. As a result, the HSC pool is protected from exhaustion and pauperization.[25–27]

The quiescent state of HSCs is tightly regulated by both intrinsic and extrinsic factors.[26,27,29]

Leading intrinsic players regulating HSCs quiescence are the cyclins involved in the regulation of the cell cycle, either favoring (cyclin-dependent kinases, CDKs) or inhibiting (CDK inhibitors, CKIs) its progression.[26,30,31]

The critical role played by several CKIs of either the *Ink4* (p15, p16, p18, p19) or *Cip/Kip* (p21, p27 and p57) gene families in the regulation of HSCs quiescence has been described. p21 (Cdkn1a) is the lowest expressed member of the family in LT-HSCs, however its role in the maintenance of quiescence is well established. In homeostatic conditions, *p21* knock-out (KO) mice show an increased number of proliferating HSCs and, upon myeloablative stress, they die due to HSCs depletion. Furthermore, serial BM transplantation revealed an impaired self-renewal potential for *p21* KO HSCs.[28,30,32] Another member of the CIP/KIP family, p57 (Cdkn1c), has the highest expression in LT-HSCs and its deficiency correlates with defects in HSCs self-renewal potential. Moreover, *p57* KO HSCs showed higher levels of p27 (Cdkn1b), suggesting a functional overlap between the two genes in controlling HSCs quiescence and homeostasis.[33] p57 and p27 drive HSCs quiescence through the interaction with the cyclin D1-Hsc70 complex, which, in turn, prevents cyclin D1 nuclear translocation and the consequent activation of CDK4 and -6. In the absence of these CDKs, retinoblastoma (Rb) proteins remain unphosphorylated and bind the transcription factor E2F, preventing S phase entry.[34] The members of the other CKI family, INK4, inhibit both CDK4 and CDK6, but their contribution to HSCs quiescence is lower compared to the one exerted by the CIP/KIP family. To date, p18 is the only member of the INK4 family that has been linked to HSCs maintenance and found upregulated in *p57* deficient HSCs.[35,36]

In addition to CKIs, CDKs regulation also contributes to HSCs maintenance. Indeed, CDK6 or cyclin D2 repression induces HSCs quiescence. Accordingly, CDK6 is expressed at low levels in LT-HSCs, favoring cell cycle arrest, while it is highly expressed in ST-HSCs, promoting a rapid cell cycle entry.[37]

The expression of genes involved in HSCs quiescence, self-renewal and differentiation is controlled and regulated by multiple transcription factors.

Firstly, p53, having p21 among its effectors, was found to be highly expressed in homeostatic LT-HSCs and repressed upon LT-HSCs activation, enabling cell cycle entry. Moreover, *p53* deficient HSCs were more proliferative.[38] p53 may also play a role in inducing quiescence by favoring the expression of two transcriptional repressors, the growth factor independent 1 (Gfi1) and the Necdin. Although the exact mechanism exerted by Gfi1 and Necdin has not been fully understood, they are both known to prevent E2F activation.[39,40]

In addition, STAT5 and FoxO transcription factors, members of the signal transducer and activator of transcription (STAT) and Forkhead box (Fox) family respectively, have been shown to control p27 and p57 expression, mediating HSCs quiescence.[28,41,42] To maintain FoxO activity, LT-HSCs take advantage of two different mechanisms that desensitize them to PI3K/Akt-activating trophic factors. First, PTEN (phosphatase and tensin homologue), highly expressed in LT-HSCs, prevents PI3K-mediated Akt activation. Accordingly, *Pten* inactivation in HSCs triggers cell cycle entry.[43] The second mechanism involves the microRNA miR126, which represses the expression of some PI3K-Akt components and targets CDK3, known to control the G0/G1 transition, favoring cell cycle entry.[44]

Last, CKI expression is regulated also by c-Myc (c-Myelocytomatosis viral oncogene homolog), which acts either as transcriptional repressor or antagonist of both p21 and p27.[45]

In addition to intrinsic factors, the HSCs cell cycle is determined by extrinsic, niche-derived signals, which control the activity of transcription factors and the consequent expression of cell cycle regulators. The BM microenvironment, constituted by the endosteal and the vascular niche, is fundamental for HSCs maintenance, controlling their proliferation, differentiation and self-renewal through secreted factors and physical cell-cell and cell-extracellular matrix (ECM) interactions (**Figure 1.3**).[25,28]

Osteopontin (OPN), secreted by osteoblasts and bone marrow mesenchymal stromal/stem cells (BMSCs), is a matricellular protein acting as a bridge between the cell surface and the ECM.[46] HSCs, through the expression of OPN-binding integrins, are kept in the BM niche in a quiescent state. *Opn* deficiency, indeed, has been described to enhance LT-HSCs proliferation.[47] CXC motif chemokine ligand 12 (CXCL12), also known as stromal-derived factor 1α (SDF1α), is a chemokine expressed by osteoblasts, BMSCs and endothelial cells, binding CXCR4 and CXCR7.[48] The CXCL12-CXCR4 axis plays a role in HSCs quiescence, since *Cxcr4*$^{-/-}$ HSCs demonstrated impaired engraftment and hyperproliferation.[49,50] CXC motif chemokine ligand 4 (CXCL4), produced by megakaryocytes (MKs) and LT-HSCs, plays a role in hematopoiesis by signaling through CXCR2.[51] In particular, both *Cxcr4*$^{-/-}$ and *Cxcl4*-deficient mice showed reduced HSCs self-renewal and enhanced cycling. Moreover, while MKs depletion reduced HSCs quiescence, CXCL4 injection increased it.[51,52] Transforming growth factor beta (TGFß), a cytokine secreted by osteoblasts, Schwann cells and MKs, is another key mediator of LT-HSCs quiescence.[53,54] Indeed, blocking the TGFß-1 signaling with a neutralizing antibody enhanced HSCs proliferation, underlying the role played by TGFß in maintaining HSCs in a quiescent/slow cycling state. Similarly, while

MKs ablation resulted in loss of HSCs quiescence, TGFß-1 injection restored it.[53,54] Among the described mechanisms of TGFß-mediated quiescence, both p57 and *Cxcr4* expression has been described.[55,56]

Trombopoietin (TPO), produced by BMSCs, binds the MPL (myeloproliferative leukemia virus protooncogene), which is highly expressed in LT-HSCs but not in ST-HSCs. *Tpo* deficiency, indeed, leads to HSCs proliferation and LT-HSCs depletion, in association with reduced expression of CKIs (p57 and p19).[57] Last, angiopoietin 1 (Ang1), mainly produced by osteoblasts, drives HSCs quiescence through the Ang1/Tie2 signaling, even if the exact mechanism is poorly understood.[58,59]

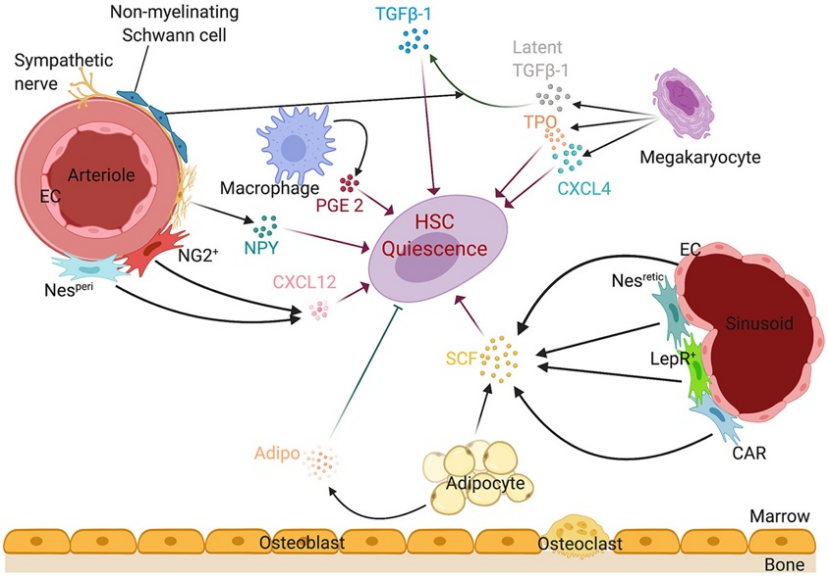

Figure 1.3 Bone marrow cells regulating HSCs quiescence and maintenance. BM resident cells secrete a series of molecular cues that are fundamental in driving HSCs quiescence. Bone marrow mesenchymal stromal cells (Nes^{peri}, $NG2^{+}$, CAR, $LepR^{+}$ and Nes^{retic}) secrete SCF and CXCL12. Sympathetic nerves produce a neuropeptide (NPY), while non-myelinating Schwann cells secrete the transforming growth factor beta (TGFß). Megakaryocytes produce TGFß-1, TPO and CXCL, while macrophages secrete prostaglandin E_2 (PGE_2) (from O'Reilly *et al*., Blood Reviews 2021).[28]

In addition to secreted factors, the ECM plays a pleiotropic role in HSCs maintenance. First, it facilitates the engraftment of HSCs in a quiescence-mediating niche through adhesion molecules, such as integrins, selectins, cadherins and CD44. Secondly, both its composition and biochemical properties regulates HSCs quiescence (e.g. fibronectin-rich endosteal niche supports HSCs quiescence).[60] Last, the ECM retains factors and cytokines favoring the establishment of quiescence.[61]

Despite their quiescent state, HSCs can rapidly react to cell-intrinsic and extrinsic regenerative stimuli and proliferate, ensuring the production of blood cells.[19,23,25–27] Quiescent HSCs can enter the cell cycle and fulfil the increased energy demand by switching their metabolism from glycolysis to oxidative phosphorylation (OXPHOS) that, in turn, controls a series of enzymes capable of modifying DNA and histones, regulating the decision between self-renewal and differentiation. In addition, dividing HSCs are protected from apoptosis and necroptosis thanks to the inhibition of programmed cell death pathways. When the demand for new blood cells is satisfied, HSCs restore their quiescent state by returning to glycolysis, in part through autophagy-dependent mitochondrial clearance (**Figure 1.4**).[23,26,27]

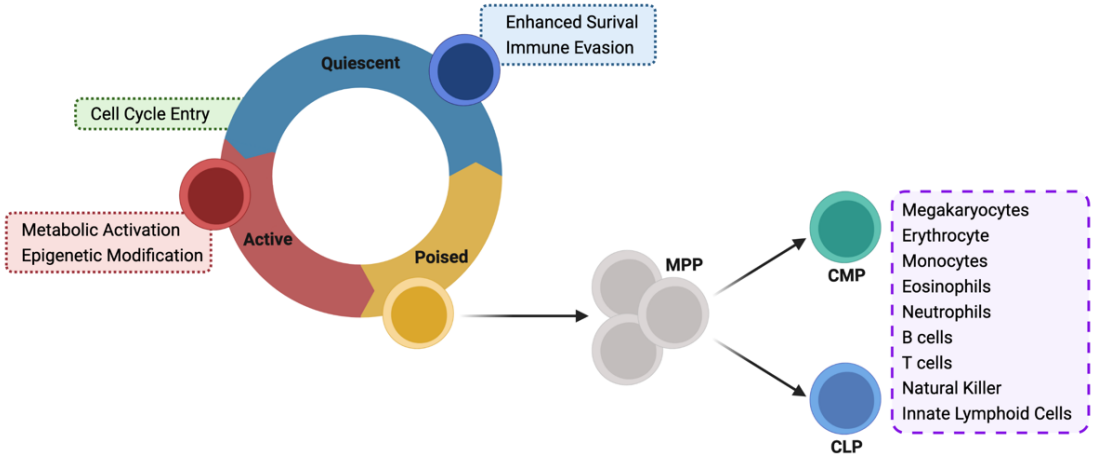

Figure 1.4 Regulation of HSCs activity. At steady state, most of the HSCs are quiescent. If stimulated by regenerative stimuli, they enter the cell cycle and differentiate into downstream progenitors (adapted from Yamashita *et al*., Nature Reviews Cancer 2020).[23]

In response to pathological conditions, such as infections and injuries leading to an acute loss of mature blood cells, HSCs can rapidly enter the cell cycle and differentiate to restore homeostasis.[23,62] The tight and dynamic regulation between the quiescent and active state allows HSCs to satisfy the request for blood cell production both in steady state and regeneration processes. However, a persistent activation or deregulation of this mechanism can lead the way to a malignant transformation.[23,62]

1.3 The process of leukemogenesis

AML develops through the progressive accumulation of mutations occurring in HSCs or immature progenitors. These alterations dysregulate HSCs self-renewal or provide self-renewal capacity to the progenitors, induce hyperproliferation and inhibit the differentiation,

resulting in the accumulation of abnormal, immature myeloid cells in the BM and PB, while hematopoiesis is suppressed.[18,63] However, not all the AML subtypes arise *de novo* from normal hematopoiesis but may also represent the evolution of other conditions characterized by clonal expansion or selection of mutated HSCs.[23,28,64,65] In age-related clonal hematopoiesis (ARCH), a somatic mutation occurring in a single HSC causes a relative expansion of single clones, without evident changes to the lineage output of the hematopoietic system. Although some individuals may remain disease-free throughout their entire life, ARCH increases the risk of developing hematological malignancies.[66] During AML development, the genetic heterogeneity of mutated HSCs and the selective environmental pressure drive the clonal evolution of pre-leukemic HSCs. In myeloproliferative neoplasms (MPNs), selected clones accrue mutations that favor the expansion of the HSPCs pool and the overproduction of mature cells. On the other hand, the inhibition of progenitor differentiation associated with increased HSCs self-renewal leads to impairment of blood production and eventually to BM failure in MDSs. Ultimately, in MPNs and MDSs the increased selective pressure for the acquisition of further driver mutations can set the stage for a full transformation to AML.[65]

Considering the pre-leukemic mutational landscape, early mutations usually occur in DNA-methylating enzymes, leading to enhancement or acquisition of self-renewal properties and defective differentiation, with consequent competitive fitness of pre-leukemic HSCs.[23,67,68] The quiescence state of HSCs favors error prone DNA repair mechanisms with subsequent genomic rearrangements or mutations. [68,69] Moreover, HSCs aging can increase the acquisition of spontaneous mutations.[64,68,70] The generation of a favorable BM microenvironment, together with a dysregulation of inflammatory signals by the pre-leukemic HSCs, ultimately promotes their clonal expansion, mutagenesis, and oncogenic potential.[68] Late mutations, usually involving molecules within signaling pathways and transcription factors, induce proliferation and differentiation block leading to AML development.[67,71]

Once the leukemia clones are generated in the BM space, they are able to enter the blood stream to extravasate in secondary BM locations and additional metastatic sites (e.g. spleen, lymph nodes, central nervous system),[72,73] adopting HSPCs and/or mature leukocytes trafficking abilities.[74,75] When leukemic cells reach the new BM location, they can co-opt a series of HSCs signaling pathways and localize in specialized niches functional to their thrivingness.[76] While the vascular niche fuels leukemia proliferation, the endosteal and

adipocytes-rich niches promote dormancy (**Figure 1.5**).[77,78] Last, leukemic blasts are able to remodel the BM niche to favor AML growth over HSCs.[79]

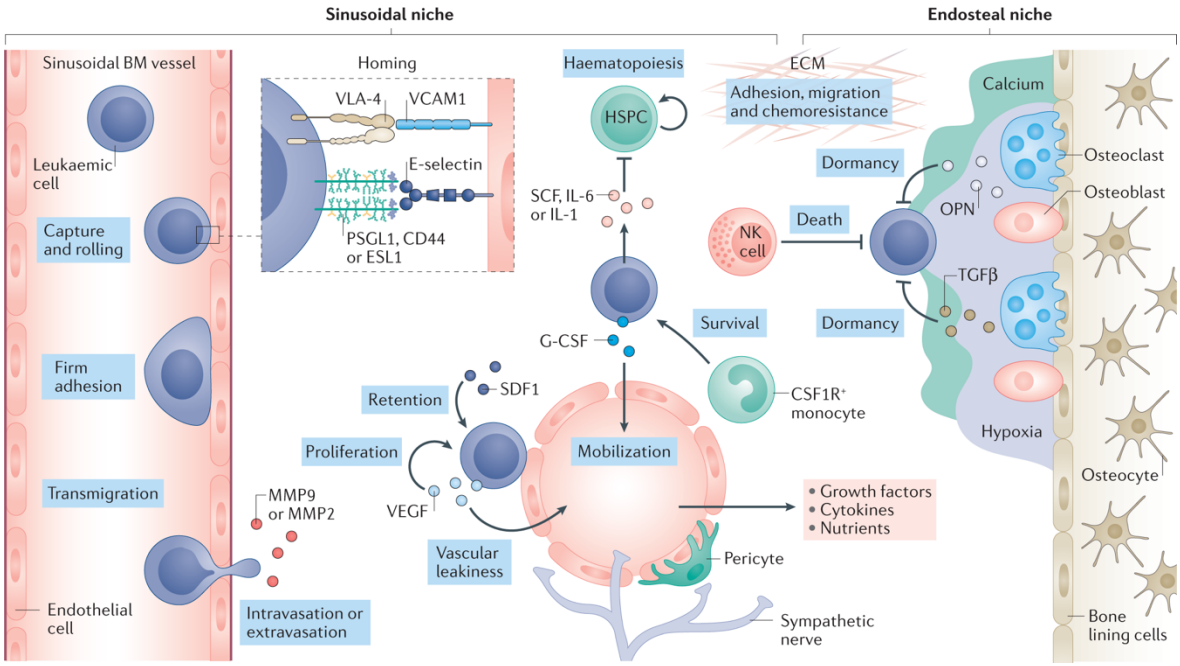

Figure 1.5 The leukemia bone marrow microenvironment. Leukemia cells homing is mediated by a series of adhesion molecules (VCAM-1 and E-selectin) and soluble factors (SDF1). Once the new BM location is reached, leukemic blasts can remodel the BM niche to promote their own growth and survival or migrate to pro-dormancy endosteal niches (from Whiteley *et al*., Nature Reviews Cancer 2021).[75]

AML, as other hematological malignancies, is composed of a small population of cells that share phenotypical and functional features with normal HSCs: the leukemia stem cells (LSCs). LSCs are functionally defined as cells able to: 1) self-renew and 2) recreate and propagate AML in immunodeficient mice.[68,80,81] LSCs usually represent a rare leukemic subpopulation that can originate either from transformed pre-leukemic HSCs or more committed progenitors that gain self-renewal properties.[23,24,67,68,81] LSCs, in addition to disease initiation and propagation, thanks to their lower proliferative rate and niche localization, are able to escape chemotherapy treatment and immune surveillance, leading to post-therapy relapse of AML.[68,82,83]

1.4 The mutational landscape of AML

The first model proposed to support AML pathogenesis was suggested by Gilliland and Griffin and called “the two-hit model”. In this model the prerequisite for AML development

was represented by the cooperation between two different lesions, not sufficient to cause AML alone: class I mutations (e.g. mutated *FLT3-ITD*, *cKIT* or *NRAS*), which confer a proliferative advantage and class II mutations (e.g. AML fusion genes), which interfere with the hematopoietic differentiation process.[84] However, more recent whole-genome and whole-exome sequencing studies have set the stage for a better understanding of leukemogenesis, rendering the two-hit model an oversimplification of the process. Indeed, it is becoming evident that AML evolution is a multistep process, with a primary mutation which manifests together with a complex interplay of epigenetic and genetic mutations (two to six current somatic mutations), which can be acquired or lost over time (clonal selection).[17,63,85]

An important aspect of clonal evolution is that the earliest mutational events, represented by somatic mutations in the *DNMT3A*, *TET2*, *JAK2*, *ASXL1* and *SF3B1* genes, can occur in both healthy individuals (ARCH) and MDSs, MPNs and AML patients.[15,64] *DNMT3A* and *TET2*, which are the most frequently mutated genes in ARCH, confer a strong competitive advantage to LT-HSCs, rendering them potential pre-leukemic clones. Indeed, the clonal expansion of mutated HSCs is permissive for the accumulation of secondary and tertiary mutations leading to AML development.[23,67] However, AML can also follow patterns of clonal evolution alternative to ARCH. In fact, only in the 20% of cases the *DNMT3A* mutation is present in both AML blasts and residual non-leukemic hematopoietic cells (T lymphocytes), indicating that the mutation occurred in ancestral cells, affecting both the myeloid and the lymphoid lineages before AML development.[86,87]

Exon 12 mutations in the *NPM1* gene are among the most common AML driver mutations, occurring in 35% of AML cases and in 55% of those with a normal karyotype (NK-AML).[88,89] Moreover, within the same patient, $NPMc^+$ co-occurs together with the internal tandem duplication mutation in *FLT3* (FLT3-ITD) in 40% of cases and/or with the *DNMT3A* mutation in almost 60% of the cases, implying molecular synergisms among these three mutations in promoting AML development. [89–92] In the WHO classification, the AML harboring the *NPM1* mutation represents a distinct entity, and, in the absence of co-occurring mutations, it is generally associated with a favorable prognosis.[10,12,88] *NPM1* encodes for nucleophosmin, a phosphoprotein primarily located in the nucleus, but able to shuttle between the nucleus and the cytoplasm, thanks to the presence of both a nuclear localization signal (NLS) and a nuclear export signal (NES) inside the protein.[93] NPM has been reported to play a role in many basic cellular processes, in the maintenance of genomic stability and

in the control of the cell cycle.[89,93] The mutation at exon 12 of *NPM1*, which is usually a 4 base-pair insertion, causes a frameshift in the C-terminus of the gene that results in the creation of an additional NES and, ultimately, in the aberrant cytoplasmic localization of the mutant protein (NPMc$^+$).[89] Unlike mutations of *DNMT3A*, *TET2*, *JAK2*, *ASXL1* and *SF3B1,* NPMc$^+$ has not been detected in individuals with ARCH.[87] In AML with ARCH, indeed, while *DNMT3A* mutation has been detected across different non-leukemic HSCs, progenitors and mature populations, NPMc$^+$ was selectively present in multilymphoid and/or granulocyte monocyte progenitors, suggesting that *DNMT3A* mutations precede NPMc$^+$ during leukaemogenesis.[87] However, since the majority of NPMc$^+$ / *DNMT3A* mutated AMLs do not show evidence of ARCH, it was suggested that NPMc$^+$ may play different functions during AML development.[86]

NPMc$^+$ is typically present in *de novo* AMLs in the dominant leukemic clone together with other sub-clonal mutations, such as FLT3-ITD.[15] However, even if it is known that NPMc$^+$ is critical for leukemogenesis, the associated molecular mechanisms are still under investigation. First, it was shown that in transgenic mouse models, NPMc$^+$ expression alone leads to myeloproliferation in BM and spleen, without being sufficient to cause AML development.[94] Later on, it was demonstrated that NPMc$^+$ knock-in (KI) mouse models develop leukemia late in life and with low penetrance (about 30% of the animals), suggesting the need for additional mutations to support a full AML phenotype.[95,96] Moreover, Vassiliou *et al.* identified, through transposon insertional mutagenesis, such cooperative mutations, including the ones in the *Flt3* gene.[96] The proof of the cooperation between NPMc$^+$ and FLT3-ITD mutations in AML development came from NPMc$^+$ / FLT3-ITD mice, which were shown to quickly develop leukemia.[95] Last, the fact that NPM mutations are preserved in the 90% of relapsed AML patients suggests that they are critical for the development and maintenance of the main leukemic clone.[97]

Remarkably, main recurrent chromosomal abnormalities (e.g. PML-RARα and MLL-rearranged -MLLr) and some gene mutations (e.g. *MLL1*, *RUNX1*, *CEBPA* and *TP53*) are mutually exclusive with NPMc$^+$, strongly suggesting overlapping underlying pathological molecular mechanisms and the pivotal role of NPMc$^+$ mutation in driving AML development.[91]

Acute promyelocytic leukemia (APL), a clinical-morphological subtype of AML, accounts for the 10-15% of all adult AMLs and it is characterized by a proliferation of blasts blocked in the promyelocytic stage of myeloid differentiation.[10,98,99] The 95% of APL cases harbor

the promyelocytic leukemia (PML) – retinoic acid receptor α (RARα) oncogenic fusion protein, known as PML-RARα, as a result of a balanced translocation between the chromosomes 15 and 17. Less commonly, *RARα* can be fused to other partner genes, such as *NPM*, *PLZF* and *NuMA*.[100,101] The resulting RARα fusion proteins disrupt the physiological RARα signaling, ultimately leading to aberrant repression of genes necessary for a proper myeloid differentiation.[100] This differentiation block was overcome, together with PML-RARAα oncoprotein degradation, by the adoption of differentiating agents (*all-trans* retinoic acid -ATRA and the arsenic trioxide -ATO) in chemotherapy free regimens.[98,102–104] Noteworthy, ATRA monotherapy is associated with disease relapse, while combination therapy with ATRA and ATO leads to high cure rates.[98,103,104] Additionally, ATRA administration to treat non-APL AML (e.g. $NPMc^+$ AML), in association with chemotherapy, leads to both ATRA-induced differentiation and $NPMc^+$ degradation.[105] The basis for $NPMc^+$ AML sensitivity to ATRA has been linked to ATRA-induced differentiation.[102] ATRA treatment, indeed, degrades mutant NPM1 leading to PML upregulation, PML nuclear body formation, growth arrest and activation of p53 signaling and senescence.[106,107] These data unraveled a series of similarities between $NPMc^+$ AML and APL: an altered nuclear distribution of PML bodies, which are stress-responsive domains with growth suppressive properties, and a therapy response correlating with mutated NPM1 or PML/RARα degradation, PML upregulation and p53 activation causing cell senescence.[105,107,108] Further, these data support the presence of common pathological molecular mechanisms and may explain the observed $NPMc^+$ and PML-RARα mutually exclusiveness in AMLs patients.

Rearrangements of the mixed-lineage leukemia (MLLr) gene *KMT2A* are among the most common chromosomal abnormalities in AML, accounting for around the 5-10% of the cases in adults.[109] MLLr leukemia represents an heterogenous group of AMLs, since more than 70 different fusion partner genes have been described so far and, among them, the most common involves *AF9*, *AF4, AF10* and *ELN*.[8,110] *KMT2A*, located on the chromosome 1, encodes for a histone methyltransferase harboring a C-terminal SET domain capable of methylating histone 3 lysine 4, positively regulating multiple transcription factors.[111] The oncogenic fusion proteins, resulting from the chromosomal translocation, are characterized by the conservation of the functional N-terminal of MLL and the acquisition of the C-terminal of the translocation partner, which activates transcription.[112] In particular, *MLL* disruption by translocation positively regulates the *HOX* genes (including *HOXA9* and

HOXA7) and the HOX cofactors *MEIS1* and *PBX3*, all crucial in the process of leukemogenesis. The direct consequence of this upregulation is an enhancement in stem and progenitor cells proliferation together with a block in myeloid differentiation, ultimately leading to AML.[111,113,114] Menin, a tumor suppressor protein encoded by the *MEN1* gene and acting as an essential oncogenic cofactor of MLL fusion proteins, may represent a valuable target for *MLL*r leukemia.[115,116] Pharmacological inhibition of menin – *KMT2A* has proved effective in preclinical models by downregulating the aberrant gene expression profile (*Hox* and *Meis1*) and releasing the differentiation block. To date, multiple clinical trials with menin inhibitors have been started with early promising results.[115–119] Similarly, another potential therapeutic target in leukemias bearing MLL translocations is represented by the histone 3 lysine 79 (H3K79) methyltransferase DOTL1, known to be implicated in the development and growth of leukemias bearing MLL translocations.[120] In this regard, the antileukemic activity and the tolerability of DOTL1 inhibitors is under investigation in preclinical models.[121,122]

Of note, the upregulation in *Hoxa* and *Meis1* has been described also in NPMc$^+$ AML and it is considered the most important transcriptional trait.[123] The similarity between the gene expression profiles of these two AML subtypes has led to the hypothesis of MLL/menin involvement in NPMc$^+$ AML. Strikingly, MLL ablation or the small molecule menin inhibitor promoted differentiation and exerted a potent antileukemic effect in both NPMc$^+$ mouse models and patient-derived xenografts, while clinical trials are currently running.[117,119,124] Additionally, since in NPMc$^+$ blasts the overexpression of *HOXA* and *MEIS1* has been described in association with H3K79 di/tri-methylation, DOT1L inhibitors were tested too:[125] treatment of NPMc$^+$ KI mice exerted a survival advantage associated with myeloid differentiation, similar to the data obtained with menin inhibitors.[124,125] Although underlying molecular mechanisms are still largely unknown, these data clearly indicate the activation of common leukemic pathways in MLLr and NPMc$^+$ AML.

1.5 The intratumoral phenotypic heterogeneity

Most tumors can be considered as complex ecosystems, in part shaped by the selective pressure exerted by the microenvironment in which they reside. Such a pressure drives the diversification of cancer cells, generating a high degree of intratumoral heterogeneity (ITH).[126] In the last decades, several multiregional genome-sequencing studies identified a wide genetic diversity of malignant cells not only in primary versus metastatic lesions and

in different regions of the same tumor (spatial heterogeneity), but also in different moment of disease progression (temporal heterogeneity).[67,127,128] Notably, ITH does not refer only to the genetic variability, but includes epigenetic, transcriptional, phenotypic, metabolic and secretory components (**Figure 1.6**).[129–131] Moreover, also the non-malignant components of the tumor microenvironment, such as stromal and immune cells, are affected by ITH.[132,133]

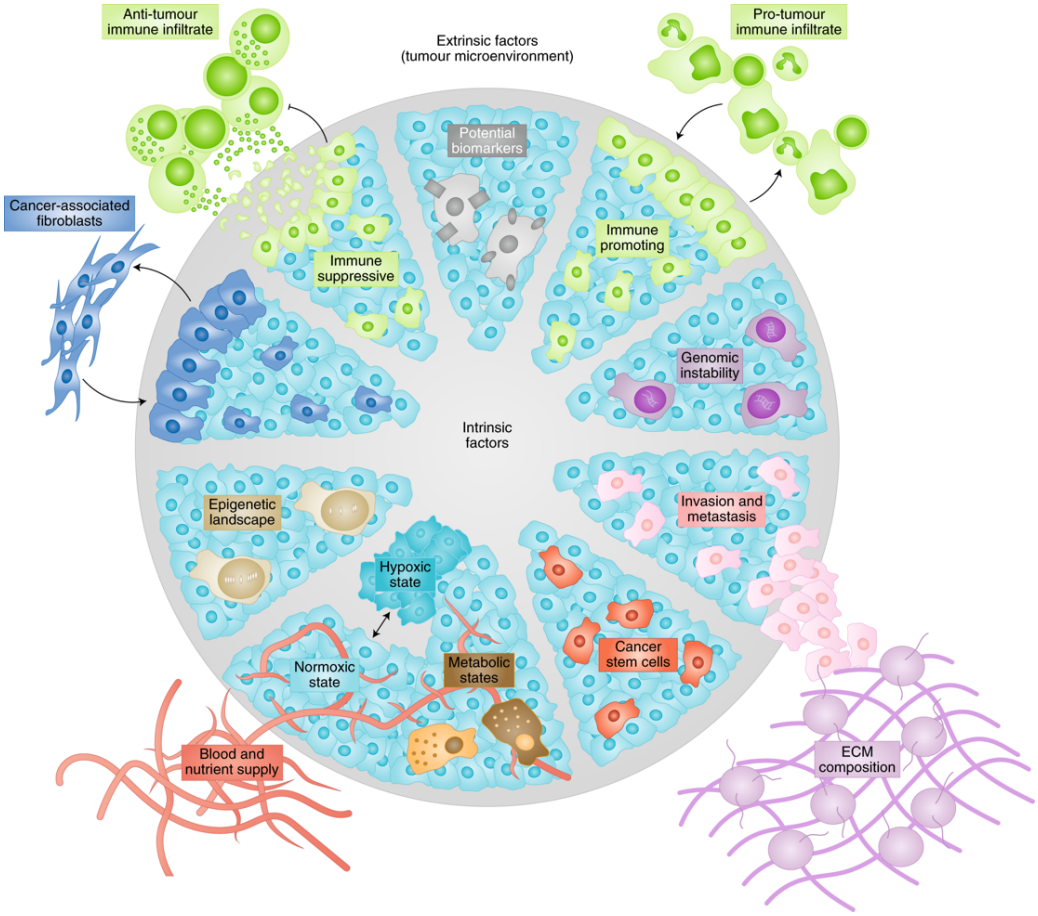

Figure 1.6 Intratumoral heterogeneity and its regulation by intrinsic and extrinsic factors. Tumors can be considered as complex ecosystems composed of heterogeneous populations of cancer cells (intratumoral heterogeneity). This heterogeneity can be driven by both intrinsic and extrinsic factors (from Lawson *et al*., Nature Cell Biology 2018).[134]

As for AML, most tumors are composed of different cell subpopulations showing different genetic features (subclones).[67,135,136] In addition, the selection forces responsible for the observed ITH acts on phenotypes, which are the result of both genetic and non-genetic influence.[128,137,138] In fact, genetically identical cancer cells can be morphologically different due to the response to different environmental stimuli: hypoxia, lack of nutrients and inflammatory cytokines, for example, induce the expression of different epigenetic modifiers, able to modulate the expression of genes linked to a specific phenotype like

differentiation, transdifferentiation or epithelial-mesenchymal transition.[131,139] In addition, these stimuli can also modulate protein synthesis and translation, generating an enormous proteomic heterogeneity.[140] Last, ITH is further increased by the aberrant tumor microenvironment. Indeed, different cancer cell phenotypes can be generated as a consequence of both heterogeneity in immune cells infiltration and cellular and/or paracrine interactions produced by an altered tissue architecture.[126,128,134,138]

1.5.1 Quiescence is part of the intratumoral phenotypic heterogeneity

As previously mentioned, cancer cells show high levels of phenotypic plasticity, being able to respond to environmental perturbations through transcriptional and metabolic reprogramming.[137,141] In particular, transcriptomic, metabolic and immune intratumoral heterogeneity can generate both cycling and cell cycle restricted cells (defined as quiescent or dormant cells).[141–144] Dormant cancer cells are reported to be not proliferating cells that have undergone a transient and reversible G0-G1 cell cycle arrest.[145–147] In general, dormant cells are described as a rare population both in solid (such as breast,[148] prostate,[149] lung,[150] colon,[151] ovarian,[152] brain,[153] pancreas[154] and kidney[155] cancer) and hematologic (such as multiple myeloma[156] and leukemia[157]) tumors. Currently, dormant cancer cells are identified as cells with less RNA content[158] and negative for the expression of the cell cycle marker Ki67,[159] a nuclear protein expressed in proliferating cells and progressively degraded in the transition between the M and G1 phase of the cell cycle. Moreover, Ki67 has been employed as a clinical marker of cancer prognosis because it reflects the proliferative index of a tumor.[159]

It is important to mention that for years the terms ‘cancer stem cells’ and ‘quiescent cancer cells’ have been used interchangeably.[160] However, more recently, some important differences have been established. First, cancer stem cells have been shown to express markers and transcription factors of stemness, that are present only on some dormant cancer cells.[156,161] Moreover, cancer stem cells are self-renewing and give rise to differentiated cells, whilst there is no difference in terms of differentiation status between cycling and dormant cancer cells.[162]

Cancer cells can enter a state of dormancy to survive and adapt to different environmental stresses, such as growth factors and nutrients deprivation, hypoxia, antineoplastic treatments and immune clearance.[163] In primary tumors the alternation between proliferation and quiescence allows malignant cells to acquire additional genetic and epigenetic mutations that

are essential for disease progression, increasing tumor aggressiveness and survival in unfavorable environments.[164,165] At a later stage, dormancy can be employed to facilitate immune evasion[166,167] and resist to anticancer drugs.[168,169]

In addition, dormancy is a feature of the disseminated tumor cells (DTCs) that have left the primary tumor mass to reach secondary sites. DTCs, adapting to new microenvironments, undergo dormancy, a state that is thought to be the major culprit of therapy resistance and metastatic relapse (**Figure 1.7**).[148–157,170–172] Finally, repeated cycles of antineoplastic drugs can push cancer cells to enter quiescence, rendering them resistant and responsible for disease reoccurrence.[173]

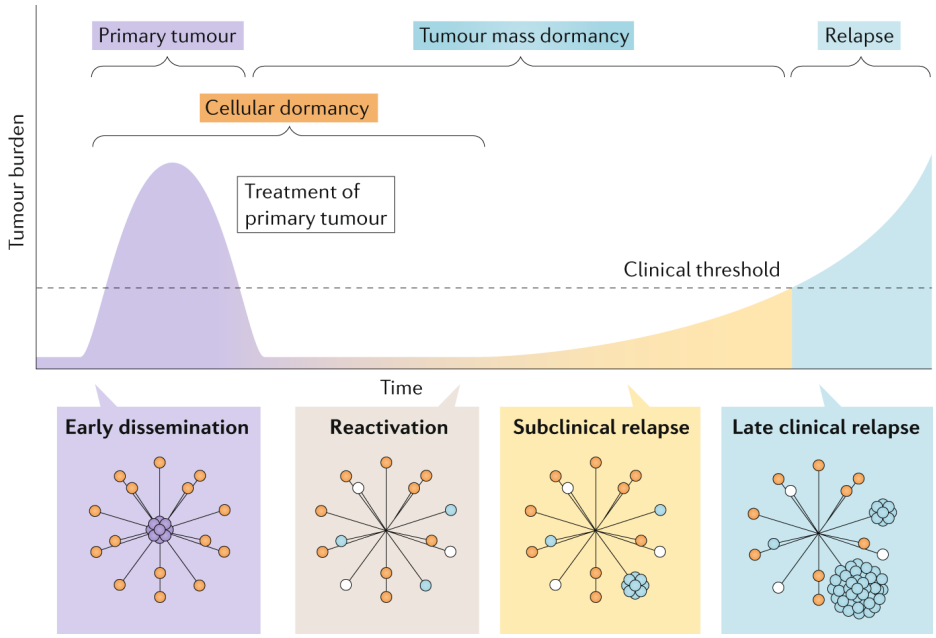

Figure 1.7 Model of cellular and tumor mass dormancy. DTCs (orange circles) can be present before the primary tumor (purple circles) is clinically detectable. Among DTCs, some do not survive (white circles), while some others remain dormant. When dormant DTCs are reactivated (blue circles), they give rise to metastatic relapse (from Phan and Croucher *et al*., Nature Reviews Cancer 2020).[146]

Based on the above consideration, dormancy is not only regulated by cell-intrinsic properties but also depends on cell-extrinsic environmental factors, and among them the niche in which the tumor cell resides. In summary, dormant cancer cells are characterized by: 1) cell cycle arrest; 2) reversibility of the state of quiescence; 3) niche dependence; 4) ability to evade the immune system; 5) drug resistance and 6) metastatic relapse, making them the main therapeutic target to eradicate the tumor.

1.5.2 Downstream effects of quiescence in solid tumors

Cancer-related deaths are mainly associated with tumor relapse and metastases, conditions that can both arise years and decades after treatment and removal of the primary tumor.[174] The main responsible for late metastatic relapse is the random reactivation of drug-resistant, dormant cancer cells, that can lodge in organs different from the primary tumor site even at early stages of the disease (**Figure 1.8**).[166,167,175,176]

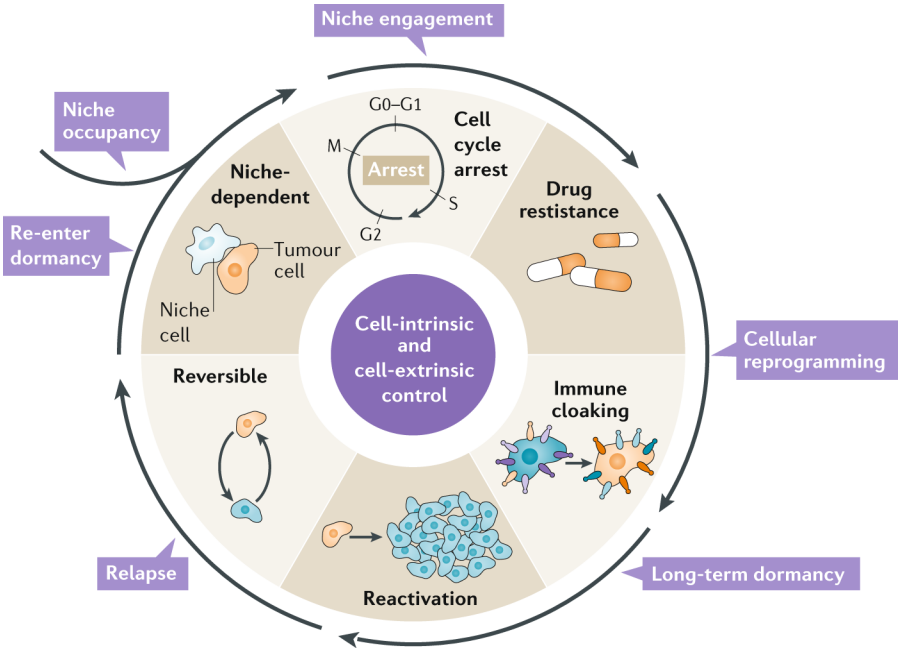

Figure 1.8 The dormant cancer cell life cycle. Cancer cells, after leaving the primary tumor, occupy the niche, entering a state of cell cycle arrest. Subsequently, they undergo cellular reprogramming allowing them to resist antineoplastic drugs and evade the immune system. Subsequently, changes in the microenvironment can reactivate these dormant cancer cells, generating a metastatic relapse (from Phan and Croucher *et al*., Nature Reviews Cancer 2020).[146]

To survive in hostile environments, DTCs can exploit various mechanisms, most of which involve the entrance into a state of dormancy. It has been demonstrated that the quiescence state correlates with the protection of normal stem cells from natural killer (NK) and T cells killing through the downregulation of the machinery necessary for endogenous antigen presentation. [177–179] The fact that the immune privilege is linked to the quiescent state and is not an intrinsic cell property was also demonstrated for quiescent DTCs in breast and lung cancer by the lab of Massagué.[166,180] In addition, dormant DTCs can "cloak" and mask themselves as immune cells belonging to the niche (immunocloaking)[156,181] and they may exploit the immune privilege that normal cells have when they occupy a specific niche,[182] which can additionally provide chemo- and radioprotection to cancer cells irrespectively of

their cell cycle status.[171,183] Lastly, some evasion mechanisms are specific to dormant cancer cells. Indeed, since chemo- and radiotherapy target highly proliferating cancer cells, causing their death, quiescent cells can survive in a passive manner because of their cell cycle status.[142,144,164,168,173,184] Moreover, dormant cancer cells actively regulate a series of pathways responsible for after-therapy adaptation and survival.[154,170,171,185]

1.5.3 Intratumoral Phenotypic Heterogeneity in AML: the Leukemia Stem Cells

As previously mentioned, normal HSCs give rise to mature blood cell types of the lymphoid, erythroid and myeloid lineages and HSCs commitment proceeds through a series of increasingly lineage-committed progenitor states.[19] In a similar way, AML is constituted of primitive (LSCs) and more differentiated cells.[186] Therefore, the bulk AML population is composed of a mosaic of leukemic cells with different features and sensitivities to anticancer therapies leading to the first level of the intratumoral AML phenotypic heterogeneity.

LSCs were firstly described by Dick and colleagues as $CD34^+/CD38^-$ leukemic cells retaining *in vivo* tumorigenic ability.[80,187] However, there is a wide intra-tumoral and inter-patient heterogeneity in the expression levels of these two surface markers. Indeed, further studies demonstrated that also $CD34^-$ cells can engraft immunocompromised mice, and *NPM1*-mutated AML contains both $CD34^+$ and $CD34^-$ LSCs.[188,189] Based on the expression of CD34, CD38 and aldehyde dehydrogenase (ALDH), Gerber *et al.* were able to identify different AML phenotypes: 1) $CD34^+/CD38^-/ALDH^{high}$, indistinguishable from HSCs and associated with poor-risk cytogenetic or *FLT3-ITD*; 2) $CD34^+/CD38^-/ALDH^{int}$ in intermediate-risk AML; 3) $CD34^+/CD38^-$ or $CD34^-$ in the most favorable AML ($NPMc^+$ and APL).[188] These phenotypes, in addition, may indicate at which stage of the hematopoietic differentiation the leukemic mutation develops, with the $CD34^+/CD38^-/ALDH^{high}$ arising from primitive HSCs, $CD34^+/CD38^-/ALDH^{int}$ from less differentiated progenitors and $CD34^-$ from the most differentiated ones.[188]

LSCs hijack a series of HSC survival mechanisms, in particular to manage stress and suppress cell death.[190,191] The AMP-dependent kinase (AMPK)-mitochondrial fission 1 (FIS1)-mediated mitophagy pathway favors the maintenance of LSCs stem properties that can be compromised by oncogenic transformation-induced stress,[192] and BCL2 expression inhibits mitochondrial pro-apoptotic pathways.[190] Additionally, LSCs are able to evade immune clearance thanks to the presence of regulatory T cells (T_{regs}) in the BM niche,[193] they escape macrophage-mediated phagocytosis through the expression of "*don't eat me*"

signals like CD47,[194] and NK-mediated immune surveillance through the upregulation of poly-ADP-ribose polymerase (PARP1) and the subsequent NKG2D ligand downregulation (**Figure 1.9**).[195]

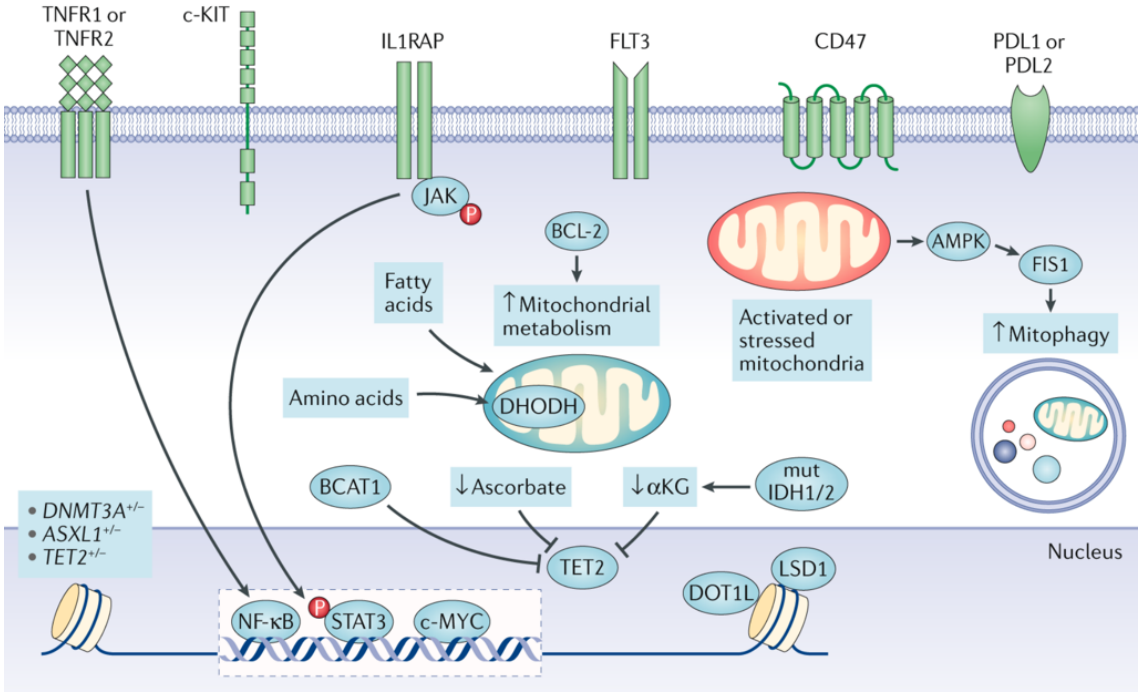

Figure 1.9 LSCs pro-survival and immune escape pathways. LSCs co-opt pro-survival and immune-evasion pathways from HSCs. Via TNF receptors (TNSRs) and IL-1 receptor accessory protein (IL1RAP) upregulation, LSCs potentiate the signaling pathways of chronic inflammation. In addition, LSCs sustain their proliferation and survival through the upregulation of cKIT and FLT3, while CD47, PDL1 and PDL2 carry out an immune-inhibitory role. Then, the mitochondrial metabolism increases, fueled by non-glucose energy substrates (fatty acids and amino acids) (adapted from Yamashita *et al*., Nature Reviews Cancer 2020).[23]

Like HSCs, most LSCs benefit from their quiescence state which, however, can be reverted, leading to cell cycle entry, whenever it is necessary to react to environmental stresses.[196] As of today, it is known that quiescence regulation in LSCs is similar to normal HSCs, with the endosteal niche of the BM playing a central role in dormancy maintenance.[28,76,156,197] However, while HSCs can switch from quiescence-associated glycolysis to OXPHOS, LSCs, even if unable to use glycolysis, are extremely plastic from a metabolic point of view and they can rely on amino acid catabolism and OXPHOS as well as on fatty acid oxidation.[190,198] Both intrinsic (cell cycle regulators and transcription factors) and extrinsic (niche-derived) factors tightly regulate LSCs quiescence, as described in the section 1.2 for HSCs; however, some differences exist between HSCs and LSCs quiescence. A recent study by Sheng *et al.* has shown that the Fox family member FoxM1 is highly expressed in MLLr

AML, inducing p21-dependent LSCs quiescence, and FoxM1 KO MLL-AF9 mice exhibit LSCs quiescence loss.[199] Additionally, in chronic myeloid leukemia (CML) the microRNA miR300 induces LSCs quiescence at low concentration in a FoxM1-dependent manner.[200] In AML miR126, has been linked to LSCs quiescence, and its deficiency drives LSCs proliferation and differentiation, ultimately leading to LSCs pool exhaustion.[44] Moreover, during AML development, alterations of the BM stroma like decline in the overall BMSC numbers, increased expression of OPN and reduced expression of adhesion molecules (VLA4 and VCAM1), CXCL12, Ang1, SCF and TGFß-1, support LSCs quiescence at the expenses of normal hematopoiesis.[79,201]

While a wide amount of information is available on solid tumor dormancy and its implication, data on AML are mainly restricted to the therapeutic implications of quiescent LSCs. Quiescent LSCs are largely considered the main culprits of the failure of conventional therapies, which mainly target actively proliferating cells.[196] Moreover, the association between quiescence and upregulation of several pro-survival mechanisms (e.g. reduced metabolic rates and expression of anti-apoptotic proteins) renders LSCs resistant to a broader range of therapeutics.[28] Indeed, most studies conducted on LSCs quiescence have been mainly focused on the identification of potential LSCs Achilles heel, including ways to break their dormancy and/or their niche related privilege to achieve a durable cure.[81,83]

LSCs can be extremely heterogeneous, from both a genetic and phenotypic point of view, not only among different AMLs, but also within the same patient. LSCs intra-patient heterogeneity can arise as a result of complex processes of clonal evolution and selection. Indeed, during AML development, the LSCs are subjected to stimuli (e.g. niche effect, immunosurveillance, inflammation, therapy...) that can potentially drive their clonal evolution from disease initiation to relapse, passing through AML progression. The presence of this aggregate of diverse populations of cells, together with their quiescence state, makes LSCs and their heterogeneity the main responsible for post-therapy AML relapse. In the last decade, many studies tried to characterize them phenotypically and molecularly, with the final aim of better predicting disease aggressiveness and developing new therapeutic strategies capable of targeting LSCs. [82,135,136,141,202]

1.6 Therapeutic strategies in AML: how to tame the intratumoral heterogeneity

As discussed in the previous chapters, AML is morphologically, immunophenotypically, (cyto)genetically and epigenetically heterogeneous, heavily affecting patient response to

treatment and outcome.[2,11] Indeed, high levels of ITH are associated with poor prognosis and outcome due to the presence, within the same tumor, of a variety of clones with different sensitivities to anticancer therapies, which can lead to therapy resistance, treatment failure and subsequent relapse, even in the presence of an initial response to first line treatments.[137,138,203,204] In addition, ITH has a significant impact on the initial classification of the disease, since not all the cell populations may be adequately represented in the biopsy of the primary tumor but they can become evident as resistant clones in post-therapy relapse.[18,137]

The current treatment approach, consisting in combination chemotherapy, hypomethylating agents (HMA) and/or HSCT, can fail to achieve a definitive eradication of the disease, ultimately leading to AML relapse.[12] More recent findings of multiple intracellular pathways critical for AML growth have set the stage for the identification of new potential molecular and immunological therapeutic targets. Moreover, the wide inter-patient heterogeneity underlines the need for personalized therapeutic strategies (**Figure 1.10**).[3,205]

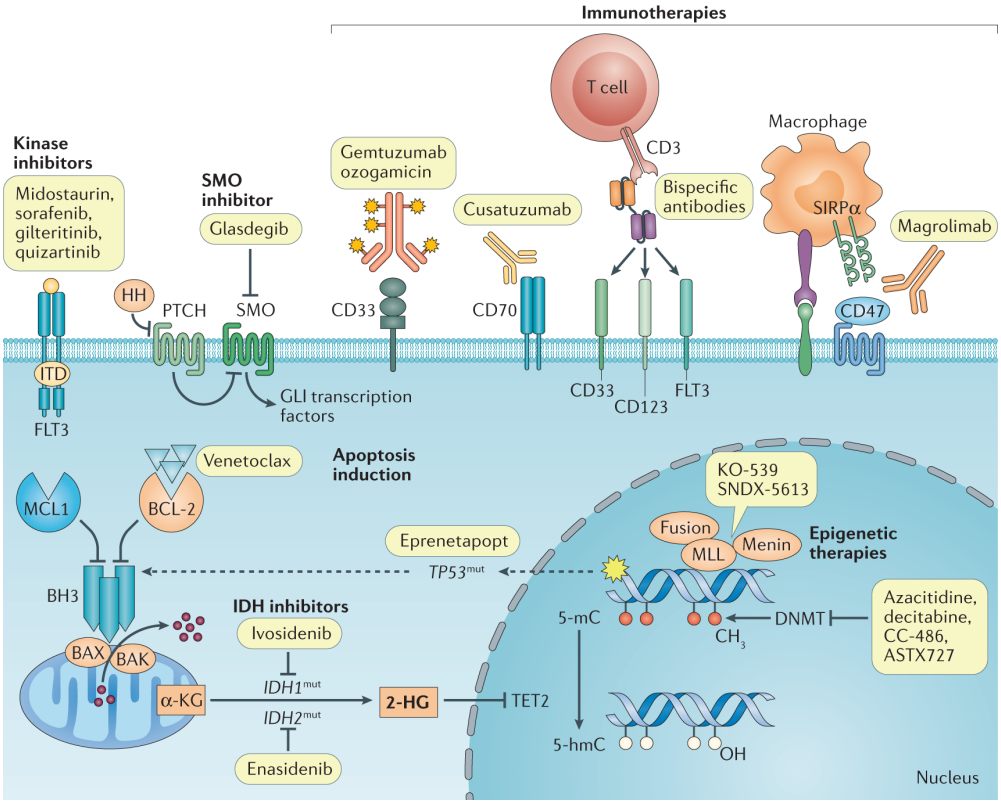

Figure 1.10 Targetable pathways for AML therapy. Inhibition of FLT3, IDH1, IDH2 and BCL2 are part of the precision medicine approach to AML. Other agents have recently entered clinical practice: epigenetic therapies, HH pathway and p53 inhibitors, and immunotherapies (from Döner *et al*., Nature Reviews Clinical Oncology, 2021).[205]

Targeting mutated proteins

FLT3, IDH1/IDH2, *KMT2A*, *NPM1* and *TP53* are among the most frequently mutated genes in AML.[63,92,141,206] The usage of small molecules inhibitors have shown a transient efficacy in relapsed and/or refractory AML when administered as single agents. However, their combination with standard therapies and novel agents allowed to circumvent both primary and acquired resistance, increasing the response rate.[207–211] In particular, these inhibitors can exert antileukemic activity (e.g. the FLT3 inhibitors midostaurin and gilternib[207] and the menin inhibitors in *KMT2A*-rearranged and *NPM1*-mutated AMLs[119]), induce cellular differentiation (e.g. ivosidenib and enasidenib, respectively IDH1 and IDH2 inhibitors,[208,209,212,213] the DOT1L inhibitor pinometostat in *KMT2A*-rearranged AMLs[214] and the inhibitors of the dihydroorotate dehydrogenase enzyme[215,216]) and cause cell cycle arrest and tumor apoptosis (e.g. eprenetapopt, a p53 inhibitor[210]).

Targeting immune evasion mechanisms

Hematological malignant cells are both poorly immunogenic and extremely immunosuppressive. Among immune cells, T cells and NK cells play a pivotal role in AML immunosurveillance. However, AML blasts can exploit immune evasion mechanisms to escape from immune system recognition.[217–220]

The most important immune evasion mechanism is represented by the expression, on leukemic blasts, of a series of ligands (PDL1, PDL2, galectin 9 and poliovirus receptor CD155) interacting with T cell co-inhibitory receptors, such as the cytotoxic T-lymphocyte associated protein 4 (CTLA4), the programmed cell death protein 1 (PD1), the T cell immunoglobulin and mucin domain 3 (Tim3), the T cell immune-receptor with Ig and ITIM domains (TIGIT) and the lymphocyte activating 3 (LAG3).[217] Targeting and blocking these inhibitory molecules may potentiate the anti-leukemic immune response.[218] Several clinical trials are ongoing to test the efficacy of anti-CTLA4 and anti-Tim3 antibodies and PD1/PDL1 and TIGIT/CD155 axis inhibition, alone or in combination with conventional chemo-, radio- or targeted therapy.[221]

Moreover, AML blasts express on their surface several antigens (e.g. CD33, CD123, CD70 and CD47) that are not expressed by HSCs and can be used as targets for antibody-mediated and cell-based immunotherapies.[194,222–225] Chimeric antigen receptor (CAR) T cells have been of limited clinical relevance in AML.[226] The main biological barrier limiting the use of CAR T cells in AML is represented by the absence of AML unique antigens, not shared with normal HSPCs and myeloid progenitors. Additionally, AML blasts can produce soluble

factors able to inhibit T cells proliferation, and they can evade the immune system through various immunosuppressive mechanisms, thus countering the therapeutic potential of CAR T cells.[227–229] In relapsed B-cell acute lymphoblastic leukemia the combination of PD1 inhibitors and CAR-T cells gave promising responses and improved CAR-T cell function and persistence, suggesting that the combination of immune check-point blockade may represent a way to overcome poor persistence and dysfunctions of CAR- T cells also in AML patients.[230] Furthermore, monoclonal antibodies, able to bind AML epitopes promoting cell death, have been tested to block the CD70-CD27 signaling pathway, crucial for AML growth, and CD47, a "*don't eat me*" molecule that inhibits macrophage phagocytosis.[224,225] Moreover, to potentiate immune cells recruitment, bispecific antibodies, recognizing both T cell (CD3) and blast (CD33 or CD123) epitopes, have been introduced.[222] Last, antibody-drug conjugates have been developed for both $CD33^+$ and $CD123^+$ AML.[223] All these immunotherapies are currently being tested in clinical trials.

Targeting anti-apoptotic mechanisms

Cancer cells frequently evade apoptosis through the overexpression of antiapoptotic proteins (BCL2 and MCL1) and downregulation of proapoptotic ones (BH3 and BAK/BAX).[231] In AML, BCL2 and MCL1 are often overexpressed leading to chemotherapy resistance. In order to increase the apoptotic rate of AML blasts, various strategies have been employed, such as the administration of proapoptotic molecules (e.g. BH3 mimetics such as obatoclax and navitoclax[232]) and the inhibition of the overexpressed antiapoptotic ones (e.g. venetoclax, a selective BCL2 inhibitor;[211,233] and MCL1 inhibitors[234]). To circumvent the development of therapy resistance, combined approaches using venetoclax and MCL1 inhibitors or BH3 mimetics or other drugs targeting AML survival pathways are under evaluation in clinical trials.[211,233,234]

Other strategies entail the targeting of signaling pathways essential for AML growth: 1) receptor tyrosine kinase (RTK) signaling pathways (c-Kit, FLT3 and TAM RTKs);[235–237] 2) Hedgehog (HH) proteins;[238] 3) c-Myc;[239] 4) DNA damage response;[240] and 5) epigenetic modification pathways.[241] In addition, since the BM niche provides a chemoprotective and anti-apoptotic environment for AML blasts and LSCs, their physical and/or molecular uncoupling from the niche could improve therapy response.[77,242,243]

Targeting LSCs

LSCs are largely considered one of the main culprits of therapy failure and relapse in AML. Indeed, these cells are able not only to survive to first line treatments but can also evolve

increasing the genetic and phenotypic heterogeneity at the time of relapse.[244] The identification of targetable LSC molecular features not shared with HSCs represents a strategy that can be exploited to achieve durable remission.

Although LSCs have some metabolic features in common with HSCs, their reliance on mitochondrial respiration (OXPHOS) and non-glucose energy sources can be therapeutically exploited, as well as their low ROS levels and high BCL2 expression.[190,233,245] However, despite the initial success of amino acid depletion in AML, some resistance occurred thanks to the metabolic plasticity of LSCs that are able to upregulate the oxidation of fatty acids and rescue OXPHOS. To overcome the high LSC adaptation abilities the combination of different metabolic therapeutic strategies is likely required.[190,198]

In addition to the aforementioned features, most LSCs are described to be in a state of quiescence/low cycling rate that can support their resistance to traditional chemo- and radiotherapy.[196]

Targeting quiescence

Traditionally, different strategies have been proposed to target dormant cells in solid tumors: 1) maintain cancer cells in a state of dormancy to prevent reactivation and metastatic relapse; 2) reawake dormant cancer cells to sensitize them to chemo- and radiotherapy; 3) target dormant cancer cells specific features to eradicate them.[146] To date, none of these approaches exerted significant results. However, targeting multiple stages of the dormant cancer cell life cycle (niche occupancy and adaptation, immune evasion and reactivation) may represent a strategy to prevent quiescence-related tumor relapse.[146]

In leukemia, several studies have been conducted with the aim of eliminating dormant LSCs.

First, mobilization of LSCs from the BM niche may break their state of dormancy while sensitizing them to chemotherapy. In AML mouse models, the administration of both granulocyte colony-stimulating factor (G-CSF) and cytarabine pushed quiescent LSCs to proliferate, leading to their successive elimination.[246] However, this therapeutic strategy did not improve patients outcome in clinical trials.[247] A phase I trial was conducted combining a CXCR4 antagonist together with decitabine: even if mobilization of LSCs was observed, the clinical benefits for patients were uncertain.[243]

Other attempts were made to force dormant LSCs to enter the cell cycle. In CML, combination therapy with Fbxw7 ablation and chemotherapy resulted in quiescent LSCs eradication and reduced CML relapse after therapy discontinuation.[248] Moreover, since

LSCs exhibit higher autophagy levels compared to their differentiated counterpart in CML, autophagy inhibitors were tested in transgenic mouse models. Interestingly, treatment with autophagy inhibitors led to reduced LSCs quiescence and drove myeloid expansion.[249]

In AML, the HH signaling pathways have been implicated in the maintenance of the LSCs population. Preclinical studies and a phase II clinical trial demonstrated that the HH inhibitor glasdegib reduced LSCs quiescence, sensitizing them to chemotherapy.[250,251] Last, Leichman and colleagues first correlated the presence of miR126 overexpression in AML with an increased fraction of quiescent, drug-resistant LSCs and an attenuated differentiation toward leukemic blasts.[44] Notably, miR126 inhibition exhausted LSCs while promoting normal HSCs expansion.[44,252]

Collectively these data strongly support the importance of targeting LSCs quiescence to achieve their eradication and a durable therapeutic response. However, the best approach and the optimal combination with other therapies in a clinical setting still need major efforts.

Chapter 2: Materials and Methods

2.1 MA9 AML mouse models

Mice were housed in a pathogen-free animal facility at the European Institute of Oncology. The procedures related to animal use have been communicated and have been approved by the Italian Ministry of Health.

MLL-AF9 (MA9) leukemia was generously provided by Dr Chi Wai So. This AML was obtained by MSCV-MLL-AF9-puro retroviral transduction and transformation assay of cKit$^+$ cells isolated from BM mononucleated cells, as previously described by Esposito *et al.*.[253] Briefly, cKit$^+$ BM cells were FACS isolated from wild-type (WT) C57BL/6-Ly5.1 mice, transduced by spinoculation with a retroviral vector expressing the MLL-AF9 oncogene, and serially re-plated in methylcellulose (MC) medium prior to injection into sub-lethally irradiated (5 Gy) C57BL/6J recipient mice.

For experiments performed in NOD-scid IL2Rgamma^{null} (NSG) mice (JAX stock #005557, the Jackson Laboratory)[254,255], the previously described MA9 AML was transduced by spinoculation with the pHIV-Luc-ZsGreen (plasmid #39196, Addgene) lentiviral vector, expressing both luciferase and the fluorescent protein ZsGreen, and injected into sub-lethally irradiated (5 Gy) C57/BL6J recipient mice for expansion.

Murine MA9 was characterized based on blasts immunophenotype and oncogene expression. Mice were sacrificed at the first signs of pain and leukemic blasts were isolated from BM and spleen, incubated in red blood cells (RBCs) lysis solution (for 1 L of purified water: 8.125 g NH_4Cl, 1 g $KHCO_3$ and 260 µl 0.5M EDTA) for 5 minutes on ice and stained with fluorochrome-conjugated antibodies against myeloid (Mac1, clone M1/70, PE-conjugated and Gr1, clone RB6-8C5, PeCy7-conjugated) and lymphoid (B220, clone RA3-6B2, PeCy7-conjugated and Cd3e, clone 145-2C11, PE-conjugated) markers, 1:100, 1 hour on ice, and analyzed by BD FACSCelesta™ cell analyzer (Becton Dickinson Bioscience). Quantitative polymerase chain reactions (qPCR), from blasts isolated from leukemic spleen, were performed according to standard techniques using primers specific for MLL-AF9 translocation (**Table 2.1**).

Blood smears were stained with May-Grünwald-Giemsa while bone marrow/spleen paraffin embedded samples were stained with hematoxylin-eosin, according to standard protocols, and used for AML diagnosis.

Table 2.1 qPCR primers used to check MLL-AF9 translocation.

Primer name	Sequence 5' -> 3'
MA9 forward	TGTGAAGCAGAAATGTGTGG
MA9 reverse	TGCCTTGTCACATTCACCAT

2.2 Validation experiments

2.2.1 Viral production

For validation experiments, single short hairpin RNAs (shRNAs) targeting candidate genes (*Socs2*, *Stat1* and *Sytl4*) were cloned into the pRSI16-U6-sh-UbiC-TagRFP-2A-Puro vector from Cellecta (plasmid # SVSHU616-L). We used shRNAs directed against Luciferase (Luc) (or empty vector -EV for experiments in NSG mice) as controls (**Table 2.2**).

Table 2.2 Target sequences of the shRNAs.

shRNA name	Sequence 5' -> 3'
Luc	ACCGGCTTCGAAATGTTTGTTTGGTTGTTAATATTCATAGCAACCAAACGAACATTTCGAAGTTTT
***Socs2* #1326**	ACCGGCTCGCCATTAACAAATGTATCGTTAATATTCATAGCGGTACATTTGTTAATGGCGAGTTTT
***Socs2* #1328**	ACCGGGCGAGAGACTTTGTCACATCAGTTAATATTCATAGCTGGTGTGGCAAAGTCTCTCGCTTTT
***Stat1* #1334**	ACCGGGCTGTTACTTTCCTAGATATTGTTAATATTCATAGCAATATCTGGGAAAGTAACAGCTTTT
***Stat1* #1337**	ACCGGGGACTGGAGTGTGAGTATTTGGTTAATATTCATAGCCAAATACTCGCACTCTAGTCCTTTT
***Sytl4* #1378**	ACCGGGCGAGAGTTTGGATAGCTATAGTTAATATTCATAGCTGTAGCTATCCAGACTCTCGCTTTT
***Sytl4* #1379**	ACCGGCGGAGATATTAGACCTTTCTTGTTAATATTCATAGCAAGAGAGGTCTAGTATCTCCGTTTT

In the pRSI16 lentiviral vector, shRNAs are cloned under the U6 promoter, while the puromycin resistance (PuroR) and the red fluorescent protein (TagRFP) are under the control of the UbiC promoter (**Figure 2.1**).

Figure 2.1 Cassette of Cellecta pRSI16 vector used to place *Socs2*, *Stat1* and *Sytl4* shRNAs.

For lentiviral production, the 2nd generation packaging vectors pMD2.G and pCMVdR8.2 were used. 293T cells were transfected using standard calcium phosphate precipitation. Briefly, 293T were plated in 20 cm dishes in DMEM (Lonza), 2 mM L-glutamine, 100 U/ml penicillin/streptomycin and 10% Fetal Bovine Serum (FBS) and transfected when 70%

confluence was reached. The DNA and the packaging vectors DNA were mixed directly with a concentrate solution of $CaCl_2$ in 1.25 ml of H20: 25 µg DNA, 10 µg pMD2.G, 15 µg pCMVdR8.2 and 153 µl 2M $CaCl_2$. This mixture was then added dropwise to a phosphate buffer (HBS) to form a fine precipitate. At the same time, 5 µl of 100 mM chloroquine were supplemented in each plate. After 10 min, the mixture was added to the 293T dishes. The medium containing lentiviral particles was collected 24, 48 and 72 hours after the transfection, and replaced with fresh medium. Lentiviral supernatant was filtered through a 0.2 µm Nalgene™ Rapid-Flow™ Sterile Disposable Filter Unit (ThermoFisher), concentrated by ultracentrifugation at 22000 rpm, 2h at 4°C with an Optima L-90K ultracentrifuge (Beckman Coulter) and stored at -80°C.

Lentiviral titer was evaluated by transducing 10^5 293T/well in 12-wells plates with serial dilution of the viral stock. 72h after infection, 293T were harvested and analyzed by BD FACSCelesta™ cell analyzer (Becton Dickinson Bioscience) for the percentage of $TagRFP^+$ cells. The viral titer was measured as transducing units per ml (TU/ml) with the following formula:[256]

$$\text{titer}\left(\frac{\text{TU}}{\mu}\right) = \frac{\text{number of target cells}\left(0.1 \times 10^6\right) * \left(\%\text{TagRFP}^+\text{cells}\right)}{\text{volume of added virus } (\mu\text{l})}$$

2.2.2 AML blasts transduction and sorting

Leukemic MA9 blasts were maintained in Iscove's Modified Dulbecco's Medium (IMDM, Lonza), 2 mM L-glutamine, 25% Fetal Calf Serum, 25% Horse Serum, 100 U/ml penicillin/streptomycin, $1x10^6$ M hydrocortisone, $5x10^5$ M ß-mercaptoethanol, 10 ng/ml interleukin 3 (IL3), 10 ng/ml interleukin 6 (IL6) and 50 ng/ml SCF (Peprotech). Cells were cultured in a humidified chamber at 37 °C and 5% CO_2.

Blasts were seeded in 24-wells plates in the presence of 5 µg/ml of polybrene and then infected with lentiviral particles (MOI=10) by spinoculation at 2500 rpm, for 90 min at room temperature (RT). In order to dilute polybrene, 4 hours after spinoculation, one volume of fresh medium was added to each well. Infected blasts were FACS sorted 72 hours after transduction as $TagRFP^+$ cells using the BD FACSJazz™ cell sorter (Becton Dickinson Bioscience).

2.2.3 RNA reverse-transcription and RT-qPCR

RNA was extracted from $TagRFP^+$ sorted cells using PicoPure™ RNA Isolation Kit (ThermoFisher) or Quick-RNA™ Miniprep Kit (Zymo Research), based on the number of

available cells, according to manufacturer protocols. 0.1-1 µg of total RNA was reverse-transcribed using ImProm-II™ Reverse Transcriptase kit (Promega). RNA was first incubated with random primers (0.5 µg/reaction) at 70°C for 15 minutes and then immediately placed on ice. The following mix was then added:

ImProm-II™ 5X reaction buffer	10 µl
$MgCl_2$ 25 mM	5 µl
dNTPs (10 mM each)	2.5 µl
recombinant RNAse inhibitor	1.5 µl
ImProm-II™ Reverse Transcriptase	1 µl
Nuclease-free water	to 50 µl

The reaction was incubated at 42°C for 60 minutes and then at 70°C for 15 minutes. Complementary DNA (cDNA) was stored at -20°C.

For gene expression analysis, RT-qPCR was performed using 10-20 ng of cDNA, 0.2 µM of both primers and 10 µl of FAST SYBR™ Green Master Mix (Thermofisher) in a final volume of 20 µl per reaction in 96-wells plates. Fluorescence accumulation during qPCR reaction was detected on a ViiA 7 Real-Time PCR Detection System (Thermofisher). Relative mRNA quantification was performed by comparative ΔΔCt method using *Tbp* for normalization. Primers used are listed in the **Table 2.3.**

Table 2.3 qPCR primers used to check gene silencing.

Primer name	Sequence 5' -> 3'
***Socs2* forward**	TGAAGCATGAGCCTTTCCTC
***Socs2* reverse**	GCAGACACTGTCACCCAC
***Stat1* forward**	GCCGAGAACATACCAGAGAATC
***Stat1* reverse**	GATGTATCCAGTTCGCTTAGGG
***Sytl4* forward**	AATGGTGTGAGGCTGGAAG
***Sytl4* reverse**	ACCACTTCGCCATTACTGATC
***Tbp* forward**	TAATCCCAAGCGATTTGCTG
***Tbp* reverse**	CAGTTGTCCGTGGCTCTCTT

2.2.4 *In vivo* validation

1-2x10^5 $TagRFP^+$ sorted MA9 blasts were intravenously (i.v.) injected into sub-lethally (5 Gy) irradiated C57BL/6J 8-12 weeks old mice. The level of engraftment was monitored once

a week by FACS evaluation of the percentage of TagRFP$^+$ blasts (CD45.1$^+$) in peripheral blood (PB). In details, PB obtained from the tail vein of the animals was incubated twice in RBCs lysis solution for 5 minutes on ice. The obtained white blood cells (WBCs) were subsequently stained with BB515-conjugated anti-CD45.1 antibody (clone A20, Thermofisher) at a concentration of 1:100, 1 hour on ice. Samples were then acquired by BD FACSCelesta™ cell analyzer (Becton Dickinson Bioscience) and analyzed using the version 10 of the FlowJo software (Becton Dickinson Bioscience). Latency in leukemia development was monitored and mice were sacrificed when moribund, according to the animal facility guidelines. Leukemic infiltration was assessed in PB, BM, spleen and liver by FACS evaluation of the percentage of TagRFP$^+$ blasts (CD45.1$^+$), as previously described.

To evaluate the level of target genes knock-down (KD) at the moment of sacrifice, TagRFP$^+$ and TagRFP$^-$ blasts (CD45.1$^+$) were FACS sorted and their RNA was extracted an reverse-transcribed as reported in the section 2.2.3. A RT-qPCR was performed to evaluate *Socs2*, *Stat1* and *Sytl4* expression levels as described in the section 2.2.3.

2.3 Analyses of the effects of *Socs2* and *Stat1* silencing on cell cycle distribution of MA9 blasts *in vivo*

10^5 TagRFP$^+$ sorted MA9 blasts were i.v. injected into sub-lethally (5 Gy) irradiated C57BL/6J 8-12 weeks old mice. Silencing efficiency was checked at sorting time, 72h post transduction, through a RT-qPCR (see the section 2.2.3). The level of engraftment was monitored once a week by FACS evaluation of the percentage of TagRFP$^+$ blasts (CD45.1$^+$) in PB, as described in the section 2.2.4. Animals were sacrificed either at specific time points post transplantation (e.g. *Socs2* experiment) either when a specific level of engraftment in the PB was reached (e.g. *Stat1* experiment).

For *in vivo* experiments aimed at evaluating the cell cycle status of MA9 blasts, total BM cells were isolated by grinding bones from posterior limbs, vertebral column and sternum. Single cell suspensions were incubated in RBCs lysis solution for 5 minutes on ice. Cells were washed in 1x PBS and 10^7 cells were used for subsequent staining. Cells were then fixed in BD Cytofix/Cytoperm™ buffer for 30 minutes on ice, washed with Perm/Wash™ buffer (P/W) and re-fixed in BD Cytofix/Cytoperm™ plus buffer for 10 minutes on ice. Last, cells were washed with P/W and incubated with BD Cytofix/Cytoperm™ buffer for 5 minutes on ice and washed again. Fixed cells were then stained with PeCy7-conjugated anti-

Ki67 antibody (clone B56, Becton Dickinson Bioscience), 1:40, and anti-cleaved Caspase3 antibody (Cell Signaling), 1:200, 1 hour on ice. Cells were washed with P/W and incubated with secondary Alexa488-conjugated anti-rabbit antibody (Jackson Immuno Research), 1:100, 1 hour on ice. Finally, cells were washed with P/W and re-suspended in 1 ml of 1x PBS containing DAPI (5 µg/ml) and incubated overnight at 4°C. Samples were then acquired by BD FACSCelesta™ cell analyzer (Becton Dickinson Bioscience) and analyzed using the version 10 of the FlowJo software (Becton Dickinson Bioscience).

2.4 Analyses of the effects of *Socs2*- and *Stat1* silencing on the clonogenic activity, cell cycle distribution and survival of MA9 blasts *in vitro*

2.4.1 Colony-forming efficiency assay

500 TagRFP$^+$ sorted MA9 blasts were seeded in MethoCult M3434 (StemCell Technologies) in 35 mm dishes (Corning®). One week after plating, colony formation was manually quantified through an inverted microscope (DMi1, Leica). In addition, the number of TagRFP$^+$ colonies was assessed with a EVOS™ FL fluorescence microscope (Invitrogen).

2.4.2 Cell proliferation, apoptosis and cell cycle assays

MA9 leukemic blasts were infected with *Socs2* and *Stat1* shRNAs, with Luc as control, and sorted as described in the section 2.2.2. Sorted TagRFP$^+$ cells, once *Socs2* and *Stat1* down-regulation was confirmed by RT-qPCR (see the section 2.2.3), were seeded in a 6-wells plate at a density of 4x10^5 cells per ml in 3 ml of medium per well in duplicate. The proliferation of these blasts was assessed through manual counting performed every 24h for one week. To determine the viability of the cells over time, 0.4% Trypan Blue Solution (Thermofisher Scientific) was used. In detail, cell clusters in the culture were disrupted by gently pipetting up and down and a 10 µl sample was taken daily and mixed 1:1 with Trypan Blue. A total volume of 10 µl was loaded into a hemocytometer (Marienfeld Superior) and both live and death cells were counted in nine squares (0.1 mm^3) to determine the number of cells per ml.

To evaluate the level of counterselection of TagRFP$^+$ blasts over time, the day of sorting and 6 days later 500.000 cells per sample were harvested to be FACS analyzed. Moreover, 3 days post sorting, 500.000 blasts per sample were also taken for Annexin V / 7-ADD staining to evaluate the percentage of early apoptotic and necrotic cells. Cells were washed twice in 100 µl of Annexin V buffer (1M HEPES, 5M NaCl, 1M $MgCl_2$ 50mM KCl in H_2O) and stained in 50 µl of the same buffer with FITC-conjugated anti-Annexin V antibody

(Biolegend) at a concentration of 1:50, 1 hour at room temperature. After the staining, cells were incubated for 10 minutes with 10 µl of 7-ADD solution (Becton Dickinson Bioscience) and then FACS analyzed to evaluate the percentage of early apoptotic (Annexin V^+ / 7-ADD^-) and necrotic (Annexin V^+ / 7-ADD^+) $TagRFP^+$ blasts.

Lastly, 3 and 8 days from the beginning of the growth curve, $2x10^6$ blasts per sample were harvested for cell cycle and Ki67 staining (see the section 2.3) and to quantify by RT-qPCR the level of target genes KD over time (see the section 2.2.3).

2.5 Single cell RNA sequencing on $TagRFP^+$ *Socs2*/*Stat1* KD blasts

2.5.1 Single-cell library preparation and sequencing

$TagRFP^+$ blasts were FACS sorted from the BM of the mice used in the *Socs2* time course (31 days post transplantation) experiment and diluted in 1x PBS 0.04% BSA, according to the ChromiumTM Single Cell 3' v2 protocol. A 10X Genomics Chromium machine was used to capture ~$5x10^3$ single-cells from each mouse into Gel Bead-In-EMulsions (GEMs) and cDNA was prepared according to the manufacturer protocol. The libraries were prepared using the Chromium Single Cell 3′Reagent Kits (v2): Single Cell 3′Library & Gel Bead Kit v2 (PN-120237), Single Cell 3′Chip Kit v2 (PN-120236) and i7 Multiplex Kit (PN-120262) (10x Genomics) and following the Single Cell 3′Reagent Kits (v2) User Guide (manual part no. CG00052 Rev C). Libraries were sequenced on NovaSeq 6000 Sequencing System (Illumina) 1 with an asymmetric paired-end strategy (28 and 91 bp read length for R1 and R2 mate respectively) with a coverage of about 50,000 reads/cell.

2.5.2 ScRNAseq data analysis

Sequencing results were demultiplexed and converted to FASTQ format using Illumina bcl2fastq software. Sample demultiplexing, barcode processing and single-cell 3' gene counting were obtained using a custom pipeline. The cDNA insert was aligned to the GRCm39 (mm39) reference genome and associated with a gene using the GENCODE gtf file (downloaded from: ftp.ebi.ac.uk/10/pub/databases/gencode/Gencode_mouse/release_M16/). Only confidently mapped, non-PCR duplicates with valid barcodes and unique molecular identifiers were used to generate the gene-by-cell matrix. Basing on the distribution of different parameters, we removed cells with fewer than 1,500 transcripts, more than 27,000 transcripts, less than 300 expressed genes, and more than 10% mitochondrial gene expression and genes expressed in

fewer than 5 cells. After such quality filtering, we obtained 5,119 cells for Luc and 1,945 cells for *Socs2*. For each cell, expression of each gene was normalized to the sequencing depth of the cell using the scran R package and log-transformed. Number of UMI per cell was regressed out of the data as a potential confounder, using the Seurat R package. Further analyses (including identification of highly variable genes, dimensionality reduction, Louvain algorithm for unsupervised clustering and differential expression analysis) were performed using the Seurat R package analyzing both single and merged samples.

2.6 RT-qPCR to *in vitro* evaluate the expression levels of immune check-point molecules

MA9 leukemic blasts were infected with *Socs2* and *Stat1* shRNAs, with Luc as control, and sorted as described in the section 2.2.2. Sorted TagRFP^{+} cells, once *Socs2* and *Stat1* downregulation was confirmed by RT-qPCR (see the section 2.2.3), were also analyzed for the expression of immune check-point molecules (Cd24a, LSGAL9 and VISTA). Primers used are listed in the **Table 2.4** and were designed through the Universal Probe Library (Roche Molecular Systems, Inc).[257]

Table 2.4 qPCR primers used to check the expression of immune check-point molecules.

Primer name	Sequence 5' -> 3'
***Cd24a* forward**	CTGGGGTTGCTGCTTCTG
***Cd24a* reverse**	CAACAGATGTTTGGTTGCAGTAA
***LSGAL9* forward**	GCATTGGTTCCCCTGAGATA
***LSGAL9* reverse**	TCCAGTAAAGGGGATGATCG
***VISTA* forward**	CCACATGCATGGCGTCTA
***VISTA* reverse**	AGGATTCCCACGATGCAG

2.7 Macrophage depletion *in vivo*

2.7.1 Macrophage depletion in immunocompromised animals using an anti-Cd115 antibody

To systematically deplete macrophages, an anti-colony stimulating factor 1 (CSF-1) receptor antibody (clone AFS98, BioXCell), a rat monoclonal anti-murine Cd115 antibody (immunoglobulin G 2a) that inhibits CSF-1-dependent cell growth by blocking the binding

of CSF-1 to its receptor, was used. As a control, an isotype-matched rat anti-trinitrophenol antibody (clone 2A3, BioXCell) was employed. Both the antibodies were administered intraperitoneally (i.p.) weekly starting 5 days after the i.v. injection of NSG mice with 10^5 ZsGreen$^+$/TagRFP$^+$ sorted MA9 blasts infected with Luc or *Socs2* (#1326) shRNA constructs, at doses of 2 mg/mouse, as previously described.[258] Silencing efficiency was checked 72h post infection by RT-qPCR (see the section 2.2.3). The effectiveness of macrophage depletion was tested three days after anti-Cd115 and anti-trinitrophenol administration on PB WBCs (obtained as described in the section 2.2.4) by FACS measuring the percentage of CD115$^+$ cells (gated ZsGreen$^-$) after the staining with a BV421-conjugated anti-Cd115 antibody (clone T38-320, Becton Dickinson Bioscience), 1:100, 1 hour on ice. Latency in leukemia development was monitored and animals were sacrificed when moribund, according to the animal facility guidelines. Leukemic infiltration was assessed in peripheral blood, BM, spleen and liver by FACS evaluation of the percentage of TagRFP$^+$ blasts (ZSGreen$^+$) as previously described (see the section 2.2.4) and 10^7 BM-derived TagRFP$^+$ blasts were collected for cell cycle and Ki67 staining (see the section 2.3).

2.7.2 Macrophage depletion in immunocompetent animals using clodronate liposomes

To systematically deplete macrophages *in vivo*, clodronate encapsulated in liposomes was used in C57BL/6J mice. Control liposomes contained phosphate-buffered saline (PBS) only. Each animal received 0.01 ml/g (5 mg of clodronate per 1ml of the total suspension volume) of clodronate liposomes or control liposomes via i.p. injection,[259] 1 week after the i.v. transplantation of C57BL/6J mice with 10^5 TagRFP$^+$ sorted MA9 blasts infected with Luc or *Socs2* (#1326) shRNA constructs. The clodronate and control liposomes were obtained from Liposoma, research liposomes (Amsterdam, The Netherlands). Silencing efficiency was checked 72h post infection by RT-qPCR (see the section 2.2.3). The effectiveness of macrophage depletion was tested one week after control and clodronate liposomes administration on PB WBCs (obtained as described in the section 2.2.4) by FACS measuring the percentage of CD115$^+$ cells (gated Cd45.1$^-$) after the staining with a BV421-conjugated anti-Cd115 antibody (clone T38-320, Becton Dickinson Bioscience), 1:100, 1 hour on ice. Latency in leukemia development was monitored and animals were sacrificed when moribund, according to the animal facility guidelines. Leukemic infiltration was assessed in peripheral blood, BM, spleen and liver by FACS evaluation of the percentage of TagRFP$^+$ blasts (CD45.1$^+$) as previously described (see the section 2.2.4) and 10^7 BM-derived TagRFP$^+$ blasts were collected for cell cycle and Ki67 staining (see the section 2.3).

To evaluate the level of macrophage depletion at the time of sacrifice, single cell suspensions obtained from the liver were incubated in RBCs lysis solution for 5 minutes on ice. Cells were washed in 1x PBS and 10^6 cells were used for subsequent staining. First, a staining of the surface molecules with FITC-conjugated anti-Cd11b (clone M1/70, Becton Dickinson Bioscience), APC-conjugated anti-F4-80 (clone T45-2342, Becton Dickinson Bioscience) and BV510-conjugated anti-Cd45.1 (clone A20, Becton Dickinson Bioscience) antibodies, 1:100, 1 hour on ice, was performed. Cells were then fixed in BD Cytofix/Cytoperm™ buffer for 30 minutes on ice, washed with Perm/Wash™ buffer (P/W) and re-fixed in BD Cytofix/Cytoperm™ plus buffer for 10 minutes on ice. Last, cells were washed with P/W and incubated with BD Cytofix/Cytoperm™ buffer for 5 minutes on ice and washed again. Fixed cells were then stained with BV421-conjugated anti-Cd68 (clone Y1/82A, Becton Dickinson Bioscience), 1:100, 1 hour on ice. Cells were washed with P/W and re-suspended in 1 ml of 1x PBS. The percentage of macrophages was evaluated by BD FACSCelesta™ cell analyzer (Becton Dickinson Bioscience) as $CD11b^+/F4\text{-}80^+/CD68^+$ cells (gated in the $CD45.1^-$ population).

Chapter 3: Preliminary data and rational of the project

3.1 Preliminary Data

As part of a more general project aimed at defining the role of quiescence in the maintenance of LSCs self-renewal potential in AMLs, a prior Ph.D. student in our group (Dr. Giulia De Conti) investigated the transcriptional changes induced by the expression of AML-associated oncogenes (NPMc$^+$, PML-RARα and MLL-AF9) in HSCs. A global gene expression analysis of LT-HSCs obtained from the BM of pre-leukemic mouse models was performed. Additionally, a previously reported transcriptional profile of MLL-AF9 (MA9) pre-leukemic LSK cells (Lin$^-$, Sca1$^+$ and cKit$^+$) derived from MA9 KI mice, was used.[260] Unexpectedly, gene set enrichment analyses of genes differentially regulated upon oncogene expression revealed, in all the three datasets, upregulation of a quiescence-related gene signature (**Figure 3.1**), suggesting that enforcement of quiescence might be a selectable leukemia trait.

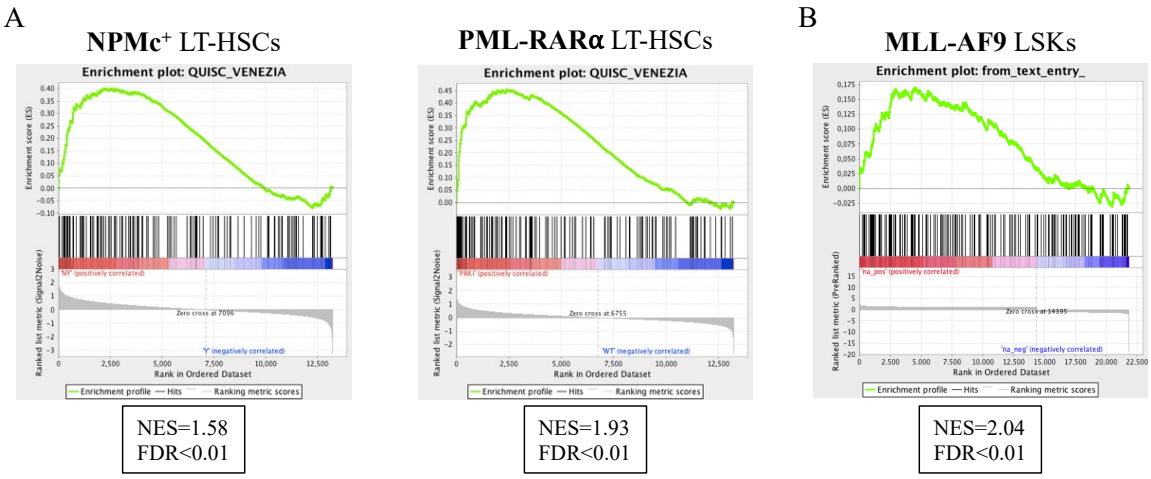

Figure 3.1 NPMc$^+$, PML-RARα and MA9 expression in pre-leukemic HSCs enforced a transcriptional program promoting quiescence. Gene Set Enrichment Analysis (GSEA) plots demonstrating enrichment levels of a quiescent-related gene signature in **A.** NPMc$^+$ and PML-RARα long term HSCs (LT-HSCs) and **B.** MA9 pre-leukemic LSK (Lin$^-$, Sca1$^+$ and cKit$^+$) compared to WT LT-HSCs.

To test this hypothesis, an *in vivo* reverse genetic screening, aimed at identifying leukemia dependencies of quiescence-related genes, was performed using a shRNA library of ~100 genes known to induce cell cycle restriction in HSCs and HSPCs.[27] As a model, MA9 AML was chosen due to its relatively higher frequency of leukemia initiating cells (1:471;

unpublished data), as compared to the other models, sufficient to cover the library complexity. Analyses of the shRNAs found depleted during *in vivo* AML growth led to the identification of 8 quiescence related genes (*Socs2*, *Stat1*, *Sytl4*, *Gfi1*, *Tie1*, *Hoxa5*, *Esr2* and *Brd4*), potentially involved in quiescence induction and AML maintenance.

3.2 Rational of the research project

The general aim of this research project is to investigate the role of quiescence in the maintenance of the transformed phenotype in AML. In particular, understanding the molecular mechanisms underlying oncogene-induced quiescence might shed light on key pathways in AML development, maintenance and response to therapies, thus providing the basis for innovative anti-leukemic strategies.

The specific aims of my project stem from the preliminary data obtained in our group, described in the section 3.1 and include the biological validation of three of the genes identified by the *in vivo* shRNA screening (*Socs2*, *Stat1* and *Sytl4*), which role in the maintenance of AML quiescence was largely unknown, with respect to: 1) their role in supporting leukemia growth/maintenance, by testing the effect of specific shRNAs on leukemia growth *in vivo*; and 2) their function in the regulation of leukemia cells quiescence, including LSCs and bulk blasts, both *in vivo* and *in vitro*.

Once validated biologically, the molecular mechanisms underlying their effects, starting from the analysis of cell phenotypes *in vivo*, will be dissected by scRNAseq of silenced and control blasts.

Chapter 4: Results

4.1 Silencing of *Socs2*, *Stat1* or *Sytl4* prevented MA9 leukemia outgrowth *in vivo*

Three of the 8 genes identified by the shRNA screening (*Socs2*, *Stat1* and *Sytl4*) were validated by analyzing the effects of their silencing on leukemia growth *in vivo*, using the same model system. MA9 blasts were transduced with lentiviruses expressing the red fluorescent protein (TagRFP), as selectable marker, and shRNAs targeting *Socs2* (#1326 or #1328), *Stat1* (#1334 or #1337), *Sytl4* (#1378 or #1379), or Luciferase (*Luc*) as control. TagRFP^{+} cells were FACS sorted 72 hours after infection to obtain a pure population of shRNA- or Luc-expressing blasts. RT-qPCR on sorted blasts confirmed silencing of the targeted genes, as compared to the Luc control (**Figure 4.1**).

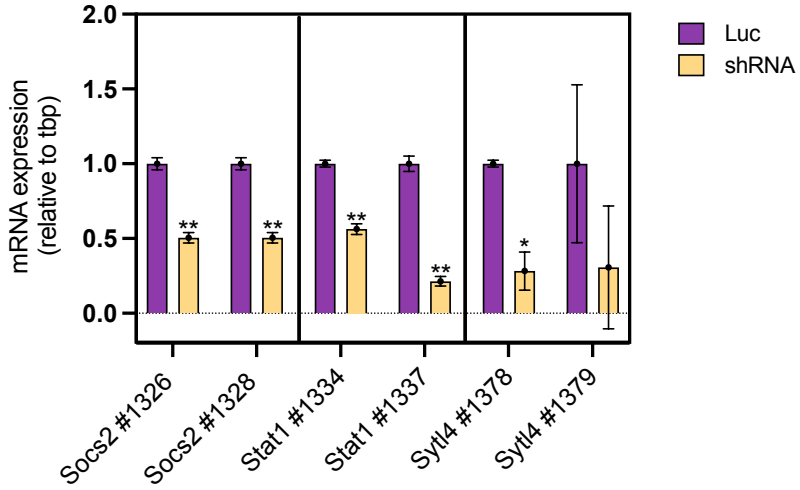

Figure 4.1 Transduction with shRNAs specific for *Socs2*, *Stat1* and *Sytl4* reduced target gene expression in AML blasts. Socs2, Stat1 and Sytl4 mRNA levels were evaluated by RT-qPCR analysis in *Socs2*-, *Stat1*- and *Sytl4*-interfered or control (Luc) MA9 blasts. Results were normalized to the *Tbp* housekeeping gene. Error bars represent the standard deviation of two technical replicates (*p<0.05 and **p<0.01, t-test).

2x10^{5} TagRFP^{+} sorted blasts transduced with *Socs2*, *Stat1*, *Sytl4* or Luc shRNAs were then intravenously (i.v.) injected into sub-lethally irradiated (5Gy) C57BL/6J recipient mice. Luc mice succumbed to AML with the same latency observed for non-infected MA9 cells, confirming that lentiviral infection does not alter MA9 leukemia growth *in vivo* (**Figure 4.2, A**). Silencing of the targeted genes, instead, significantly prolonged the survival of leukemic mice, as compared to controls (median survival: Luc=36.5 days; *Socs2*#1326=42.5 days;

Socs2#1328=59.5 days; *Stat1*#1334=59 days; *Stat1*#1337=54 days; *Sytl4*#1378=77 days and *Sytl4*#1379=58 days) (**Figure 4.2, B-D**).

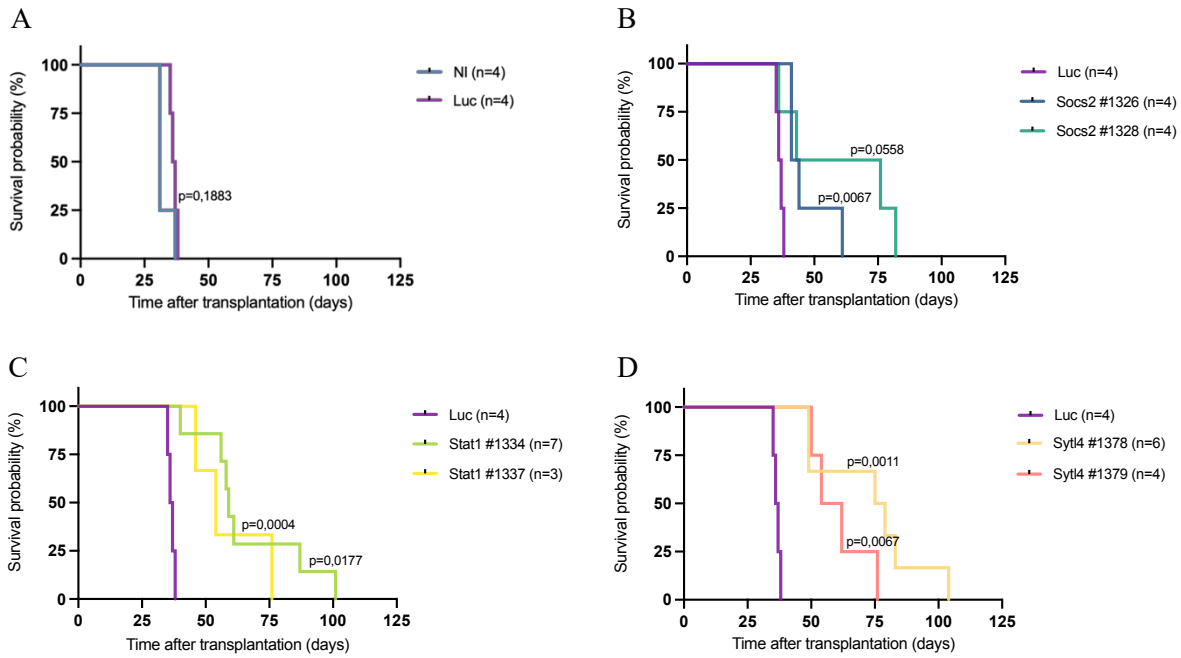

Figure 4.2. Delayed *in vivo* growth of AML blasts transduced with of *Socs2*, *Stat1* or *Sytl4* shRNAs. A. Kaplan–Meier overall survival curves in mice transplanted with non-infected (N=4) or Luc-shRNA infected (N=4) blasts. Statistical significance was calculated using the logrank (Mantel Cox) test. **B-D.** Kaplan–Meier overall survival curves in mice transplanted with *Socs2*- (#1326 N=4 and #1328 N=4) (B), *Stat1*- (#1334 N=7 and #1337 N=3) (C), or *Sytl4*- (#1378 N=6 and #1379 N=4) (D) and Luc- (N=4) interfered blasts as control group. Statistical significance of differences between shRNA-interfered and control groups was calculated using the logrank (Mantel Cox) test (values are given for each comparison in each panel) (*p<0.05, **p<0.01 and ***p<0.001).

Socs2, *Stat1* or *Sytl4* silencing, however, did not modify the penetrance of the disease, as shown by the finding that all the interfered animals, like the controls, eventually died of leukemia, with massive infiltration of the peripheral blood (PB), bone marrow (BM) and spleen (**Figure 4.3, A-B**).

To investigate whether leukemia outgrowth in *Socs2*-, *Stat1*- and *Sytl4*-shRNA samples was due to a partial effect of the interference or the selection of revertant cells, we analyzed the frequencies of TagRFP$^+$ blasts in the PB, BM and spleen of leukemic animals sacrificed at late stages of the disease (≥80% blast infiltration of the PB in all samples). Blasts were identified based on the expression of the CD45.1$^+$ congenic marker. Strikingly, while CD45.1$^+$ blasts were almost all TagRFP$^+$ in Luc-shRNA control samples (>95%), they were

highly depleted of TagRFP$^+$ cells (<5%) in all *Socs2*-, *Stat1*- or *Sytl4*-shRNA samples from all the analyzed compartments (PB, BM and spleen) (**Figure 4.3, C**).

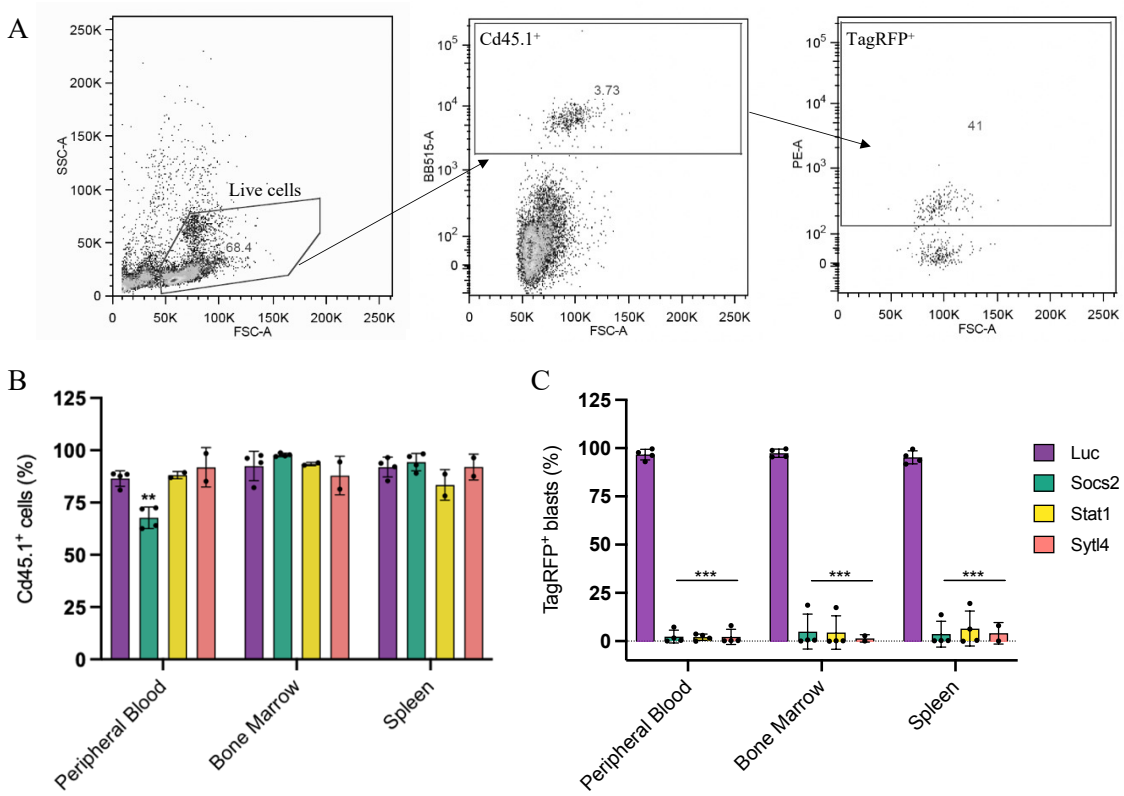

Figure 4.3 MA9 blasts harboring *Socs2*, *Stat1* and *Sytl4* shRNA were counterselected during leukemia growth *in vivo*. A. Representative FACS gating schemes for the analysis of TagRFP$^+$ blasts (Cd45.1$^+$) in the PB, BM and spleen of leukemic mice at the time of sacrifice. **B.** Percentage of CD45.1$^+$ cells isolated from PB, BM and spleen of leukemic mice at the time of sacrifice. Error bars represent the standard deviation of 4 animals (**p<0.01, t-test). **C.** Percentage of TagRFP$^+$ blasts (CD45.1$^+$) isolated from PB, BM and spleen of leukemic mice at the time of sacrifice. Error bars represent the standard deviation of 4 animals (***p<0.001, t-test).

Consistently, we found comparable levels of mRNA for each of the interfered target genes in the TagRFP$^-$ BM-derived blasts of *Socs2*-, *Stat1*- or *Sytl4*-shRNA samples, as compared to the TagRFP$^+$ BM-derived blasts of Luc-shRNA control mice (**Figure 4.4, A-C**).

Together, these results demonstrated that silencing of *Socs2*, *Stat1* or *Sytl4* expression in MA9 blasts prevented leukemia outgrowth *in vivo*. The only-modest effect on mice survival correlated with the strong counterselection of TagRFP$^+$ shRNA-expressing blasts during leukemia growth, probably due to the emergence of revertant phenotypes and/or outgrowth of residual TagRFP$^-$ blasts (CD45.1$^+$) present in the initial leukemic population.

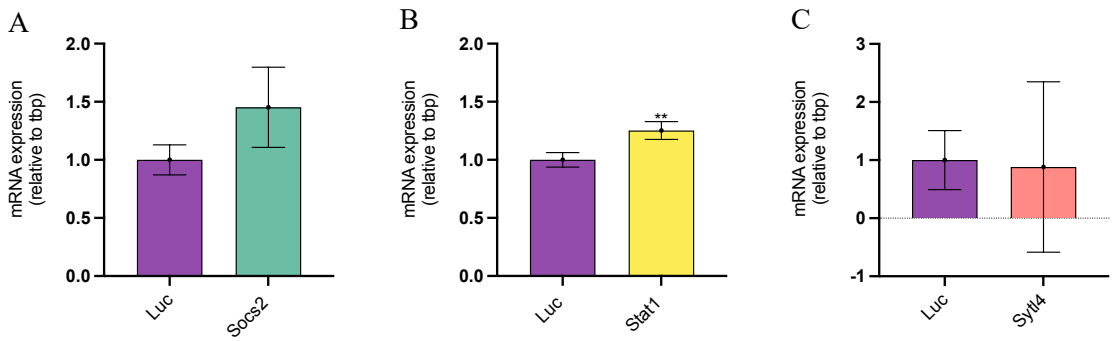

Figure 4.4 MA9 blasts harboring *Socs2*, *Stat1* and *Sytl4* shRNA were counterselected during leukemia growth *in vivo*. A-C. Socs2 (B), Stat1 (C) and Sytl4 (D) mRNA levels evaluated by RT-qPCR analysis in sorted BM-derived blasts of control (TagRFP$^+$) and *Socs2*, *Stat1*, *Sytl4* (TagRFP$^-$) animals. Results were normalized to the *Tbp* housekeeping gene. Error bars represent the standard deviation of two technical replicates (**p<0.01, t-test).

4.2 Analyses of the effects of *Socs2* and *Stat1* silencing on cell cycle distribution of MA9 blasts *in vivo*

4.2.1 *Socs2* silencing prevented the progressive accumulation of cell cycle restricted blasts in growing leukemia and induced apoptosis.

To evaluate whether silencing of *Socs2* affects the cell cycle status of growing blasts *in vivo*, MA9 cells were infected with TagRFP-lentiviruses expressing *Socs2*-shRNA (#1326) or Luc-shRNA, FACS sorted to isolate TagRFP$^+$ blasts and i.v. injected in C57BL/6J mice (10^5 cells/mouse). Silencing efficiency was checked 72h post infection (**Figure 4.5, A**) and mice sacrificed at different time points post transplantation (14, 19, 24 and 31 days) for downstream analyses.

Engraftment of injected leukemia was monitored by measuring the percentage of TagRFP$^+$/CD45.1$^+$ blasts in the BM of recipient mice. At days 14, 19 and 24 post-injection TagRFP$^+$ *Socs2*-interfered blasts showed levels of engraftment comparable to that of control blasts in the BM (~5-10%; **Figure 4.5, B**). At day 31, instead, when engraftment increased significantly in the control leukemia (~40%), percentage of *Socs2*-shRNA TagRFP$^+$ silenced blasts remained low (~5%; **Figure 4.5, B**).

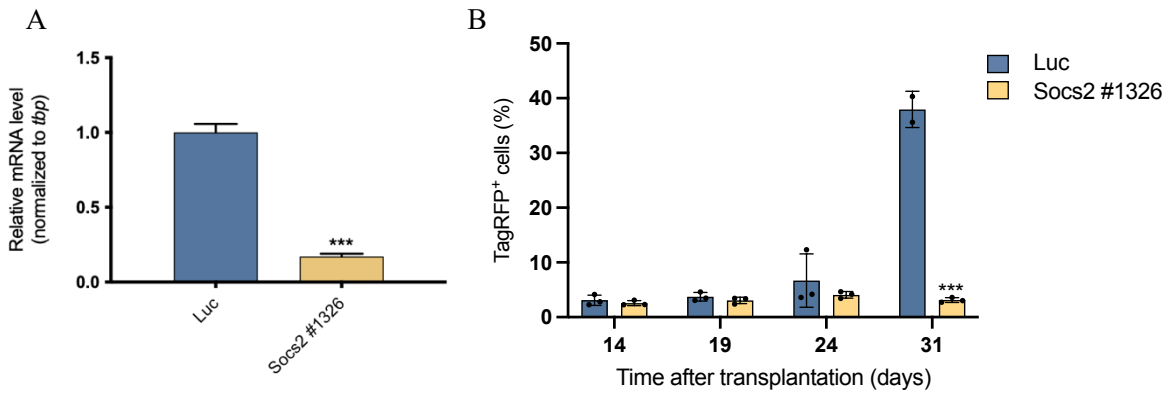

Figure 4.5 RT-qPCR confirmed *Socs2* silencing at the time of transplantation and only control MA9 leukemia engrafted in immunocompetent mice. A. Socs2 mRNA levels were evaluated by RT-qPCR analysis in *Socs2*-interfered and control MA9 blasts at 72h post infection, prior to transplantation in C57BL/6J mice. Results were normalized to the *Tbp* housekeeping gene. Error bars represent the standard deviation of two technical replicates (***p<0.001, t-test) **B.** Percentage of TagRFP$^+$ *Socs2*-interfered and Luc-shRNA control MA9 blasts evaluated in the BM by FACS at different time points post transplantation. Error bars represent the standard deviation of three animals (***p<0.001, t-test).

TagRFP$^+$ BM cells were then analyzed for cell cycle (by anti-Ki67 and DAPI staining) and apoptosis (using antibodies against cleaved caspase3).

Luc-shRNA control blasts showed a relatively high proportion of cycling cells at 14 days after injection (S+G2M = ~28%), which progressively decreased during leukemia outgrowth (~23%, ~13% and 8% at days 19, 24 and 31, respectively). Surprisingly, we observed a progressive increase in the fraction of G0/quiescent blasts (DAPI=2n and Ki67$^-$), which went from ~8% at day 14 to ~60% at day 31, paralleled by decreasing proportions of G1 cells (DAPI=2n and Ki67$^+$; from ~60% at day 14 to 30% at day 31) (**Figure 4.6, A**). The existence of a variable fraction of quiescent blasts in AML, including functional LSCs, is known. However, the role of quiescent bulk-blasts (e.g. non-LSCs) in the maintenance of leukemia growth, if any, is unclear.

Strikingly, in mice injected with *Socs2*-interfered MA9 blasts, instead, the fraction of quiescent AML cells did not increase and remained markedly low in all the analyzed time points (5-15%) (**Figure 4.6, A**). Overall, the fraction of cycling cells was higher than in control cells and persisted during leukemia outgrowth (~20-25% of S-G2M cells). Finally,

we observed increased frequency of apoptotic cells (10-15% of cleaved caspase3$^+$ cells), that was particularly evident at 24 days post transplantation (**Figure 4.6, B**).

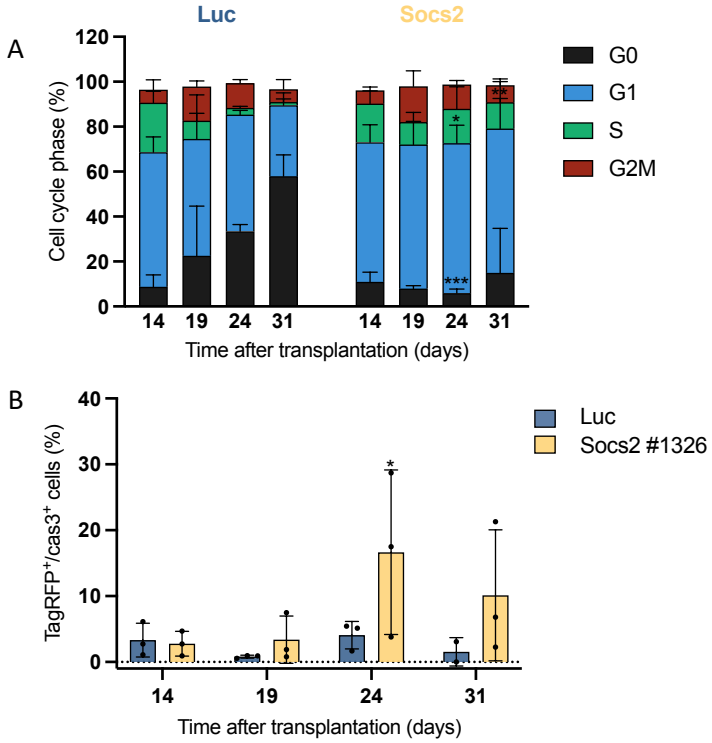

Figure 4.6 *Socs2* silencing prevented AML blasts quiescence *in vivo* and increased the fraction of apoptotic blasts. A. Cell cycle analysis of BM-derived TagRFP$^+$ MA9 blasts harboring Luc- and *Socs2*- shRNA determined at different time points post transplantation. Quiescent (G0) cells were defined as Ki67$^-$ cells with a 2n DNA content. Error bars represent the standard deviation of three animals (*p<0.05, **p<0.01 and ***p<0.001, t-test). **B.** Percentage of Caspase3$^+$/TagRFP$^+$ BM-derived MA9 blasts harboring Luc- or *Socs2*- shRNA at different time points post transplantation. Error bars represent the standard deviation of three animals (*p<0.01, t-test).

In summary, we observed significant changes of the cell cycle distribution of control AML blasts during leukemia outgrowth, characterized by progressive decline of G1 and S/G2M cells and marked increase of G0 cells. *Socs2*-interfered blasts, instead, did not outgrow, and showed the same cell cycle distribution in all the analyzed time points, with significantly increased cycling cells, markedly reduced quiescent blasts and appearance of apoptosis. These data established a phenomenological link between leukemia outgrowth, quiescence accumulation and survival, which are lost upon *Socs2* silencing.

4.2.2 *Stat1* silencing prevented the progressive accumulation of cell cycle restricted blasts in growing leukemia.

We then investigated if *Stat1* silencing induces similar effects on MA9 blasts cell cycle. As for *Socs2*, C57BL/6J syngeneic mice were i.v. injected with MA9 blasts transduced with *Stat1*- (#1334) or Luc-shRNA and FACS sorted to isolate TagRFP$^+$ blasts. Silencing efficiency was analyzed prior to transplantation, at 72h post-infection (**Figure 4.7, A**). Engraftment of injected leukemias was monitored by measuring the percentage of CD45.1$^+$/TagRFP$^+$ blasts in the PB of recipient mice at different time points post injection. Analysis of the cell cycle was performed at the time of sacrifice on BM TagRFP$^+$ blasts by anti-Ki67 and DAPI staining.

Since the delay in AML growth upon *Stat1* silencing was higher than observed for *Socs2*-interfered blasts (**Figure 4.2, B-C**), we could not perform a synchronous time course analysis. Thus, data were analyzed by grouping animals based on the levels of CD45.1$^+$/TagRFP$^+$ blasts (low: 5-15%; intermediate: 16-35% or high: 36-100%), regardless of the timing of sampling after leukemia injection (**Figure 4.7, B**). Expectedly, *Stat1*-interfered leukemia showed a significantly lower percentage of BM-derived CD45.1$^+$/TagRFP$^+$ blasts in each of the three groups, conforming that *Stat1* expression is indispensable for MA9 leukemia outgrowth.

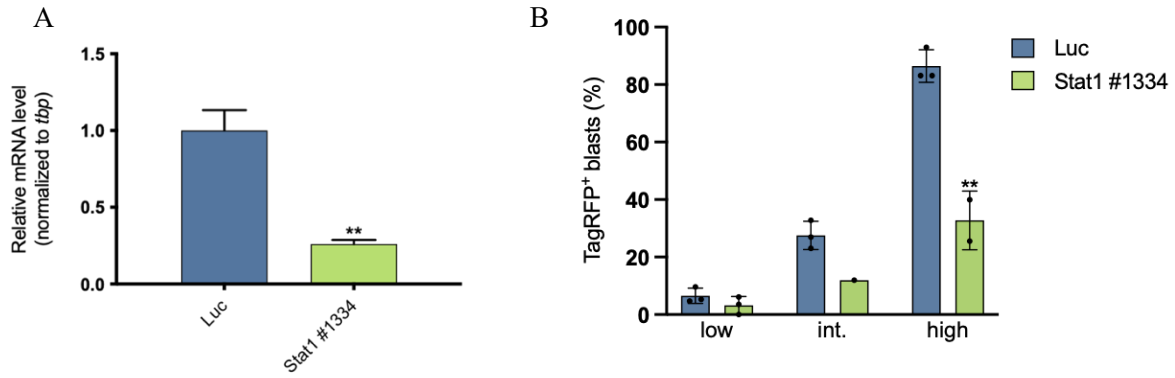

Figure 4.7 RT-qPCR confirmed *Stat1* silencing at the time of transplantation and only control MA9 leukemia engrafted in immunocompetent mice. A. Stat1 mRNA levels evaluated by RT-qPCR analysis in *Stat1*-interfered and Luc-shRNA MA9 blasts, at 72h post infection. Results were normalized to the *Tbp* housekeeping gene. Error bars represent the standard deviation of two technical replicates (**p<0.01, t-test). **B**. Injected mice were grouped according to the levels of CD45.1$^+$ /TagRFP$^+$ blasts in the BM: low (5-15%), intermediate (16-35%) and high (36-100%). Error bars represent the standard deviation of two/three animals (**p<0.001, t-test).

Cell cycle analysis of control Luc-shRNA leukemia (**Figure 4.8**) showed that the percentage of G0/quiescent (DAPI=2n and Ki67$^-$) cells increased proportionally to the level of engraftment: from ~15% in the group of mice with low engraftment, to ~20% and 45% in

the intermediate- and high-engraftment group, respectively, suggesting a progressive accumulation of quiescent blasts during leukemia outgrowth, as previously observed (see the **Figure 4.6, A**). In *Stat1*-interfered blasts, instead, the fraction of quiescent AML cells did not increase and was markedly low in all three groups (5-10%) (**Figure 4.8**).

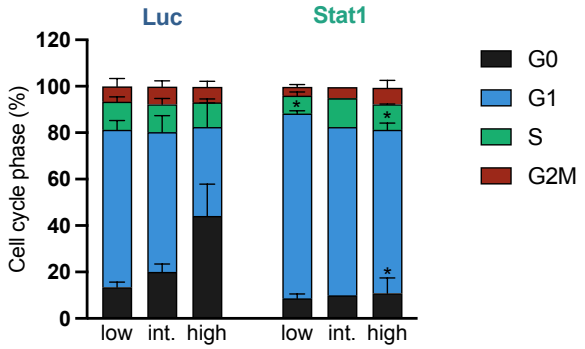

Figure 4.8 *Stat1* silencing prevented AML blasts quiescence accumulation *in vivo*. Cell cycle analysis of TagRFP$^+$ BM-derived MA9 blasts obtained from *Stat1*-interfered and Luc-shRNA control mice. Quiescent (G0) cells were defined as Ki67$^-$ cells with a 2n DNA content. Error bars represent the standard deviation of two/three animals (*p<0.05, t-test).

Notably, evaluation of the percentage of quiescence in CD45.1$^+$/TagRFP$^+$ versus CD45.1$^+$/TagRFP$^-$ blasts obtained from the same animal (sacrificed at different time points post transplantation: Luc ~35 days, *Socs2* ~45 days and *Stat1* ~55 days) showed higher levels of G0 cells in the CD45.1$^+$/TagRFP$^-$ compartment of both *Stat1*- and *Socs2*-shRNA samples, as compared to the control Luc-shRNA, confirming that low proportion of G0 cells in these mice was a specific effect of *Stat1* or *Socs2* silencing (**Figure 4.9**).

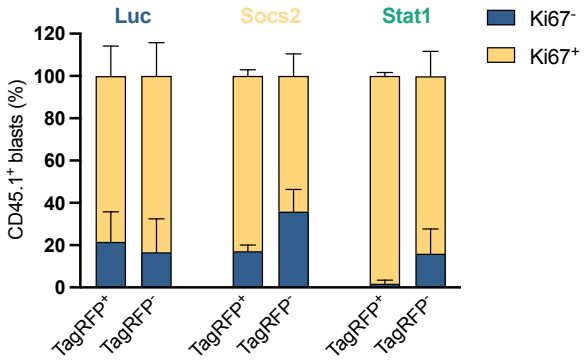

Figure 4.9 CD45.1$^+$/TagRFP$^+$ blasts of *Socs2*- and *Stat1*-shRNA samples were less quiescent as compared to the CD45.1$^+$/TagRFP$^-$ counterpart in the same animals. Percentage of Ki67$^-$ and Ki67$^+$ MA9 blasts evaluated by FACS in the CD45.1$^+$/TagRFP$^+$ or CD45.1$^+$/TagRFP$^-$ compartments of control (N=3), *Socs2*- (N=2) and *Stat1*- interfered (N=2) BM-derived cells. Blasts were obtained from the BM of mice sacrificed at ~35 (Luc), ~45 (*Socs2*) and ~55 (*Stat1*) days after leukemia injection.

Thus, *in vivo Stat1* silencing, as previously observed for *Socs2*, prevented both the accumulation of quiescent blasts and leukemia outgrowth.

4.3 Analyses of the effects of *Socs2* and *Stat1* silencing on the clonogenic activity, cell cycle distribution and survival of MA9 blasts *in vitro*

In the previous chapters we showed that silencing of *Socs2*, *Stat1* or *Sytl4* prevented MA9 leukemia outgrowth *in vivo*. The experimental setting involved the expression of specific shRNAs in MA9 cells and the subsequent transplantation of transduced cells into recipient mice, thus implying a direct effect on the regenerative potential of leukemia initiating cells or LSCs. LSCs represent a rare subpopulation in MA9 AML, since we estimated they have a frequency of 1:471 by limiting dilution experiments.

Surprisingly, we documented a dramatic effect of *Socs2* and *Stat1* silencing (the two genes analyzed so far) on the cell cycle and survival properties of the bulk of leukemia blasts: marked decrease of G0/quiescent blasts, accompanied by a parallel increase of G1 and S/G2M cells, and induction of apoptosis. Thus, silencing of *Socs2* and *Stat1* inhibited the regenerative potential of LSCs and induced a significant reprogramming of the cell cycle and survival properties of AML blasts. It was not clear, however, whether their silencing had direct effects on LSCs, bulk blasts or both.

To address these questions, we preliminarily evaluated the biological effects of *Socs2* and *Stat1* silencing on colony-forming cells, which represent a leukemia sub-population enriched in LSCs/progenitors, and cell cycle and survival properties on bulk blasts *in vitro*. To this end, MA9 blasts were transduced with *Socs2*- and *Stat1*-shRNAs, sorted for TagRFP-positivity and analyzed *in vitro* for their clonogenic potential, proliferation, cell cycle distribution and frequency of apoptosis.

4.3.1 Silencing of *Socs2* and *Stat1* significantly decreased clonogenic activity of MA9 blasts *in vitro*.

500 TagRFP$^+$ FACS sorted blasts from each sample were plated in methylcellulose (MC) medium in triplicate and colonies manually counted after one week. Silencing efficiency was analyzed on the sorted TagRFP$^+$ population, at 72h post-infection (**Figure 4.12, A-B**). The number of colonies was significantly reduced in both *Socs2*- and *Stat1*- interfered blasts (14±2.6 and 8.6±0.6 in *Socs2*-shRNA #1326 and #1328 samples, respectively; 7.6±4.5 and

2.3±1.5 in *Stat1*-shRNA #1334 and #1337 samples, respectively), as compared to controls (250±16 in Luc-ShRNA sample) (**Figure 4.10, A**). Strikingly, while almost all Luc colonies were TagRFP$^+$ (~97%), only a small percentage of them was TagRFP$^+$ in *Socs2*- and *Stat1*-interfered blasts (~5-30%) (**Figure 4.10, B**).

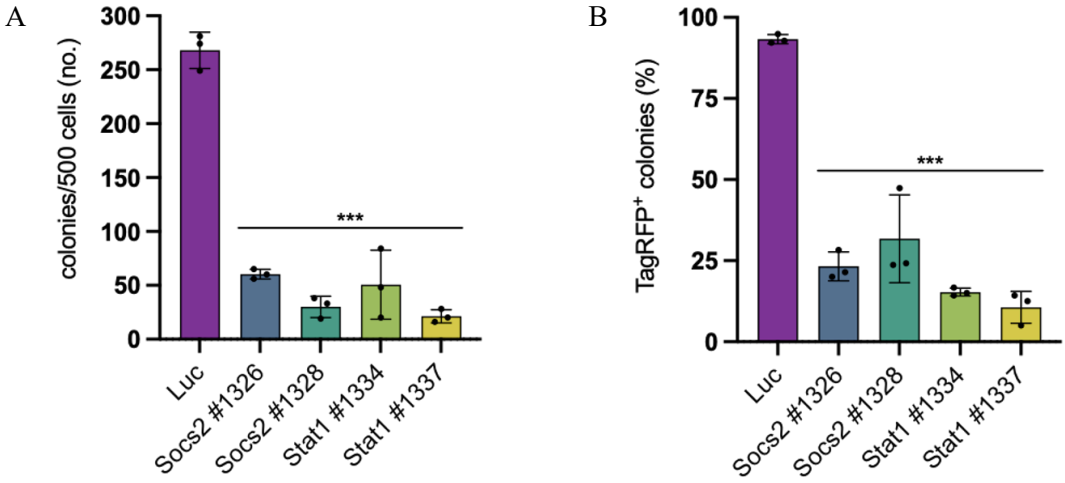

Figure 4.10 shRNA interference of *Socs2* and *Stat1* in AML blasts resulted in reduced colonies formation in methylcellulose culture. A. Number of colonies generated by *Socs2*- and *Stat1*-interfered or control MA9 blasts. AML cells were infected with lentiviruses expressing *Socs2*-, *Stat1*- or Luc-shRNAs, FACS sorted for TagRFP expression, and plated into MC (500 cells/well). Colonies were manually counted one week after plating. Error bars represent the standard deviation of three technical replicates (***p<0.001, t-test). **B.** Percentage of TagRFP$^+$ colonies generated by 500 *Socs2*- and *Stat1*- interfered or control MA9 blasts (same experiment as in A). TagRFP$^+$ colonies were manually assessed using a EVOS fluorescence microscope one week after plating. Error bars represent the standard deviation of three technical replicates (***p<0.001, t-test).

Thus, silencing of *Socs2* and *Stat1* significantly reduced clonogeneic activity of MA9 blasts.

4.3.2 Silencing of *Socs2* and *Stat1* did not affect growth of MA9 cells *in vitro*.

1.5x10^6 TagRFP$^+$ FACS sorted blasts from each sample were plated in a 6-wells plate at a density of 4x10^5 cells/ml in duplicate. Silencing efficiency was evaluated on sorted TagRFP$^+$ population, at 72h post-infection (**Figure 4.12, A-B**). Total number of cells was assessed manually every 24h over the period of one week (**Figure 4.11, A**), while percentage of alive cells was determined using a 0.4% Trypan Blue Solution (Trypan Blue Exclusion Test) (**Figure 4.11, B**). We observed a modest, yet statistically non-significant reduction of cell growth in *Socs2*- or *Stat1*-interfered cells, as compared to controls, and no significant differences in terms of cell viability.

FACS analysis for TagRFP-positivity in control Luc sample showed the same value (~97%) at the beginning (day=0) and at the end (day=6) of the culture. In *Socs2*- and *Stat1*-interfered blasts we have not observed any difference in TagRFP$^+$ cells with *Socs2*#1326 shRNA (~96%), and a modest, yet statistically non-significant, reduction at day 6 with *Socs2*#1328 (from 94% to 87%), *Stat1*#1334 (from 92% to 84%) or *Stat1*#1337 (from 97% to 80%) shRNAs (**Figure 4.11, C**).

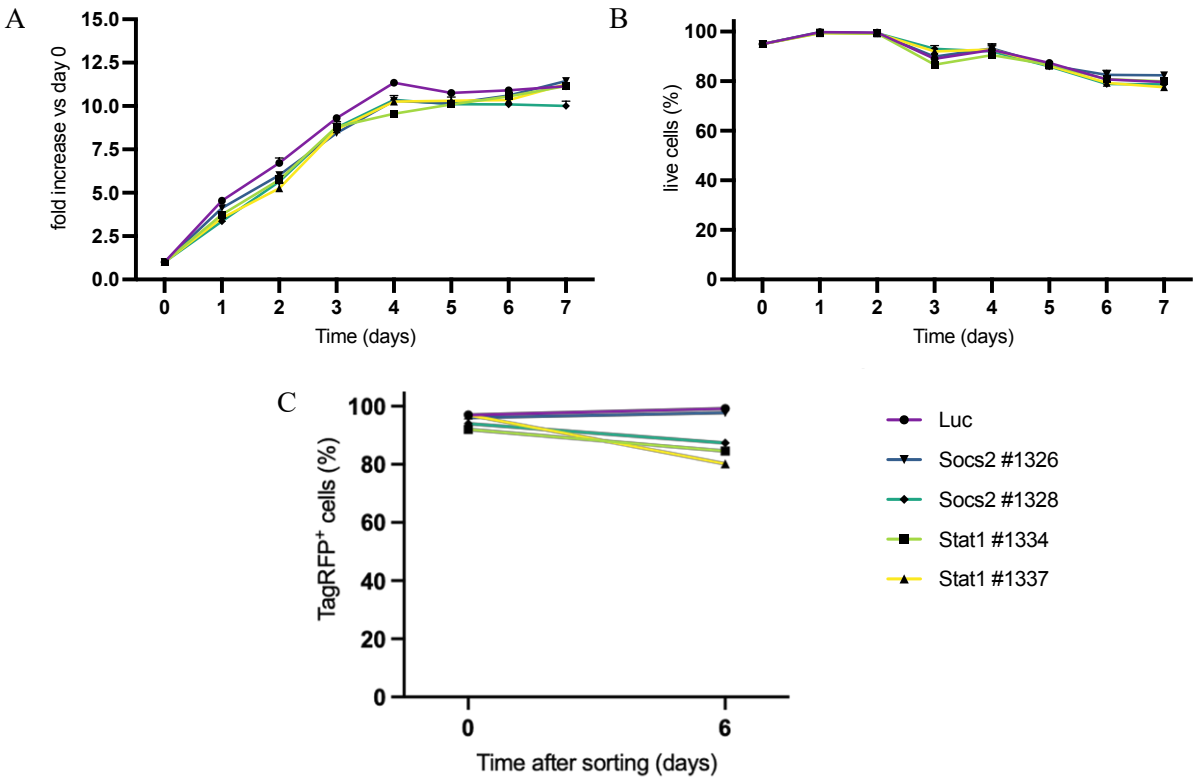

Figure 4.11 MA9 blasts harboring *Socs2* and *Stat1* shRNA maintained proliferation capability and viability over time *in vitro*. **A.** Cell numbers were manually determined and normalized to the number of plated cells (T0). Error bars represent the standard deviation of two independent experiments. **B.** Alive cells were identified manually by a Trypan Blue exclusion test (using a 0.4% Trypan Blue Solution). Error bars represent the standard deviation of two independent experiments. **C.** Percentage of TagRFP$^+$ blasts assessed on 500.000 cells by FACS analysis of the sorted population (T=0) and after 6 days of culture.

Consistently, *Socs2*-silencing was slightly reduced at the end of the culture, suggesting the existence of a modest counterselective pressure for cells with reduced *Socs2*-expression (**Figure 4.12, A-B**).

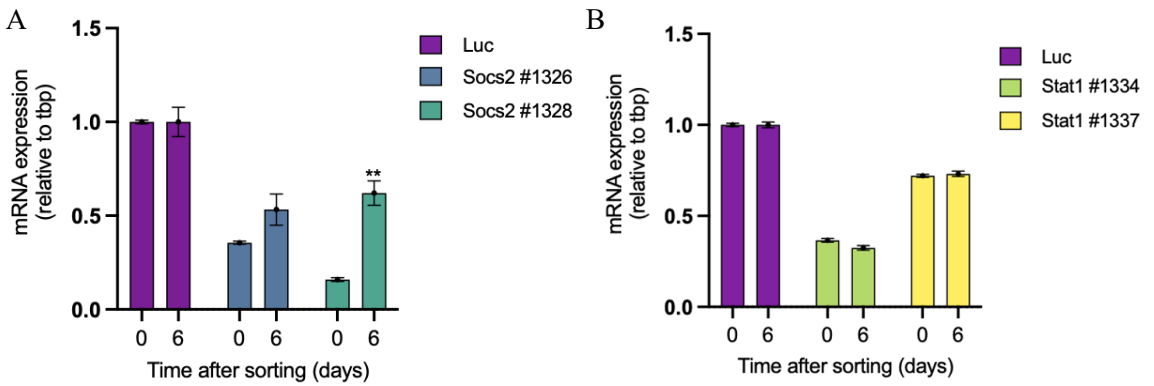

Figure 4.12 TagRFP⁺ MA9 blasts counterselection correlated with reduced *Socs2* and *Stat1* KD levels over time. A-B. Socs2 (A) and Stat1 (B) mRNA levels evaluated by RT-qPCR analysis in *Socs2*- and *Stat1*-interfered or control MA9 blasts at sorting time and 6 days later. Results were normalized to the *Tbp* housekeeping gene. Error bars represent the standard deviation of two technical replicates (**p<0.01, t-test).

4.3.3 Silencing of *Socs2* and *Stat1* did not induce alterations of the cell cycle or apoptosis/necrosis of MA9 cells *in vitro*.

1,5x10^6 TagRFP$^+$ FACS sorted blasts from each sample were plated in a 6-wells plate at a density of 4x10^5 cells/ml in duplicate. Silencing efficiency was checked on the sorted TagRFP$^+$ population, at 72h post-infection (**Figure 4.12, A-B**).

Cell cycle analysis was performed on TagRFP$^+$ cells at days 3 and 8 of cultures (**Figure 4.13**). A slight accumulation of quiescent blasts (DAPI=2n and Ki67$^-$) was observed during the culture in both control and *Socs2*- or *Stat1*-shRNA samples (from ~7% to ~20% at days 3 and 8, respectively). The three samples, however, showed the same proportion of G0/quiescent cells at 3 or 8 days.

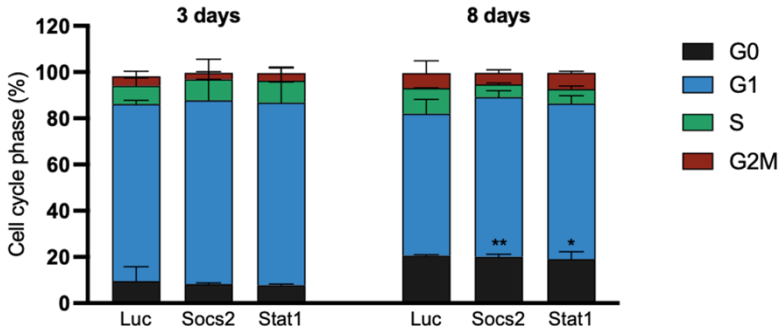

Figure 4.13 *Socs2* and *Stat1* silencing did not prevent the accumulation of quiescence *in vitro*. Cell cycle analysis of TagRFP$^+$ MA9 blasts expressing *Socs2*-, *Stat1*- or Luc-shRNA at 3 or 8 days of culture. Quiescent (G0) cells were defined as Ki67$^-$ cells with a 2n DNA content. Error bars represent the standard deviation of two independent experiments (*p<0.05 and **p<0.01, t-test).

Percentage of early apoptotic (AnnexinV$^+$/7-ADD$^-$) and necrotic (Annexin V$^+$/7-ADD$^+$) TagRFP$^+$ cells was assessed by FACS analysis after 3 days in culture (**Figure 4.14**). We did not observe differences in the frequency of apoptotic or necrotic cells between interfered and control blasts.

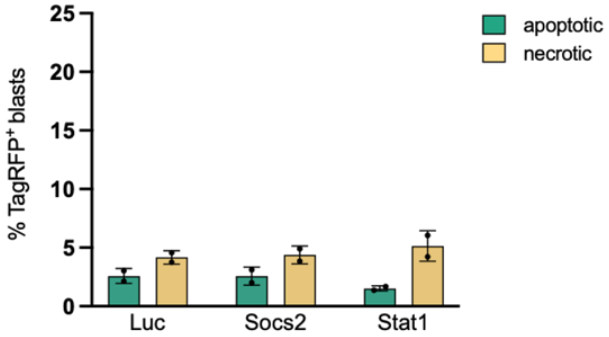

Figure 4.14 *Socs2* and *Stat1* silencing did not increase apoptotic and necrotic rates in MA9 blasts. Percentage of early-apoptotic (Annexin V$^+$ / 7-ADD$^-$) and necrotic (Annexin V$^+$ / 7-ADD$^+$) TagRFP$^+$ cells assessed by FACS at 3 days post sorting. Error bars represent the standard deviation of two independent experiments.

Conclusions. Analysis of the effects of *Socs2* and *Stat1* silencing on MA9 blasts *in vitro* showed inhibition of their clonogenic activity, which is consistent with the inhibition of the regenerative potential of LSCs observed *in vivo*. We did not observe, instead, any significant effect of *Socs2* and *Stat1* interference on proliferation, cell cycle distribution and survival of bulk blasts, as instead observed *in vivo*. Thus, it appears that *Socs2* and *Stat1* silencing affects growth/survival potential of both LSCs/progenitors and more differentiated bulk blast population. Underlying mechanisms, however, appear to be dependent on the *in vivo* context of the leukemia, which is dispensable for their effect on LSCs/progenitors (cell-autonomous effect), while it is indispensable for their effect on bulk blasts (non cell-autonmous effect). Though *Socs2* and *Stat1* interference clearly prevented proliferation of leukemia clonogenic-cells *in vitro*, we could not directly assess its effect on LSCs cell cycle status and apoptosis, either *in vivo* or *in vitro*, due the rarity of these cells and the lack of suitable markers for their prospective isolation.

4.4 scRNAseq analysis of *Socs2*-interfered cells showed marked downregulation of genes that characterize the dormant status of quiescent HSCs and activation of the apoptotic gene program.

To investigate underlying molecular mechanisms, we performed scRNAseq analysis of

Socs2-interfered and control blasts. TagRFP$^+$ MA9 blasts were FACS sorted from the BM of mice transplanted either with *Socs2*- or Luc-shRNA infected MA9 blasts. Cells were collected at 31 days after transplantation (same experiment as described in the **Figure 4.5, B**). Control leukemia was fully engrafted at this time point, with ~40% of TagRFP$^+$/CD45.1$^+$ blasts in the BM. *Socs2*-interfered leukemia, instead, did not expand and showed only ~5% of *Socs2*-shRNA TagRFP$^+$ blasts in the BM (**Figure 4.5, B**). ~5.000 cells per sample were processed accordingly to the ChromiumTM Single Cell 3' v2 protocol and sequenced on Illumina NovaSeq 6000 Sequencing System (see the section 2.5). scRNAseq data were visualized using the Uniform Manifold Approximation and Projection (UMAP) method (see the section 2.5).

The UMAP representation showed a clear separation of the two samples, suggesting a substantial difference in their transcriptomes (**Figure 4.15**).

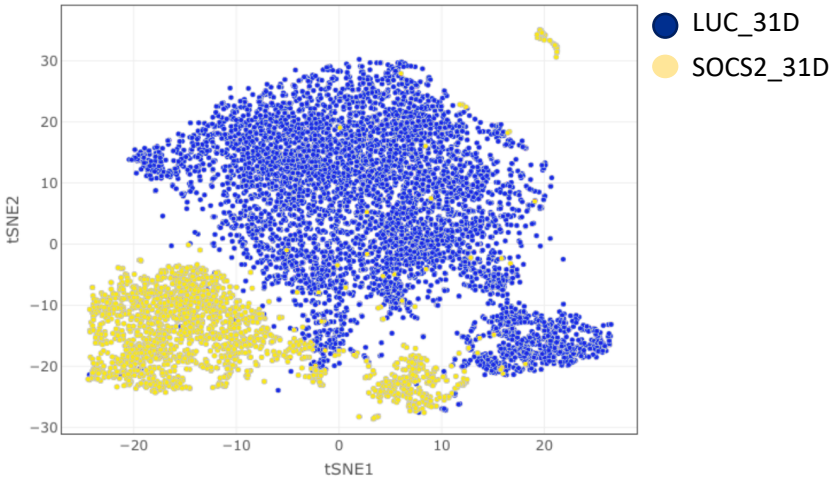

Figure 4.15 scRNAseq showed significative differences in the transcriptomes of *Socs2*-interfered and control blasts. Bidimensional tSNE plot representation of single-cell transcriptomes of TagRFP$^+$ *Socs2*-interfered and Luc-control BM-derived MA9 blasts FACS sorted for TagRFP-positivity and analyzed by scRNAseq.

Cell cycle analysis was performed with the Seurat tool, which assigns the cell cycle phase of each cell based on the expression of S- and G2M-specific genes (**Figure 4.16, A**).[261] Results confirmed the ~2 fold-increased proportion of cycling cells in sh*Socs2* blasts (S-G2M cells: ~60% versus ~35% in the control) (**Figure 4.16, B**), as previously observed by FACS analysis (Ki67$^+$ and >2n DAPI cells: ~20% versus ~8% in the control) (**Figure 4.16, C**). Absolute levels of cycling cells predicted by the Seurat tool were significantly higher than the ones obtained by FACS analysis, consistent with a tendency of Seurat to over-estimate the number of cycling cells (our unpublished observations). Accordingly, the

frequency of G0/G1 cells in *Socs2*-shRNA blasts was significantly lower than in the control (~40% versus ~70%), as observed by FACS analysis (DAPI=2n cells: ~80% versus ~90%) (**Figure 4.16, B-C**).

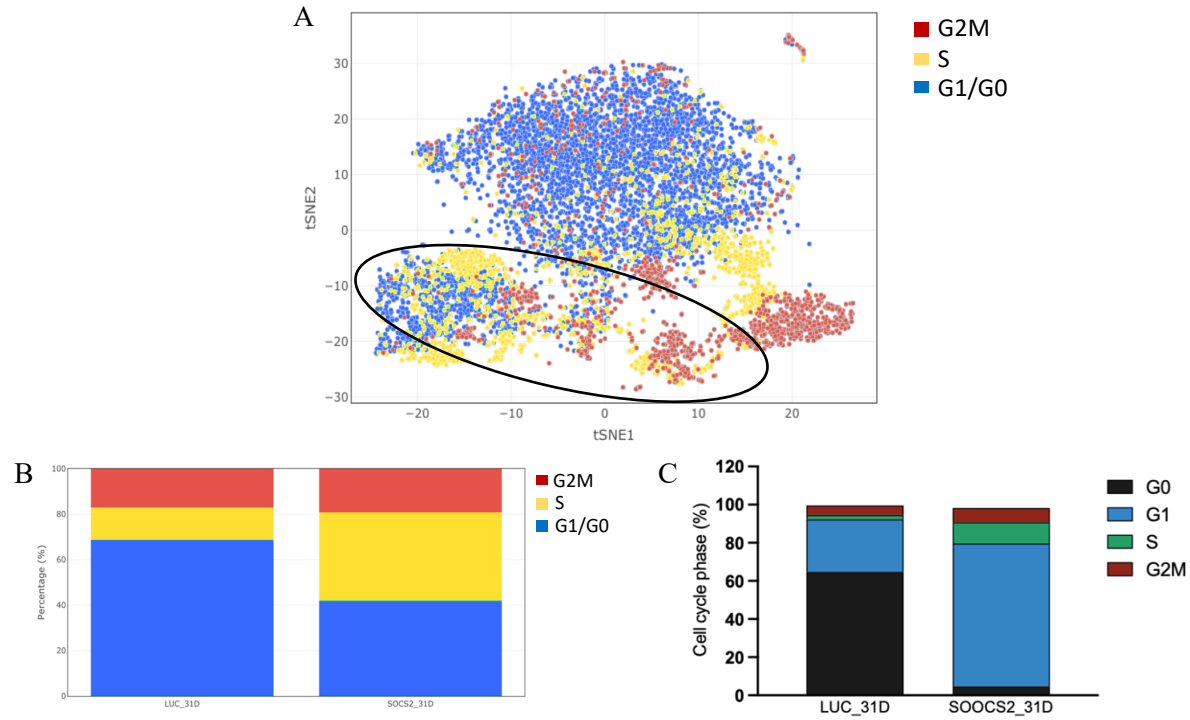

Figure 4.16 scRNAseq analysis confirmed the same cell cycle phenotype previously observed by FACS. A. Bidimensional tSNE plot visualizing the cell cycle status of each cell, as determined by the Seurat tool. The region corresponding to *Socs2*-interfered blasts is highlighted with a circle. **B.** Graphical representation of the percentage of cells assigned to different cell cycle status by the Seurat tool. **C.** Cell cycle analysis of BM-derived TagRFP^{+} MA9 blasts harboring Luc- and *Socs2*- shRNA determined at 31 days post transplantation. Quiescent (G0) cells were defined as Ki67^{-} cells with a 2n DNA content (same experiment as shown in the **Figure 4.6, A**).

The Seurat tool, however, does not discriminate G0/quiescent from G1 cells, thus preventing appreciation of the main cell cycle differences between the two samples, such as the markedly reduced fraction of G0/quiescent cells observed in *Soc2*-shRNA blasts (~5% versus ~60% in the control). Thus, we evaluated the average expression of a set of genes that characterizes quiescent HSCs. To this end, we used a gene signature derived from whole-transcriptome analyses of dormant HSCs, a subpopulation of quiescent HSCs that is at the top of the hematopoietic hierarchy.[27,262] Quiescent HSCs can dynamically switch between two phenotypic states: dormant HSCs (dHSCs), with the highest self-renewal potential, very infrequent cell division and stress signals-dependent activation, and active HSCs (aHSCs), which have limited self-renewal and, though mostly quiescent, enter the cell cycle more

frequently and participate in the maintenance of homeostasis in hematopoiesis.[263] Strikingly, the quiescent/dormant HSCs gene signature was significantly downregulated in *Socs2*-silenced blasts, as compared to Luc blasts (**Figure 4.17, A**). Analysis of the quiescence/dormant signature at single cell level showed a population of cells in the Luc-shRNA control sample with relatively high levels of expression, which largely overlapped with G0/G1 cells identified by Seurat (compare the dark blue cells in the panel A of **Figure 4.16** and **Figure 4.17**). Notably, a similar cell population was largely under-represented in the *Socs*-shRNA sample (**Figure 4.17, B**).

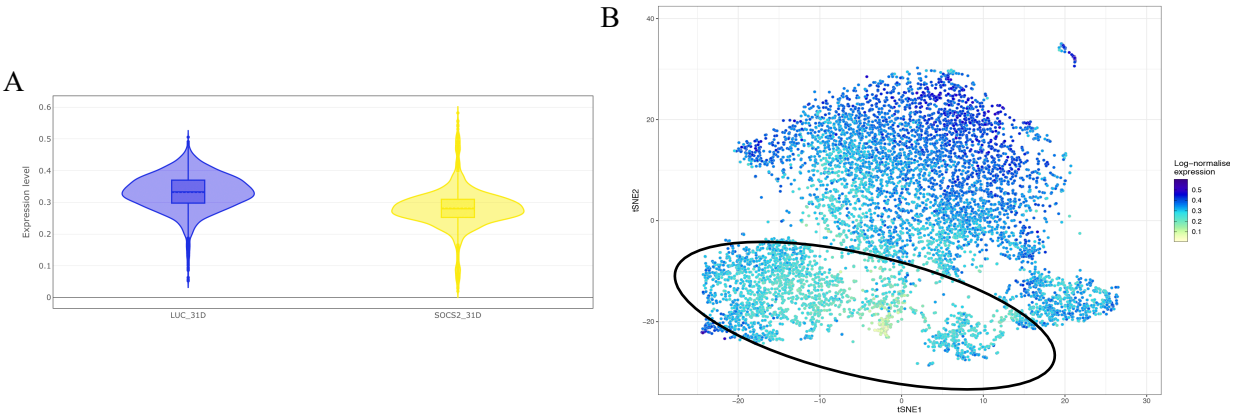

Figure 4.17 scRNAseq analysis confirmed the marked reduction of quiescent blasts in *Socs2*-interfered blasts. **A.** Violin plot representation of the normalized mean expression of a quiescent/dormant HSCs gene signature[262] in Luc-shRNA control (blue) and *Socs2*-shRNA (yellow) blasts. The Y axis shows the mean normalized read count. **B.** Bidimensional tSNE plot showing the mean expression of the quiescent HSCs gene signature in each cell. A color code scale is applied (dark blue = highest mean expression). The region corresponding to *Socs2*-interfered blasts is highlighted with a circle.

Finally, we investigated the expression levels of apoptosis-related genes, using an apoptosis specific gene signature (KEGG_apoptosis gene signature).[264] As observed *in vivo* by FACS analysis (**Figure 4.18, A**), in the sh*Socs2* sample there was a significant enrichment of genes related to the apoptotic pathway (**Figure 4.18, B**).

Thus, scRNAseq analysis of *Socs2*-interfered and control blasts showed a net separation of the two samples, suggesting a profound transcriptional reprogramming of *Socs2*-interfered blasts. Analysis of scRNAseq datasets confirmed reduced frequency of G0/G1 cells and increased apoptosis in *Socs2*-shRNA blasts. Most notably, we found marked downregulation of genes that characterize the dormant status of quiescent HSCs, suggesting that loss of

quiescence in *Socs2*-interfered cells corresponds to the loss of a functional state that in HSCs correlates with the highest potential of self-renewal.

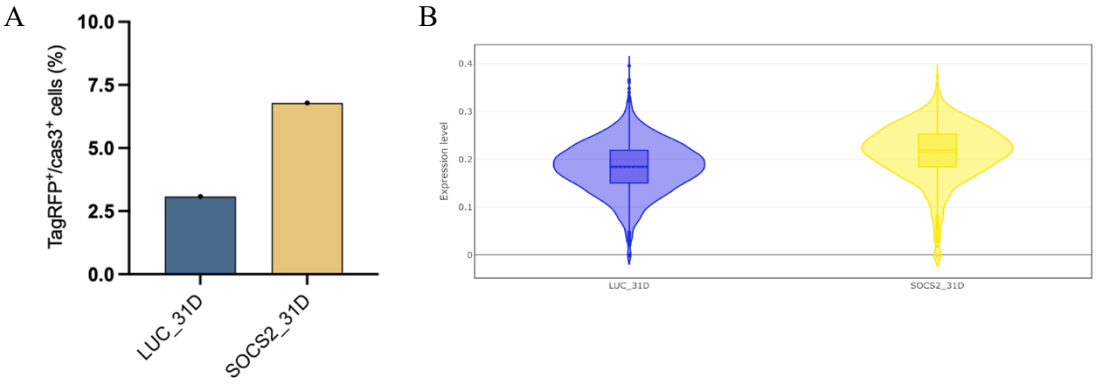

Figure 4.18 *Socs2*-interfered blasts upregulated an apoptosis-related gene signature. TagRFP$^+$ *Socs2*-shRNA and Luc-shRNA BM-derived MA9 blasts were sorted for TagRFP-positivity and analyzed by scRNAseq. **A.** Percentage of Caspase3$^+$/TagRFP$^+$ BM-derived MA9 blasts harboring Luc- or *Socs2*-shRNA at 31 days post transplantation (same experiment as shown in the **Figure 4.6, B**). **B.** Violin plot representation of the normalized mean expression of the apoptotic gene signature in *Socs2*-interefered (yellow) and Luc-control (blue) blasts. The Y axis shows the mean normalized read count.

4.5 In *Socs2*-interfered blasts, scRNAseq analysis showed marked activation of the Integrated Stress Response in both proliferating and cell cycle restricted blasts

Stress and injury signals stimulate the dormant-to-active transition of HSCs, which culminates with their entry into the cell cycle and with the expression of their regenerative potential. During the recovery phase, HSCs re-enter dormancy, allowing the restoration of a functional pool of HSCs.[263] However, if stress and/or injury signals are prolonged, or HSCs are defective in the maintenance of the dormant status, the pool of dormant HSCs is depleted and HSCs self-renewal is dramatically compromised.[25–27] Thus, we investigated whether the depletion of quiescent cells and the inability to support a fully-expressed dormant program in *Soc2*-interfered blasts correlated with the accumulation of intracellular stress, by analyzing, as indirect read-out, the activation of the integrated stress response (ISR). The ISR is a cellular stress response conserved in eukaryotic cells and activated by a variety of stressfull conditions, including accumulation of unfolded proteins in the endoplasmic reticulum (ER) or nutrient starvation, which downregulate protein synthesis (via inhibition of the phosphorylation of the eIF2α initiation factor) and induce profound transcriptional

reprogramming (through upregulation of master transcriptional regulators, such as the activating transcription factor 4, ATF4).[265] Integral to the ISR is the activation of intracellular pathways which allow cells to survive various stressors, including quiescence and autophagy, being the former a tightly regulated pathway involving lysosomal degradation of cytoplasmic organelles or cytosolic components.[266,267] Though ISR facilitates cellular adaptation to stress and it is itself a pro-survival and homeostatic program, exposure to severe stress and/or failure to resolve it can switch this signaling towards cell death.[265] A schematic representation of the ISR is given in the **Figure 4.19**.

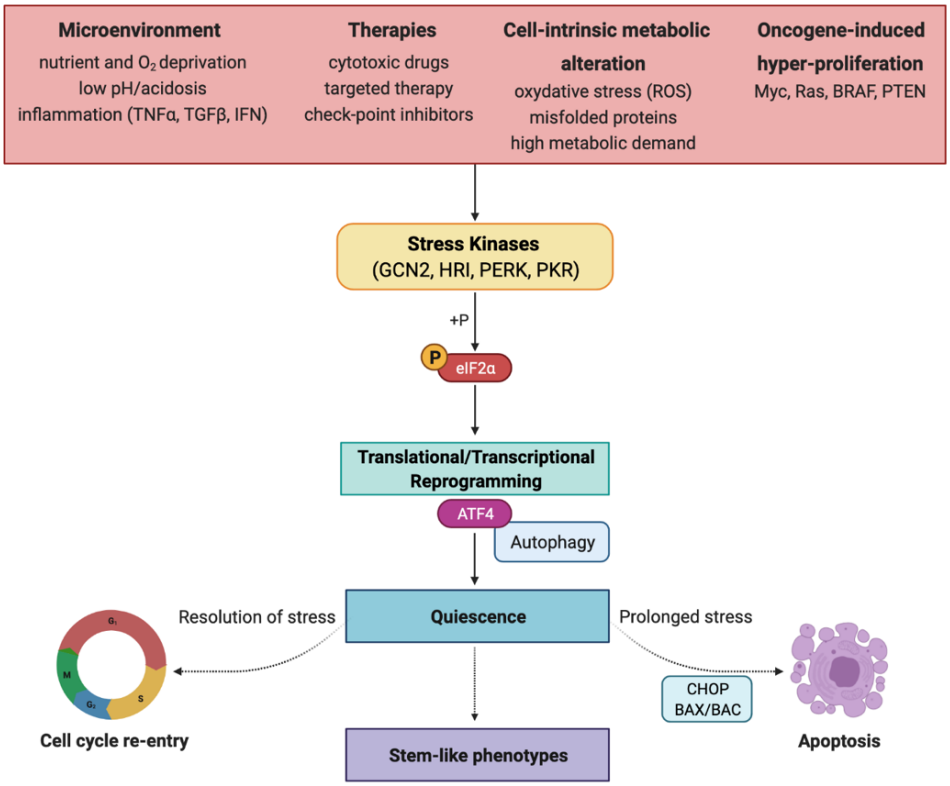

Figure 4.19 Schematic representation of the ISR. A. Microenvironmental cues, cell-intrinsic and therapy-induced stresses activate GCN2, HRI, PKR and PERK. The subsequent eIF2α phosphorylation induces activation of the ATF4 transcriptional program, followed by attenuated protein synthesis and activation of pro-survival mechanisms (autophagy, quiescence) or apoptosis, if the stressful conditions persist or the adaptative mechanisms of ISR are inefficient (adapted from Pakos-Zebruka *et al*., EMBO reports 2016).[265]

At this point, we analyzed the levels of activation of ATF4, the unfolded protein response (UPR) and autophagy, using specific gene signatures.[268,269] Strikingly, in sh*Socs2* blasts we found an increased average expression of all the three gene-signatures: the ATF4

transcriptional program (**Figure 4.20, A**), the UPR (**Figure 4.20, B**) and the autophagic pathway (**Figure 4.20, C**).

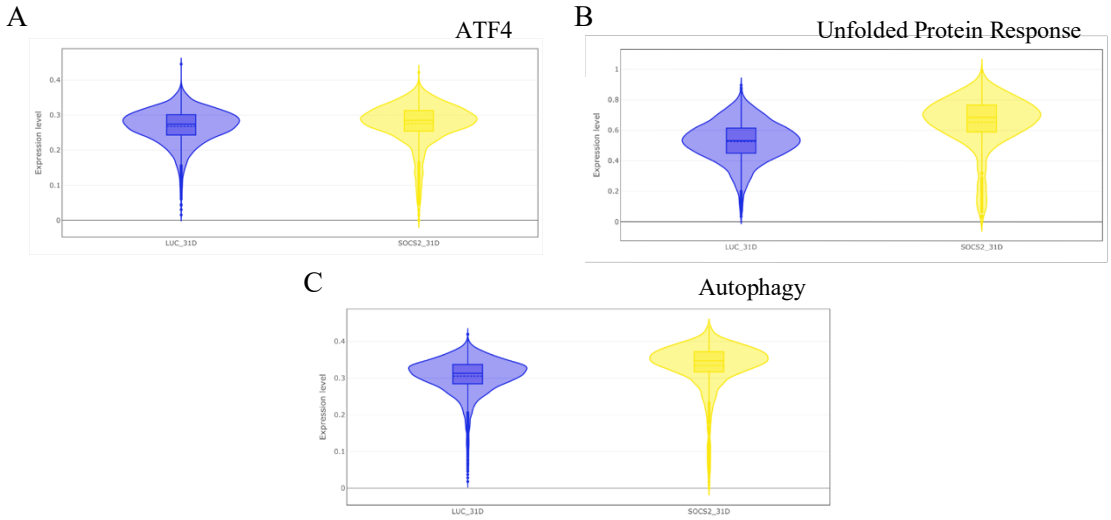

Figure 4.20 ***Socs2*-interfered blasts upregulated gene signatures related to ATF4, the UPR and the autophagic pathway.** TagRFP^{+} *Socs2*-interfered and Luc-control BM-derived MA9 blasts were sorted and analyzed by scRNAseq. **A-C.** Violin plot representation of normalized mean expression values of the ATF4 (A), UPR (B), and autophagy (C) genes signatures in *Socs2*-interefered (yellow) and Luc-control (blue) blasts. The Y axis shows the mean normalized read count.

The ISR response can also be induced by an eccessive proliferation, as shown by the induction of MYC or by the expression of oncogenic alleles of Ha-Ras, BRAF or PTEN, which drive ER stress and eIF2α phosphorylation.[270] Based on the increased cell proliferation observed in *Socs2*-interfered blasts (**Figure 4.16, B-C**), we then compared the average expression of ATF4 and genes of the UPR, autophagic and apoptotic signatures in G0/G1, S and G2M cells, as defined by the Seurat tool. In control cells, ATF4 was significantly upregulated in G2M cells (**Figure 4.21, A**), the UPR gene signature in both S and G2/M cells (**Figure 4.21, B**), while the autophagy gene signature in G0/G1 and G2M cells (**Figure 4.21, C**). In *Socs2*-silenced blasts, instead, ATF4, the UPR and autophagy gene signatures were significantly upregulated in each of the three groups (G0/G1, S and G2/M) at higher levels than their corresponding G0/G1, S and G2/M cells in the control sample (**Figure 4.21, A-C**). Levels of each gene signature varied among the groups with relative values similar to those observed in the control groups (**Figure 4.21, A-C**). Notably, the apoptotic gene signature was slightly upregulated in control G2/M cells, and consistently higher in all cell types (G0/G1, S and G2M) of sh*Socs2* cells, particularly in G2/M cells (**Figure 4.21, D**).

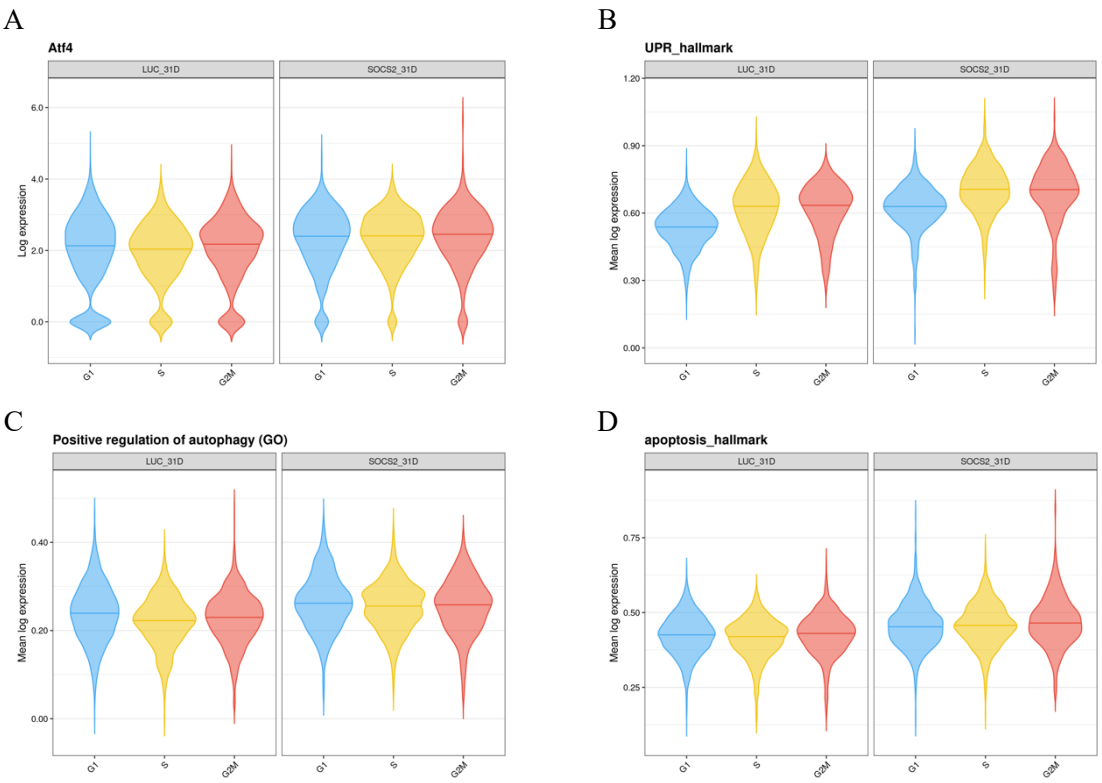

Figure 4.21 ***Socs2*-interfered blasts upregulated genes related to ATF4, the UPR, apoptotic and autophagic pathways in all the phases of the cell cycle.** TagRFP^{+} *Socs2*-interfered and Luc-control BM-derived MA9 blasts were FACS sorted and analyzed by scRNAseq. **A-D.** Violin plot representation of normalized mean expression values of ATF4 (A), the UPR (B), autophagy (C) and apoptosis (D) gene signatures in G0/G1, S and G2M cells of *Socs2*-interefered and Luc-control blasts. Cell cycle status was assigned using the Seurat tool. The Y axis shows the mean normalized read count.

To further investigate the regulation of the UPR gene signature during the cell cycle, we analyzed its expression across clustered differential gene regulations in the UMAP. The Louvain clustering algorithm yielded 11 stable and clearly separated clusters (**Figure 4.22, A**). Among the five clusters populated almost exclusively by control blasts (clusters 2, 4, 5, 6, 7) (**Figure 4.22, B**), the clusters enriched in G2/M (cluster 2) or S (cluster 5) cells showed higher expression levels of the UPR gene signature than the clusters enriched in G0/G1 cells (clusters 4, 6 and 7) (**Figure 4.22, C**). In clusters which contained mainly *Socs2*-interfered blasts (clusters 3, 9 and 10) (**Figure 4.22, B**), instead, levels of UPR gene expression were similar in proliferating (cluster 3) and less proliferating (clusters 9 and 10) clusters, and consistently higher than in clusters enriched with control cells (**Figure 4.22, D**).

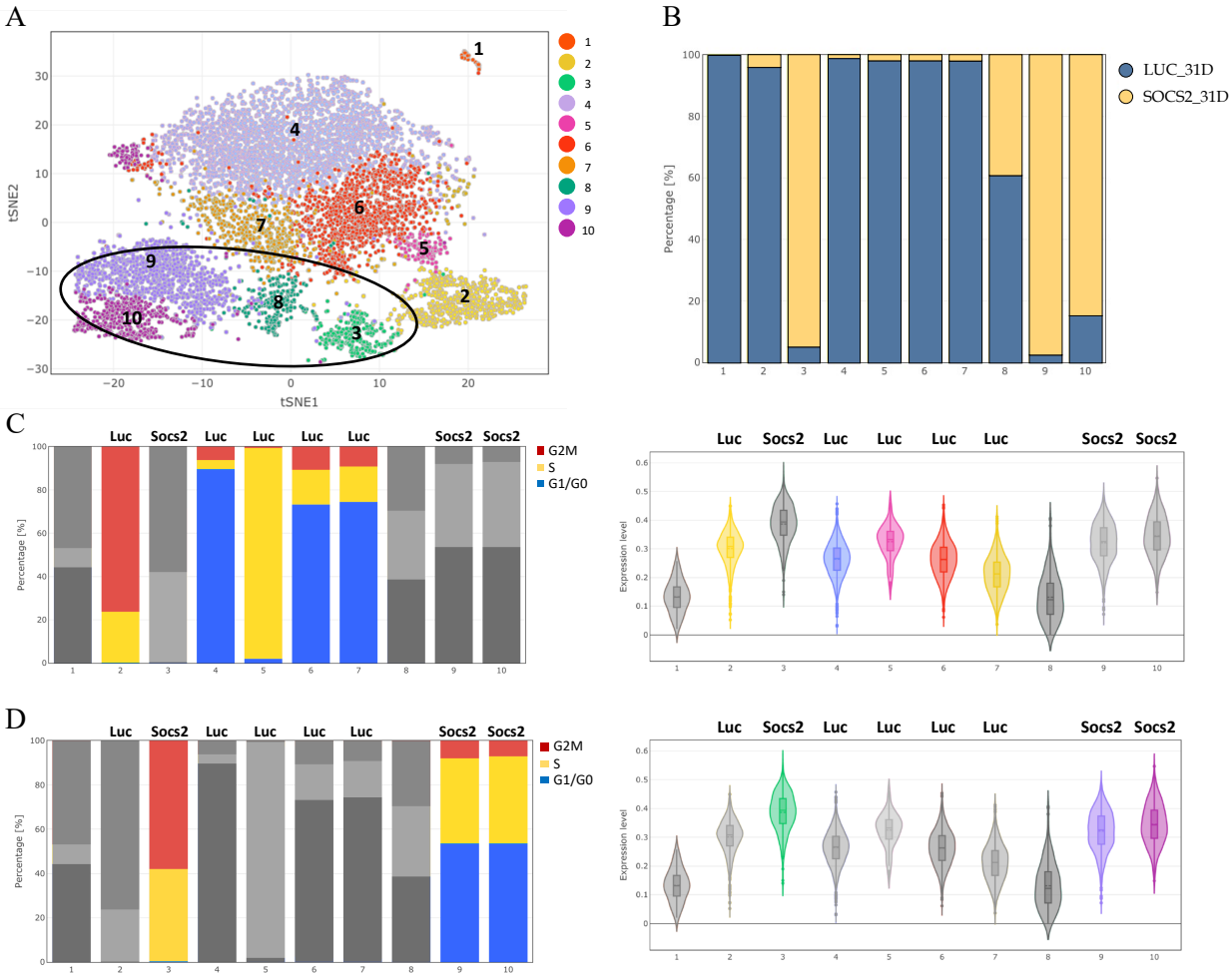

Figure 4.22 Different cell cycle regulation of the UPR gene signature in *Socs2*-interfered and control blasts clusters. TagRFP^{+} *Socs2*-interfered and Luc-control BM-derived MA9 blasts were FACS sorted and analyzed by scRNAseq. **A.** Bidimensional tSNE plot visualizing cell clusters. The region corresponding to *Socs2*-interfered blasts is highlighted with a circle. **B.** Proportion of Luc and *Socs2*-interfered blasts that contributed to each cluster. **C-D.** left panels: graphical representation of the percentage of cells assigned to different cell cycle phases in each cluster composed by shLuc (C) or sh*Socs2* (D) blasts. Right panels: violin plot representation of normalized mean expression values of the UPR genes signature for each cluster highlighted in the corresponding left panel. The Y axis shows the mean normalized read count.

Together, these data demonstrated that the ISR (ATF4, the UPR and autophagic transcriptional programs) is aberrantly activated in *Socs2*-interfered cells. Analysis of ISR gene programs in proliferating versus cell cycle restricted cells showed, in control MA9 leukemia, an upregulation of the UPR in proliferating cells and of the autophagic pathway in cell cycle restricted cells. In *Socs2*-silenced blasts, instead, both proliferating and cell cycle restricted cells activated ATF4, the UPR and autophagy, suggesting a defective

capacity of *Socs2*-interfered blasts to resolve the ISR. Consistently, *Socs2*-silenced cells showed increased expression of apoptotic genes in all the phases of the cell cycle, and particularly in G2/M cells.

4.6 *Socs2*-silenced blasts expressed reduced levels of the CD24a, galectin 9 and VISTA immune check-point molecules

Dormant/quiescent stem cells have evolved multiple mechanisms that allow the escape from immune clearance.[177] Unresolved ER stress and elevated levels of the UPR may lead to apoptosis and release or exposure on the cell surface of damage-associated molecular patterns (DAMPs), which act as danger signals and activate immune clearance.[271] Reduced dormancy/quiescence and/or sustained UPR may therefore represent a mechanism underlying the observed non cell-autonomous effects of *Socs2* interference. Thus, we analyzed the scRNAseq data for abnormal regulation of known mediators of tumor cells immune clearance. Strikingly, in *Socs2*-interfered blasts we observed marked downregulation of three distinct immune check-point molecules: CD24a, galectin 9 (LGALS9) and V-domain Ig suppressor of T cell activation (VISTA) (**Figure 4.23, A-C**).

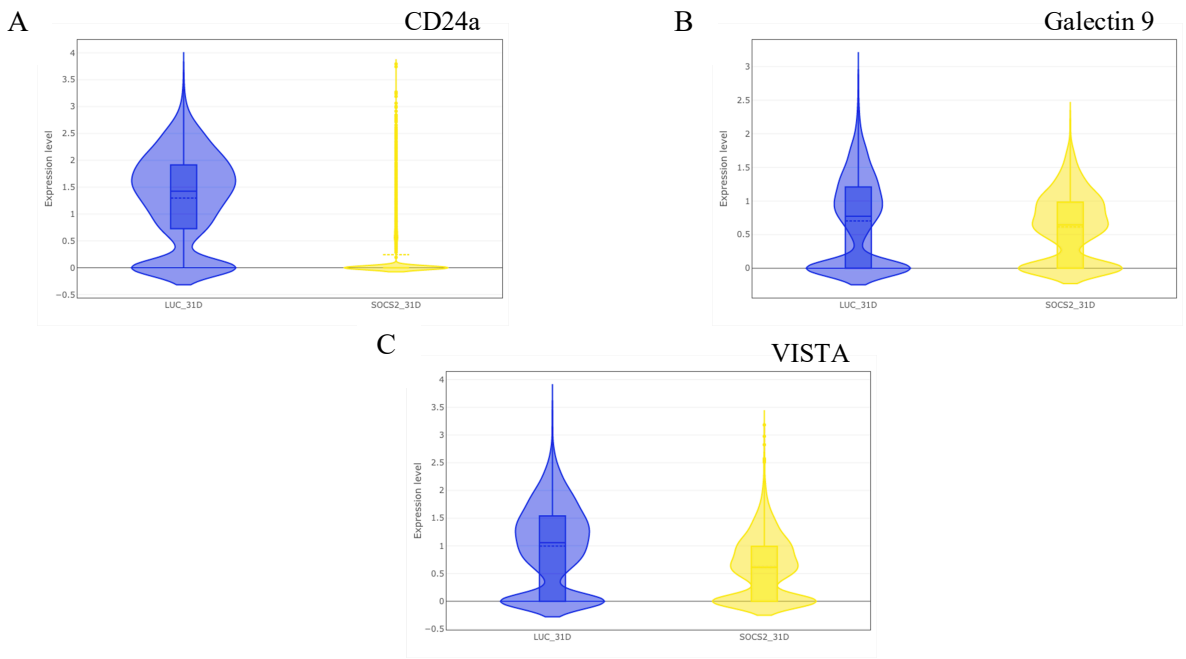

Figure 4.23 ***Socs2*-interfered blasts downregulated immune check-point molecules.** *Socs2*- and Luc-interfered BM-derived MA9 blasts were FACS sorted for TagRFP-positivity and analyzed by scRNAseq. **A-B-C.** Violin plot representation of normalized mean expression values of Cd24a (A), galectin 9 (B) and VISTA (C) genes in *Socs2*-interefered (yellow) and Luc-control (blue) blasts. The Y axis shows the mean normalized read count**.**

RT-qPCR analysis of *Socs2*- and *Stat1*-interfered MA9 blasts *in vitro* did not show any difference in the expression levels of Cd24a, LSGAL9 and VISTA, as compared to control samples (**Figure 4.24, A-B**), suggesting the existence of non cell-autonomous mechanisms regulating these immune check-point molecules expression by *Socs2* and *Stat1*.

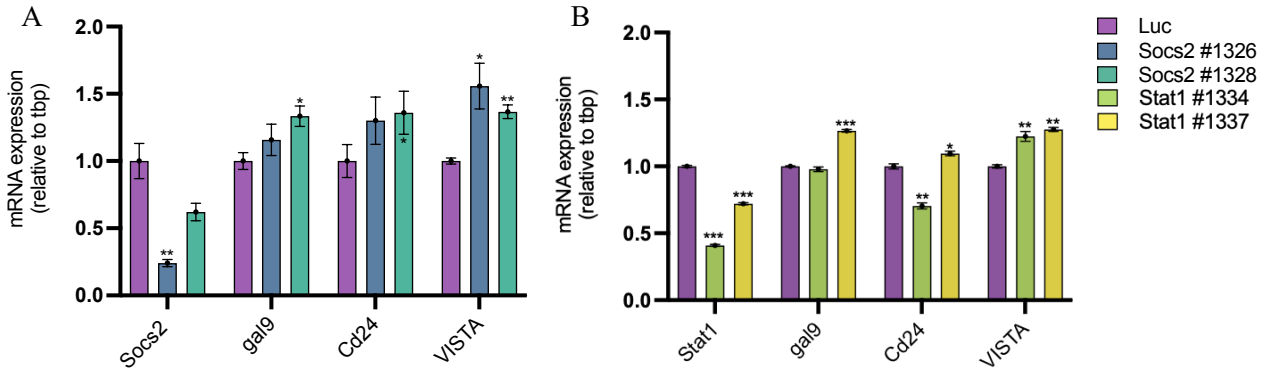

Figure 4.24 Cd24a, LSGAL9 and VISTA were not downregulated upon *Socs2* and *Stat1* silencing *in vitro*. A-B. Cd24a, LSGAL9 (gal9) and VISTA mRNA levels evaluated by RT-qPCR analysis in *Socs2*- (A) and *Stat1*- (B) interfered and control MA9 blasts. Results were normalized to the *Tbp* housekeeping gene. Error bars represent the standard deviation of two technical replicates (*p<0.05, **p<0.01, ***p<0.001, t-test).

CD24a functions as "don't eat me signal", since it has been shown to inhibit the phagocytosis of ovarian cancer cells through interaction with the macrophage receptor Siglec10 (**Figure 4.25, A**).[272] The Siglec 10 receptor is also expressed by other immune cells, including B cells, monocytes, dendritic cells and a subset of natural killer (NK) and activated T cells.[272] Galectin 9 is one of the ligand of the T cell immunoglobulin and mucin domain 3 (Tim-3) T cell inhibitory receptor.[273] Release of galectin 9 together with its receptor impairs AML cells killing by primary human NK cells, while soluble Tim-3 reduces the ability of T cells to secrete interleukin 2, required for the activation of both NK cells and cytotoxic T cells, leading to impaired immune surveillance and disease progression (**Figure 4.25, B**). [273] VISTA activity inhibits T cell activation and cytokine production. It can promote peripheral tolerance via enhanced activation of induced T cell death. VISTA mediates quiescence of mammalian myeloid and naïve T cells, and functions as an inhibitory immune check-point molecule constitutively expressed on $CD11b^+$ myeloid cells, naïve $CD4^+$ and $CD8^+$ T cells and regulatory T cells.[274] AML cells release a soluble form of the VISTA protein, enhancing the immunosuppressive activity of galectin 9, probably by forming multiprotein complexes on the surface of T cells and leading to their apoptosis (**Figure 4.25, C**).[275]

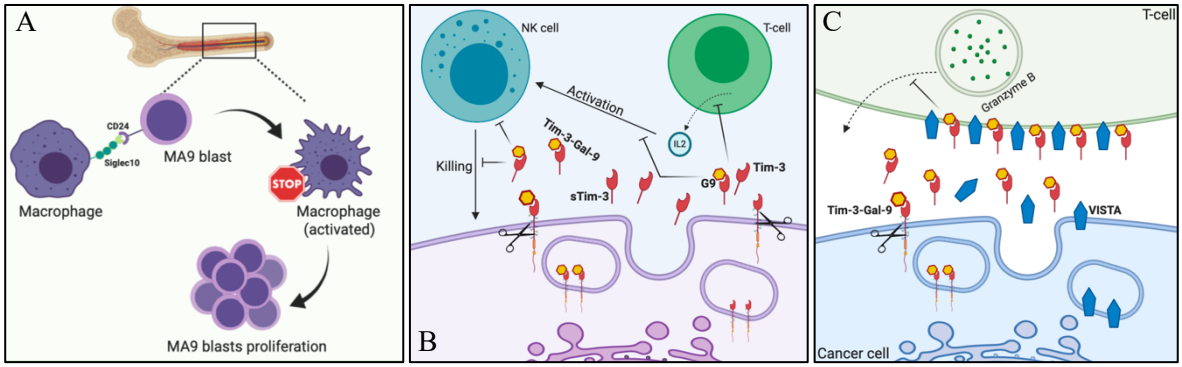

Figure 4.25 Cd24a, LGALS9 and VISTA expression favors AML immune escape. A. CD24a, through its interaction with the macrophage receptor Siglec10, inhibits phagocytosis and favors tumor growth (adapted from Barkal *et al*., Nature 2019).[272] **B.** Galectin 9 and Tim-3, secreted by AML blasts, impair NK and T cell mediated killing (adapted from Gonçalves *et al*., EBioMedicine 2017).[273] **C.** AML cells can release a soluble form of the VISTA protein, enhancing the immunosuppressive activity of galectin 9 (adapted from Yasinska *et al*., Frontiers in Immunology, 2020).[275]

Analysis of immune check-point molecules expression across clusters showed, in the Luc-shRNA control sample, the highest levels of expression for CD24a, galectin 9 and VISTA in the cluster n. 4 (**Figure 4.26, A-C**), which was the one with the largest fraction of G0/G1 cells (**Figure 4.17, B**). Relatively high levels of expression of each of the three transcripts were also observed in the cluster n. 2, which is instead composed of S and G2M cells, suggesting that CD24a, galectin 9 and VISTA are expressed throughout the cell cycle, with the highest levels in G0/G1 cells. All *Socs2*-shRNA clusters showed decreased expression of these three immune check-point molecules (**Figure 4.26, A-C**), with almost no expression of Cd24a (**Figure 4.26, D**).

Thus, *Socs2*-silenced blasts showed markedly reduced levels of CD24a, galectin 9 and VISTA, three distinct immune check-point molecules expressed by a variety of immune cells involved in cancer cells immune escape, including macrophages, NK, B and T cells. Notably, the same three molecules are mainly expressed in quiescent MA9 blasts and are not downregulated upon *Socs2* silencing *in vitro*, suggesting that *Socs2*-dependent upregulation may mediate immune escape of MA9 blasts *in vivo*.

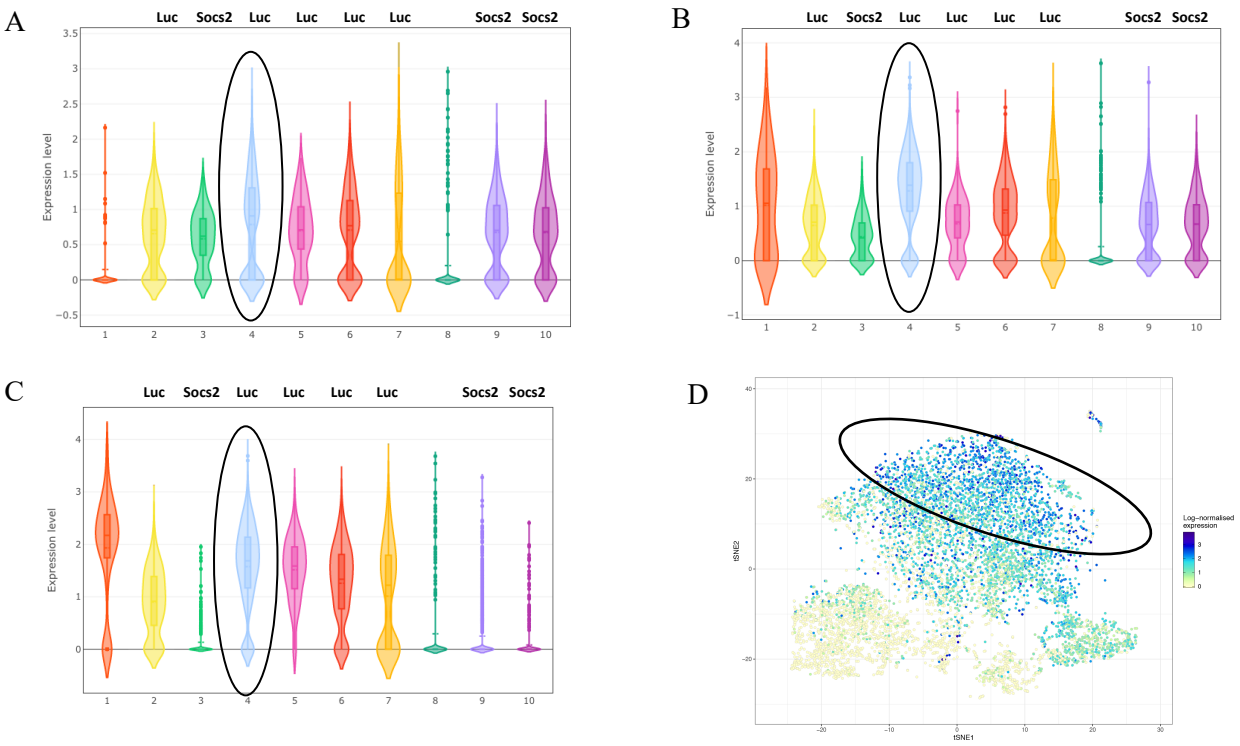

Figure 4.26 ***Socs2*-interfered blasts downregulated immune check-point molecules *in vivo*.** *Socs2*- and Luc-interfered BM-derived MA9 blasts were FACS sorted for TagRFP-positivity and analyzed by scRNAseq. **A-B-C.** Violin plot representation of normalized mean expression values of galectin 9 (A), VISTA (B) and CD24a (C) genes in each cluster. The Y axis shows the mean normalized read count. The most quiescent shLuc cluster n. 4 is highlighted with a circle. **D.** Bidimensional tSNE plot showing expression of CD24a in each cell. A color code scale is applied: dark blue = highest gene expression. The region corresponding to the cluster 4 is highlighted with a circle.

4.7 Activation of ISR and immune check-point molecules in MA9 blasts resembled the adaptive response of HSCs to oncogene-induced hyperproliferation

We then investigated if the activation of ISR and immune check-point molecules observed in MA9 blasts was part of a conserved adaptive stress response of leukemia blasts. Thus, we examined whether normal HSCs upregulate ISR and immune check-point molecules in response to stressfull conditions, such as oncogene-induced hyperproliferation. To this end, we took advantage of a scRNAseq dataset of WT versus oncogene-expressing HSCs recently generated in our laboratory (manuscript under revision). Highly purified HSCs (LT-HSCs) were obtained from transgenic mice co-expressing oncogenic alleles of NPM and FLT3-ITD by FACS sorting, using well-established combinations of antibodies against surface lineage

markers.[276] NPMc$^+$ and FLT3-ITD are the most frequently co-occurring mutations in AML, and strongly cooperate upon co-expression into murine BM.[15,89–91,95]

LT-HSCs were FACS sorted from a pool of mice for each genotype and analyzed by scRNAseq as described above. Notably, oncogene-expressing mice were sacrificed prior to leukemia development (pre-leukemic mice). At this stage, HSCs hyperproliferate but are morphologically and developmentally identical to normal HSCs, thus allowing direct evaluation of the *in vivo* effects exerted by the oncogene expression. Cell cycle analysis of merged scRNAseq datasets (2.841 WT and 3.321 oncogene-expressing cells) were performed with the Seurat tool.

First, we analyzed the average expression of ATF4 and the genes of the UPR and autophagy pathways in G0/G1, S and G2M cells within WT LT-HSCs, and across the two samples (normal versus oncogene-expressing HSCs). In control WT LT-HSCs, ATF4 (**Figure 4.27, A**) and UPR genes (**Figure 4.27, B**) were upregulated in S-phase cells, while ATF4 (**Figure 4.27, A**) and autophagy genes (**Figure 4.27, C**) in G2/M cells. In oncogene-expressing LT-HSCs, instead, ATF4, UPR and autophagy gene signatures were upregulated in all the phases of the cell cycle, at consistently higher levels than in the control cells (**Figure 4.27, A-C**). In particular, the highest levels of UPR, ATF and autophagy were observed in S-G2/M-phase cells, as in the control sample (**Figure 4.27, A-C**).

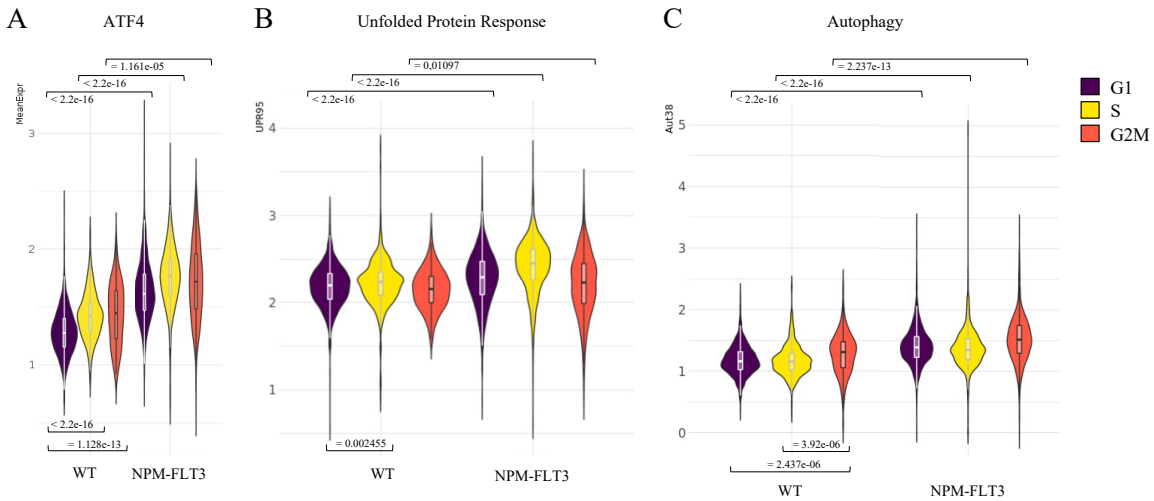

Figure 4.27 Oncogene-expressing LT-HSCs upregulated genes related to ATF4, the UPR and autophagic pathways. LT-HSCs were FACS sorted from a pool of mice for each genotype and analyzed by scRNAseq. **A-C.** Violin plots representation of normalized mean expression values of ATF4 (A), the UPR (B) and autophagy (C) gene signatures in G0/G1, S and G2M cells of WT and NPM-FLT3 LT-HSCs. Cell cycle status was assigned using the Seurat tool. The Y axis shows the mean normalized read count.

Notably, the expression levels of the ATF4 gene signature did not correlate (Pearson = 0,19) with the levels of S-phase specific genes (as defined by the Seurat tool) when analyzed in G1 cells of the two samples (~60% of all cells), while they showed a significant correlation with S-phase specific genes when analyzed in S-phase cells (~10% of all cells; Pearson = 0,39) or with G2/M genes in G2/M cells (~5% of all cells; Pearson = 0,43) (**Figure 4.28, A-C**), suggesting that ATF4 activation correlates with cell progression through the cell cycle.

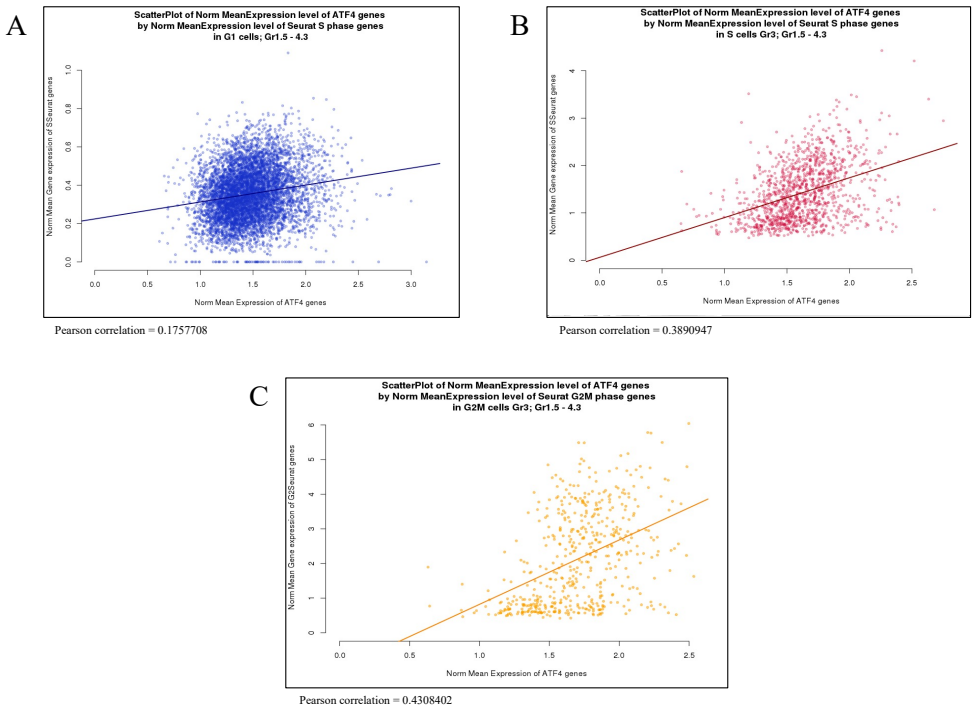

Figure 4.28 ATF activation correlated with cell progression trough the cell cycle. LT-HSCs were FACS sorted from a pool of mice for each genotype and analyzed by scRNAseq. **A-C.** Gene correlation at single cell level between the ATF4 gene signature and S-phase specific genes in the G1- (A), S- (B) and G2M- (C) phase of the cell cycle. The Y and X axes show the mean normalized read count.

At this point, we analyzed the average expression of the Cd24a and galectin9 immune check-point molecules (VISTA expression was not detectable in our dataset of WT and oncogene-expressing LT-HSCs). In control WT LT-HSCs, Cd24a was upregulated in G0/G1 cells, and, to less extent, G2M cells (**Figure 4.29, A**), while galectin 9 in G2/M and S cells (**Figure 4.29, B**). In oncogene-expressing LT-HSCs, instead, Cd24a and galectin 9 genes were upregulated in all the phases of the cell cycle, at consistently higher levels than in control cells (**Figure 4.29, A-B**). The highest levels of Cd24a and galectin 9 where reported in G2/M cells (**Figure 4.29, A-B**).

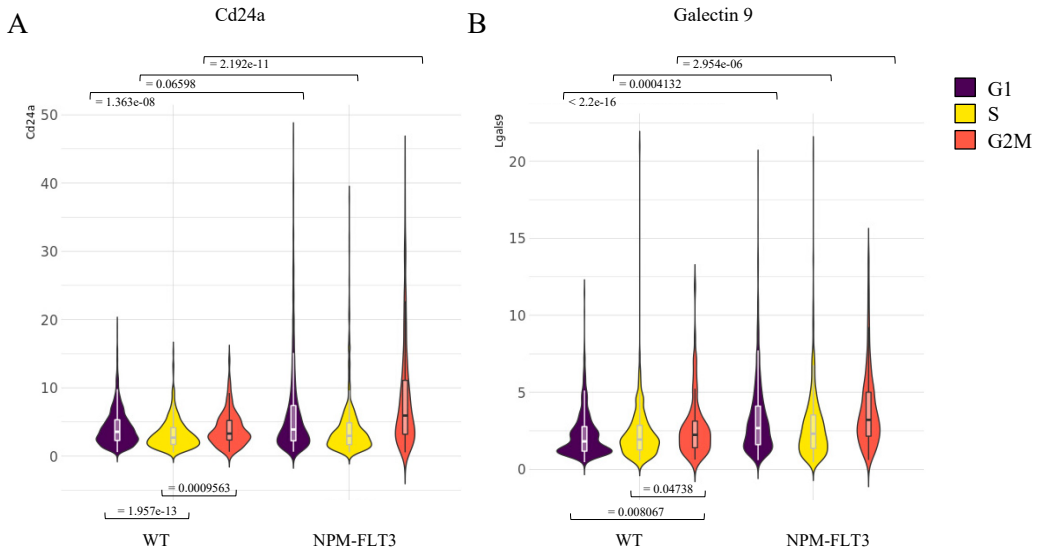

Figure 4.29 Oncogene-expressing LT-HSCs upregulated the Cd24a and galectin 9 immune check-point molecules. LT-HSCs were FACS sorted from a pool of mice for each genotype and analyzed by scRNAseq. **A-C.** Violin plots representation of normalized mean expression values of Cd24a (A) and galectin 9 (B) in G0/G1, S and G2M cells of WT and NPM-FLT3 LT-HSCs. Cell cycle status was assigned using the Seurat tool. The Y axis shows the mean normalized read count.

In summary, these data demonstrated that normal LT-HSCs activate UPR, ATF4 and autophagy during their progression through the cell cycle (S and G2/M phases) and upregulate immune check-point molecules when exiting the cell cycle (G0/G1) (**Figure 4.30, A**). These observations are consistent with emerging evidence showing that cell proliferation activates the ISR in HSCs, which is then resolved when cells exit the cell cycle.[277] Activation of check-point molecules in cell cycle restricted cells may then protect HSCs from immune clearance.[177] In oncogene-expressing HSCs, activation of the ISR and immune check-point molecules was exaggerated, as compared to normal HSCs, likely as a consequence of their hyperproliferative status. Notably, UPR, ATF4 and autophagy were hyperactivated during all the phases of the cell cycle, though their relative levels of expression in the different phases resembled those observed in normal HSCs. Immune check-point molecules were also upregulated in all the phases of the cell cycle, showing the highest levels in G2M cells. Thus, activation of the ISR and immune check-point molecules may be a conserved adaptive response of HSCs to oncogene-induced hyperproliferation.

Notably, control MA9 blasts showed similar expression patterns of the ISR and immune check-point molecules, with increased expression of ATF4, UPR and autophagy in

proliferating (S and G2M) cells, and of Cd24a and galectin 9 in cell cycle restricted (G0/G1) blasts (**Figure 4.30, B**), suggesting that MA9 blasts, like oncogene-expressing LT-HSCs, continuously activate the ISR to adapt to chronic stress generated by hyperproliferating cells (probably ER stress, considering the prominent activation of the UPR). In this context, leukemic blasts quiescence may be regarded as an immune protected status pivotal for the resolution of the ISR and fundamental to prepare cells to re-enter the cell cycle.

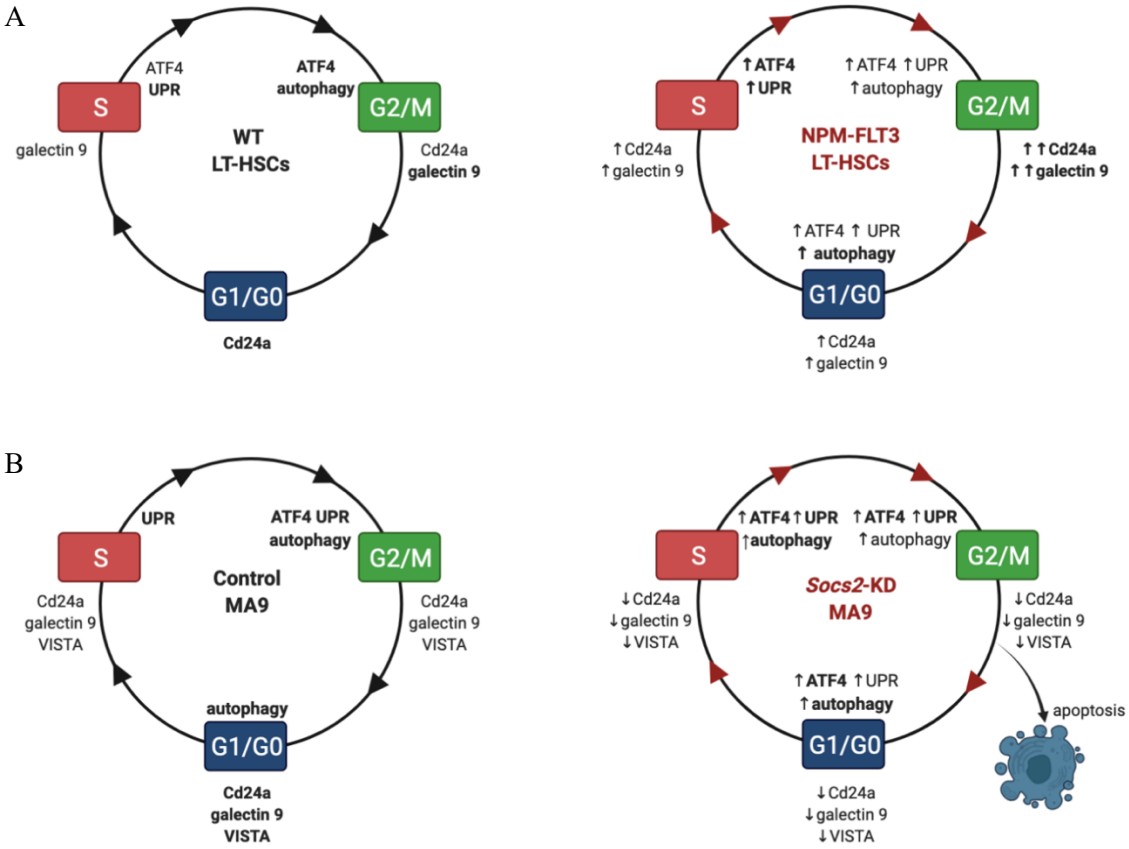

Figure 4.30 ISR and immune check-point molecules in WT versus oncogene-expressing LT-HSCs and in control versus *Socs2*-interfered MA9 blasts. A-B. Schematic representations on the connection between ISR, immune check-point molecules, proliferation and survival in WT and oncogene-expressing LT-HSCs (A), and in *Socs2*-interfered and MA9 blasts (B).

4.8 Working hypothesis: *Socs2*-depletion impedes quiescence entry of MA9 blasts, thus preventing ISR resolution and favoring immune-mediated cell death

Socs2-silencing dramatically modified the regulation of the ISR and immune check-point molecules (**Figure 30, A**). Indeed, we observed a further activation of the ISR (ATF4, UPR and autophagy) during all the phases of the cell cycle and, strikingly, a downregulation of immune check-point molecules. Hyperactivation of the ISR and downregulation of immune

check-point molecules correlated with the inability of MA9 blasts to maintain a quiescent status and with the induction of apoptosis, which may represent the primary effect of *Socs2* depletion. We then hypothesized that *Socs2* regulates the resolution of the ISR response in MA9 blats by allowing cells with activated ISR to enter quiescence and initiate further pathways of ISR resolution, including the upregulation of immune check-point molecules. In the absence of *Socs2*-mediated quiescence, cells will maintain a sustained activation of the ISR and switch toward the apoptotic module of the ISR, with the concomitant downregulation of immune check-point molecules and immune-mediated cell death (immunogenic cell death, ICD). Notably, the effect of *Socs2* on ISR-induced quiescence was observed only *in vivo*, suggesting that its capacity to allow quiescence entrance upon ISR activation involves interactions of the leukemic blasts with the tissue microenvironment. A scheme of our working hypothesis is reported in the **figure 4.31**.

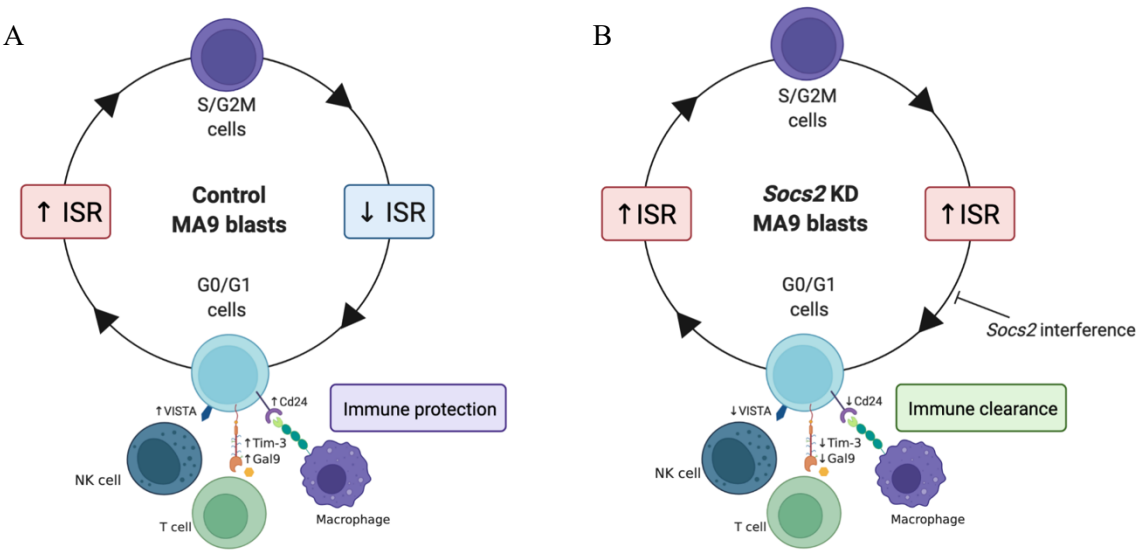

Figure 4.31 Working hypothesis: *Socs2*-depletion blocks entry of MA9 blasts into quiescence, preventing ISR resolution and favoring immune-mediated cell death. Schematic representations on the connection between ISR, immune check-point molecules, proliferation and survival under steady state conditions (A) and upon *Socs2* interference (B).

4.9 Modest growth inhibition by *Socs2*-interference in immunocompromised animals

To investigate whether immune clearance plays a role in the anti-leukemic effect of *Socs2* silencing, we evaluated growth of *Socs2*-interfered and control MA9 blasts in an

immunocompromised NOD-scid IL2Rgamma^{null} (NSG) mouse strain,[254,255] lacking B, T and NK cells.

Since the hematopoietic compartment of NSG mice expresses the same congenic marker of MA9 basts (CD45.1^{+}), to distinguish transplanted from recipient cells we engeneered MA9 blasts to express both luciferase and green fluorescent protein (Luc-ZsGreen) and monitored AML blasts in the PB of transplanted animals by double-marker expression (ZsGreen^{+}). Mice were i.v. injected with 10^5 TagRFP^{+}/ZsGreen^{+} sorted MA9 blasts infected with empty vector (EV) or *Socs2* (#1326)-shRNA constructs. Silencing efficiency was checked at sorting time, 72h post infection (**Figure 4.32, A**). Engraftment was monitored by measuring the percentage of ZsGreen^{+} blasts in PB over time and mice were sacrificed when moribund to study blasts cell cycle in the BM.

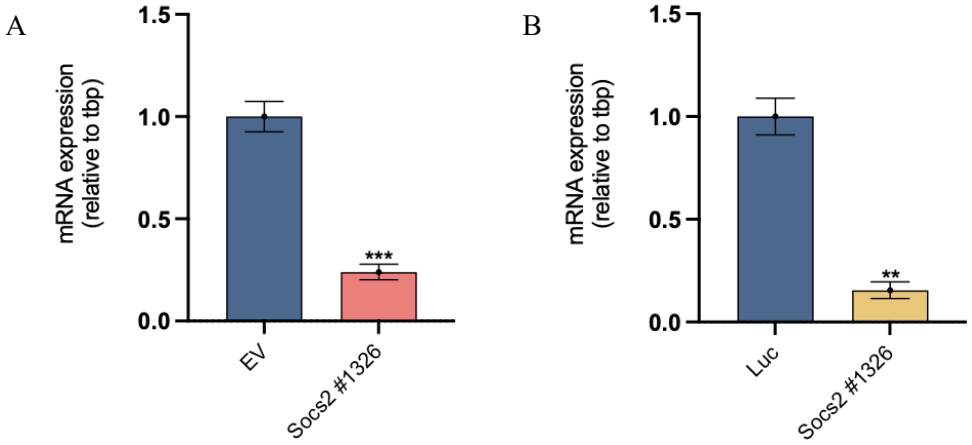

Figure 4.32 *Socs2* blasts were interfered at the time of transplantation. *Socs2* mRNA levels evaluated by RT-qPCR analysis in *Socs2*-interfered and control MA9 blasts 72h post infection and prior to i.v. transplantation in NSG (A) and immunocompetent (B) mice. Results were normalized to the *Tbp* housekeeping gene. Error bars represent the standard deviation of two technical replicates (**p<0.01 and ***p<0.001, t-test).

Silencing of *Socs2* delayed leukemia onset, as compared to control blasts (median survival: EV=27 days and *Socs2*=35 days; p=0,001) (**Figure 4.33, A**). However, the effect was more modest than observed in immunocompetent mice (median survival: Luc=34 days and *Socs2*=45 days; p<0,001) (**Figure 4.33, B**), despite similar levels of *Socs2* silencing in the two experiments (**Figure 4.32, A-B**). Most notably, while TagRFP^{+} cells were completely counterselected in sh*Socs2* MA9 cells upon injection into syngeneic mice (**Figure 4.33, C**), we observed a variable and significantly higher percentage of TagRFP^{+} blasts upon injection into NSG animals (10-60%) (**Figure 4.33, D**).

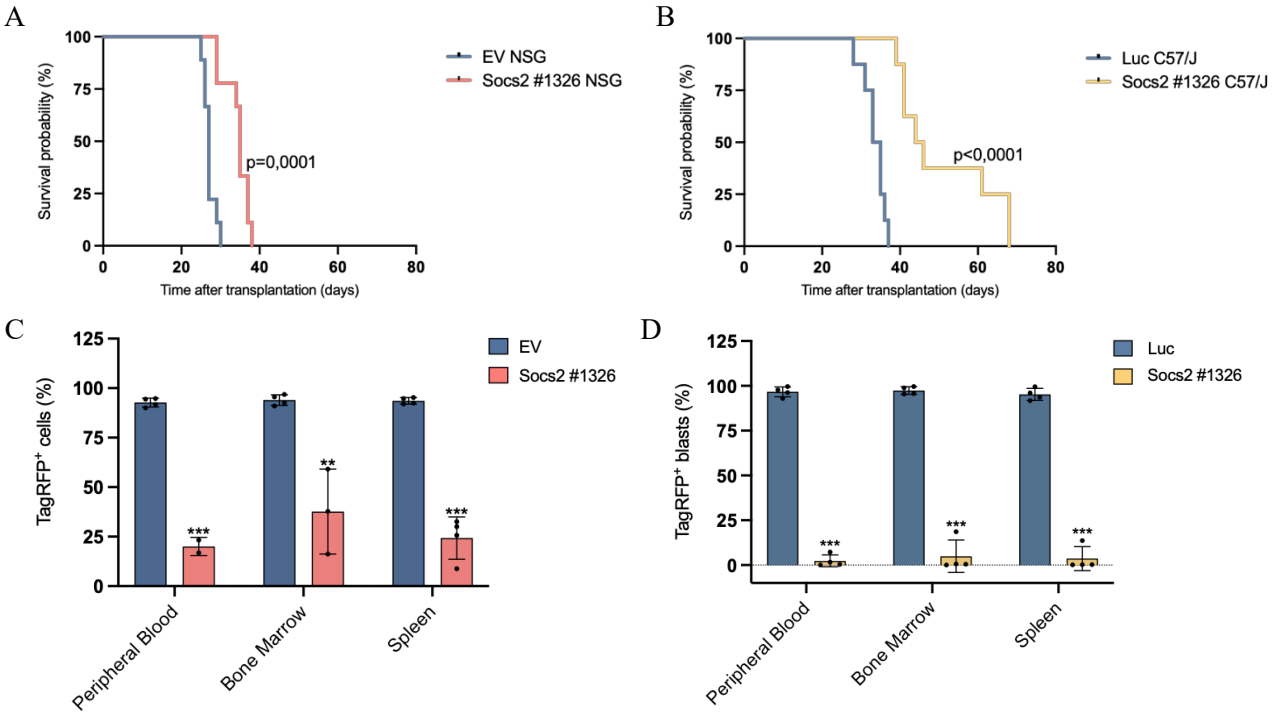

Figure 4.33 ***Socs2*-interfered blasts were capable of growing in immunocompromised animals.** **A.** Kaplan–Meier overall survival curves in NSG mice transplanted with *Socs2*-interfered (N=8) and control (N=8) blasts. Statistical significance was calculated using the logrank (Mantel Cox) test (**p<0.001). **B.** Kaplan–Meier overall survival curves in C57BL/6J mice transplanted with *Socs2*-interfered (N=8) and control (N=8) blasts. Statistical significance was calculated using the logrank (Mantel Cox) test (***p<0.0001). **C-D.** FACS analysis of the percentage of TagRFP$^+$ blasts (CD45.1$^+$) isolated from PB, BM and spleen of leukemic NSG (C) and immunocompetent (D) mice. Error bars represent the standard deviation of 4 animals (**p<0.01 and ***p<0.001, t-test).

Analysis of the cell cycle profile of TagRFP$^+$ cells did not show any difference between *Socs2*-interfered and control blasts (**Figure 4.34, A**). However, AML grown in NSG mice showed a much lower proportion of quiescent cells than observed in syngeneic immunocompetent animals (14,57% ± 1,2% versus 39,1% ± 9% **Figure 4.34, B**).

Taken together, these data supported the hypothesis that the immune system contributes to the clearance of *Socs2*-interefered blasts. Intriguingly, a significantly lower proportion of quiescent cells was documented in MA9 blasts when grown into immunocompromised mice, suggesting that immunocompetent cells might contribute to the activation of the ISR in syngeneic mice. We are currently investigating the extent of ISR activation in NSG-propagated MA9 leukemia.

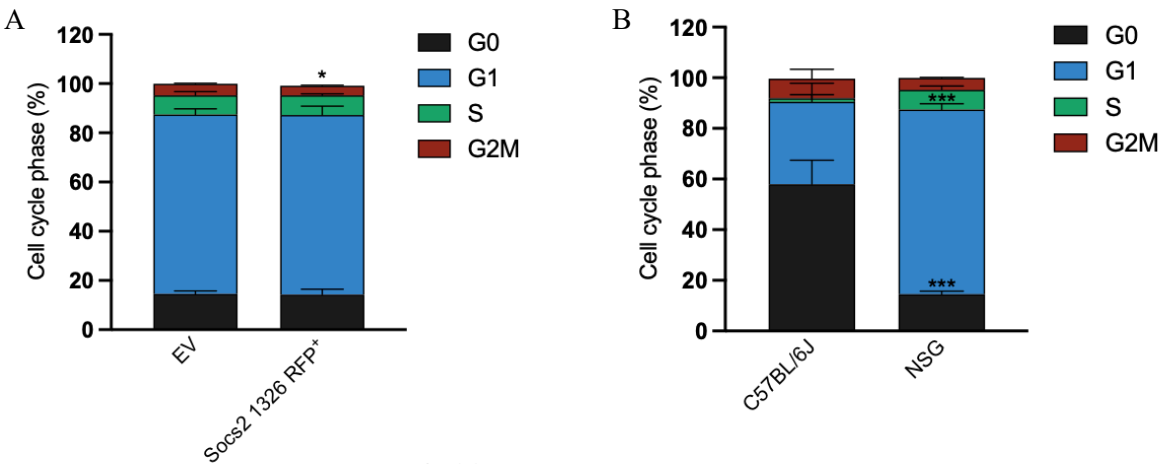

Figure 4.34 Both *Socs2*-interfered and control blasts did not accumulate quiescence in immunocompromised animals. **A.** Cell cycle analysis of TagRFP$^+$ BM-derived MA9 blasts harboring control and *Socs2*-shRNA determined at the time of sacrifice. Quiescent (G0) cells were defined as Ki67$^-$ cells with a 2n DNA content. Error bars represent the standard deviation of 4 (control) and 3 (*Socs2*) animals (*p<0.05, t-test). **B.** Cell cycle analysis of TagRFP$^+$ BM-derived MA9 blasts harboring control shRNA in C57BL/6J and NSG mice determined at the time of sacrifice. Quiescent (G0) cells were defined as Ki67$^-$ cells with a 2n DNA content. Error bars represent the standard deviation of 4 animals (***p<0.001, t-test).

4.10 Macrophage depletion did not affect the growth of *Socs2*-interfered blasts in immunocompromised animals

To explore whether the residual innate immunity in NSG mice was responsible for the modest anti-leukemic effect observed upon *Socs2* interference, we investigated the contribution of macrophages-mediated innate immunity in the clearance of *Socs2*-interfered AML blasts *in vivo*.

To systematically deplete macrophages, we used a rat monoclonal antibody (AFS98; immunoglobulin G 2a) against the murine receptor (Cd115) of the colony stimulating factor 1 (CSF-1) that inhibits CSF-1-dependent cell growth by blocking binding of CSF-1 to its receptor.[258] As control, we used an isotype-matched rat anti-trinitrophenol antibody. Both antibodies were administered intraperitoneally (i.p.) weekly (2 mg/mouse, as previously described), [258] starting 5 days after i.v. injection of 10^5 ZsGreen$^+$/TagRFP$^+$ FACS sorted Luc- or *Socs2*-shRNA (#1326) MA9 blasts. Silencing efficiency was checked at 72h post infection (**Figure 4.35, A**). The extent of macrophage depletion was tested three days after anti-Cd115 and anti-trinitrophenol administration by FACS analysis of circulating CD115$^+$

monocytes (**Figure 4.35, B**). Engraftment was monitored by measuring percentages of TagRFP$^+$ blasts (ZsGreen$^+$) in PB. Mice were sacrificed when moribund to study the blasts cell cycle in the BM.

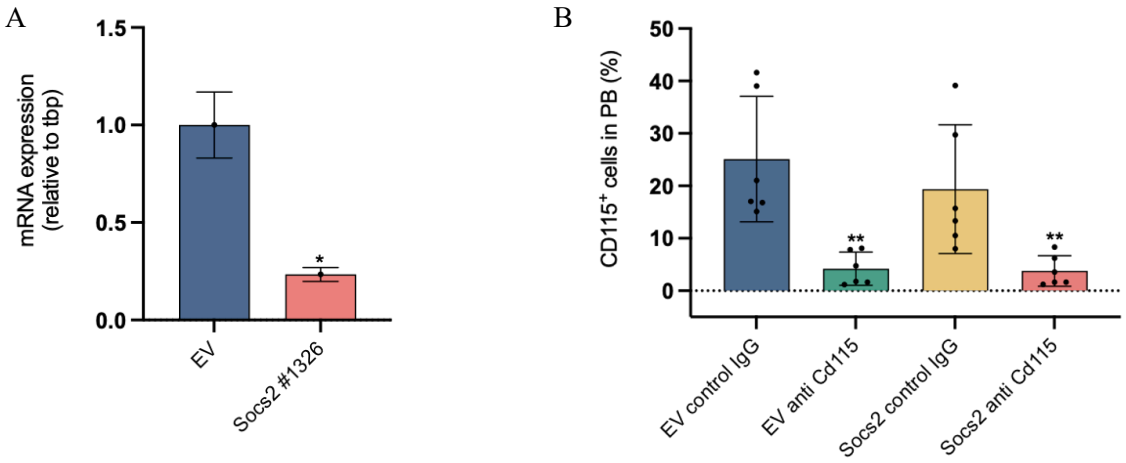

Figure 4.35 Effective *Socs2* silencing and macrophage depletion in immunocompromised animals. A. Socs2 mRNA levels evaluated by RT-qPCR analysis in *Socs2*-interfered and control MA9 blasts 72h post infection. Results were normalized to the *Tbp* housekeeping gene. Error bars represent the standard deviation of two technical replicates (*p<0.05, t-test). **B.** Percentage of CD115$^+$ cells (gated as ZsGreen$^-$) evaluated by FACS in the PB of mice three days after the i.p. treatment with control (anti-trinitrophenol) and anti-Cd115 antibody. Error bars represent the standard deviation of 6 animals (**p<0.01, t-test).

Mice transplanted with control and sh*Socs2* blasts, treated with either anti-trinitrophenol or anti-Cd115 antibody, died with similar latencies (median survival: EV anti-trinitrophenol=26 days, EV anti-Cd115=26.5 days, *Socs2* anti-trinitrophenol=34.5 days and *Socs2* anti-Cd115=33 days) (**Figure 4.36, A**).

Analyses of the cell cycle did not highlight any difference between sh*Socs2* anti-trinitrophenol and anti-Cd115 treated blasts, nor a reduction of the percentage of quiescent blasts, as compared to control animals (**Figure 4.36, B**).

These data suggested that the residual innate immunity of NSG mice (macrophages) is not responsible for the increased survival of mice transplanted with *Socs2*-silenced blasts, inferring that the residual effect of *Socs2* interference in NSG mice was due the cell-autonomous component of the *Socs2* function.

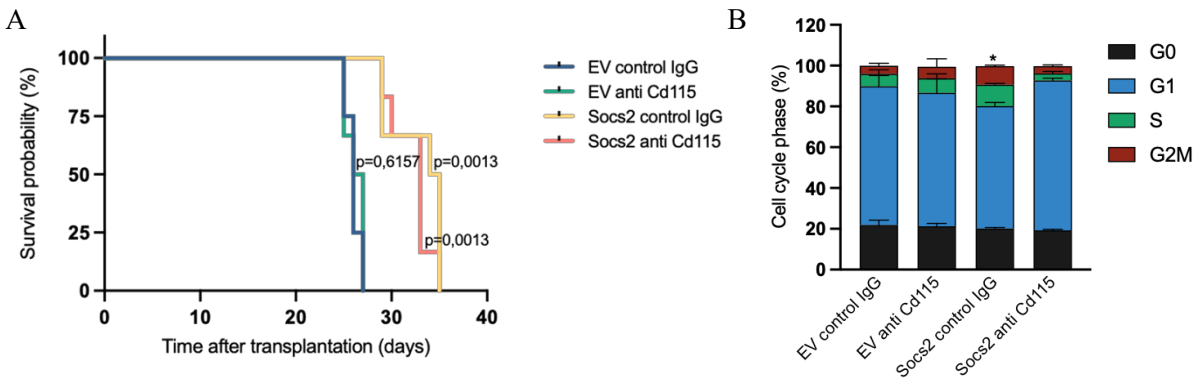

Figure 4.36 Macrophage depletion did not affect the survival and the cell cycle status of *Socs2*-interfered and control blasts in immunocompromised animals. A. Kaplan–Meier overall survival curves in mice transplanted with *Socs2*-interfered (control IgG N=6 and anti-Cd115 N=6) and EV (control IgG N=6 and anti-Cd115 N=6) blasts, i.p. treated with control or anti-Cd115 antibody three days after transplantation. Statistical significance was calculated using the logrank (Mantel Cox) test (**p<0.01). **B.** Cell cycle analysis of TagRFP$^+$ BM-derived MA9 blasts harboring empty vector and *Socs2*-shRNA determined at the time of sacrifice. Quiescent (G0) cells were defined as Ki67$^-$ cells with a 2n DNA content. Error bars represent the standard deviation of 3 animals (*p<0.05, t-test).

4.11 Macrophage depletion prolonged disease latency of immunocompetent mice transplanted with *Socs2*-interfered blasts

At this point, we investigated the contribution of macrophages-mediated innate immune response to the clearance of *Socs2*-interfered AML blasts in immunocompetent, syngeneic mice.

Macrophages were systematically depleted by i.p. injection of clodronate[259] and PBS (control) liposomes one week after the i.v. injection of mice with 10^5 TagRFP$^+$ sorted MA9 blasts infected with Luc or *Socs2* (#1326)-shRNA constructs. Silencing efficiency was checked 72h post infection (**Figure 4.37, A**). The extent of macrophage depletion was tested one week after clodronate and PBS liposomes administration by FACS analysis of circulating CD115$^+$ monocytes (**Figure 4.37, B**). Engraftment was monitored by measuring percentages of TagRFP$^+$ blasts (CD45.1$^+$) in the PB. Mice were sacrificed when moribund to evaluate levels of macrophage depletion in the liver and to study blasts cell cycle in the BM.

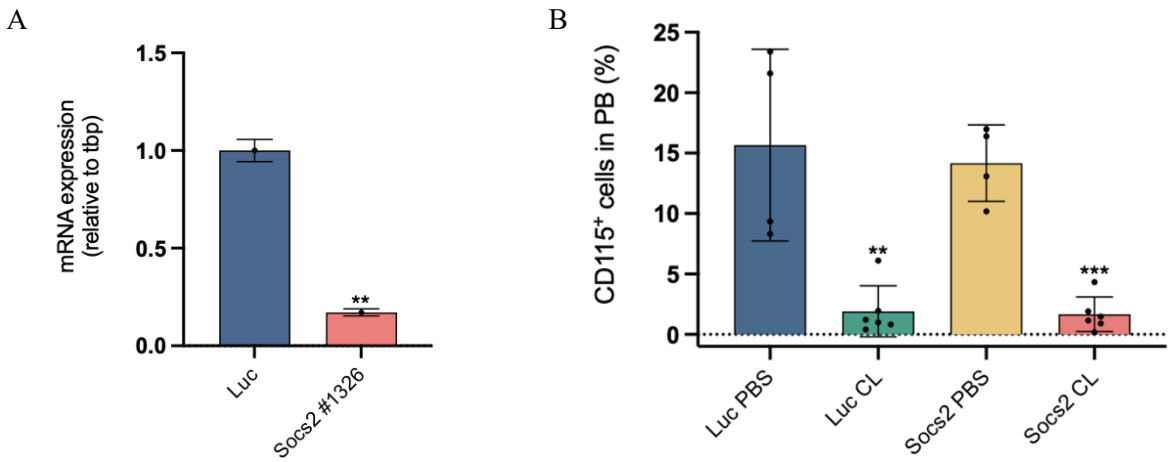

Figure 4.37 Effective *Socs2* silencing and macrophage depletion in immunocompetent animals. A. Socs2 mRNA levels evaluated by RT-qPCR analysis in *Socs2*-interfered and control MA9 blasts 72h post infection. Results were normalized to the *Tbp* housekeeping gene. Error bars represent the standard deviation of two technical replicates (**p<0.01, t-test). **B.** Percentage of $CD115^+$ cells (gated as $Cd45.1^-$) evaluated by FACS in the PB of mice one week after the i.p. treatment with control and clodronate liposomes. Error bars represent the standard deviation of 4 (Luc PBS and *Socs2* PBS) and 6 (Luc CLO and *Socs2*) animals (**p<0.01 and ***p<0.001, t-test).

At the time of sacrifice, clodronate-treated Luc- and *Socs2*-shRNA animals displayed decreased percentage of liver macrophages ($CD11b^+$/F4-80^+/$CD68^+$ cells gated in the $CD45.1^-$ population), as compared to PBS-treated controls (**Figure 4.38, A**). Average differences, however, did not reach statistical differences, probably due to the high variability among animals and the low numbers of animals.

Control mice treated with PBS and clodronate liposomes died with similar latencies (median survival: Luc PBS=32 days and Luc clodronate=32 days, **Figure 4.38, B**). Analyses of the cell cycle did not show any difference between PBS- and clodronate-treated mice (**Figure 4.38, C**).

The disease latency of mice transplanted with *Socs2*-interfered blasts and treated with clodronate liposomes was longer (median survival=43 days) than those of treated or untreated Luc mice (median survival=32 days), but shorter than PBS-treated mice transplanted with sh*Socs2* blasts (median survival=67,5 days) (**Figure 4.38, B**). Analysis of the cell cycle did not show any difference between sh*Socs2* PBS and clodronate treated blasts. *Soc2*-interfered blasts, however, showed a reduction in the percentage of quiescent blasts, as compared to shLuc controls (**Figure 4.38, C**).

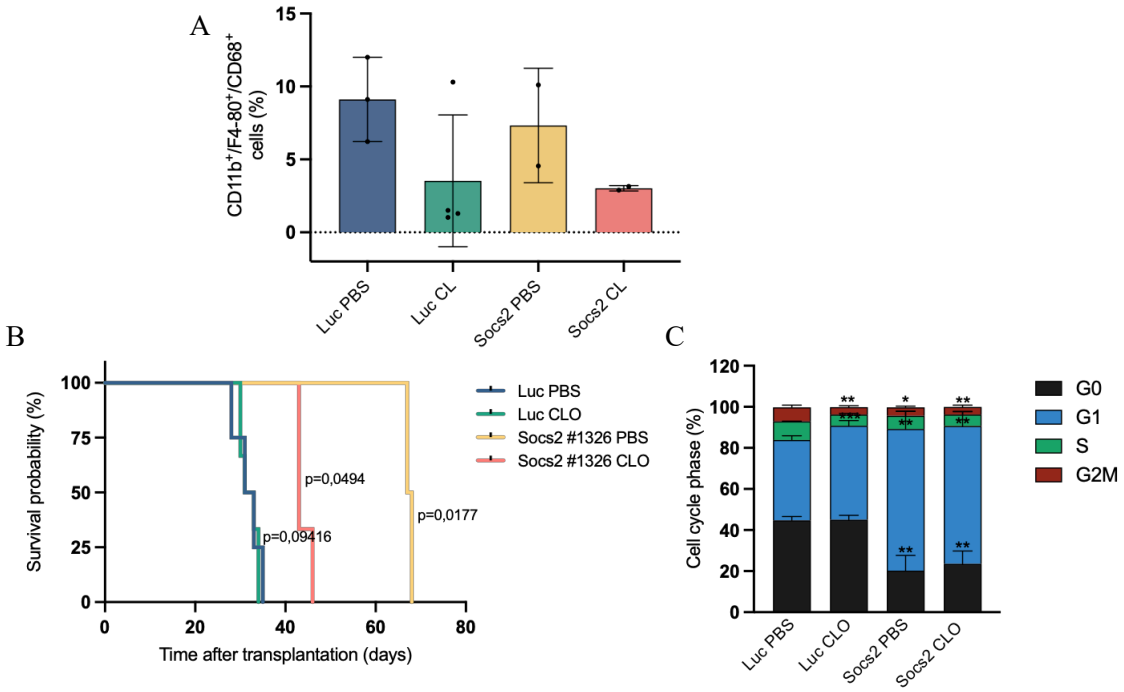

Figure 4.38 Macrophage depletion reduced the survival of mice transplanted with *Socs2*-interfered blasts. **A.** Percentage of CD11b$^+$/F4-80$^+$/CD68$^+$ cells (gated as CD45.1$^-$) evaluated by FACS in the liver of mice treated with control (PBS) and clodronate liposomes at the time of sacrifice. Error bars represent the standard deviation of 3 (shLuc, PBS), 4 (shLuc, CLO) and 2 (sh*Socs2*, PBS and CLO) animals. **B.** Kaplan–Meier overall survival curves in mice transplanted with *Socs2*-interfered (control N=2 and clodronate liposomes N=3) and Luc (control N=4 and clodronate liposomes N=6) blasts, i.p. treated with control or clodronate liposomes one week after transplantation. Statistical significance was calculated using the logrank (Mantel Cox) test (*p<0.05). **C.** Cell cycle analysis of TagRFP$^+$ BM-derived MA9 blasts harboring Luc- and *Socs2*-shRNA determined at the time of sacrifice. Quiescent (G0) cells were defined as Ki67$^-$ cells with a 2n DNA content. Error bars represent the standard deviation of 3 (Luc PBS), 4 (Luc CLO) and 2 (*Socs2* PBS and CLO) animals (*p<0.05, **p<0.01 and ***p<0.001, t-test).

These data suggested that macrophages contributed to the immune clearance of *Socs2*-interfered blasts. Macrophage depletion, however, did not modify the proprotion of quiescent *Socs2*-interfered blasts, suggesting that regulation of quiescence is the primary effect of *Socs2*-interference. Notably, under the same experimental conditions, macrophage-depletion had no effects on the outgrowth of control MA9 blats. This experiment, however, is flawed by the small size of the cohorts analyze

Chapter 5: Discussion

In AML LSCs, a rare cell population at the apex of leukemia hierarchical organisation,[80,186] are thought to be the only leukemic sub-population possessing the self-renewal properties typical of HSCs. Traditional anti-leukemic therapies have limited effects on LSCs, mainly due to their quiescent state.[196] However, the specific role of LSCs quiescence in tumor development and maintenance, and underlying mechanisms are still a matter of intense investigation.

Starting from the observation that some AML oncogenes ($NPMc^+$, PML-RARα and MLL-AF9) are able to enforce a quiescent-related transcriptional program in pre-leukemic HSCs, we decided to investigate the relevance of quiescence in AML growth through an *in vivo* loss-of-function genetic screening, searching for shRNAs selectively depleted during AML expansion from a library of ~1000 shRNAs targeting ~100 genes implicated in the regulation of quiescence. The aim of my Ph.D. project was to validate three of the eight identified hits (*Socs2*, *Stat1* and *Sytl4*) and to further investigate underlying cellular and molecular mechanisms.

STAT1, a transcription factor member of the STAT proteins family, is activated in response to interferons, and it is involved in various biological processes, including immune response, cell proliferation, survival, apoptosis, and differentiation.[278] STATs proteins, upon phosphorylation mediated by receptor-associated kinases and Janus Kinases (JAK), form homo- or heterodimers that translocate to the nucleus and regulate transcription of a series of target genes.[279] The role of *Stat1* in the regulation of quiescence is controversial. In HSCs, *Stat1* has been described as a negative regulator of quiescence, since interferon α treatment induces cell cycle entry of dormant HSCs in a *Stat1*-dependent manner.[280] Moreover, HSCs hyperproliferation, as induced by genetic ablation of *Irgm1*, a positive regulator of HSCs quiescence, is rescued upon *Stat1* depletion, likely through interruption of interferon signaling.[281] On the other hand, *STAT1* activation correlates with cell growth arrest in response to interferon γ, and STAT signaling appears to be a negative regulator of the cell cycle through CKIs induction.[282] Consistently, STAT1 has been described to play either tumor suppressor or pro-tumorigenic functions in several cancer types.[283] Additionally, the JAK2 /STAT1/IRF1(interferon regulatory factor 1) signaling pathway regulates interferon γ – mediated PDL1 overexpression in cancer.[284] Constitutive activation of STAT has been described in both primary AML blasts and leukemic cell lines,[285,286] as well as *Stat1*

maintains high major histocompatibility complex 1 (MHC I) expression and its depletion decreases MHC I expression leading to immune-mediated blasts clearance.[283]

SOCS genes are transcriptional targets of the JAK/STAT signaling pathway, which regulate HSCs quiescence, activation, self-renewal and differentiation through the secretion of various cytokines (e.g. SCF, TPO, GM-CSF…).[287] SOCS proteins negatively regulate JAK/STAT signaling via a classical negative feedback loop. *SOCS2* is overexpressed in HSCs, particularly LT-HSCs, as compared to the more differentiated populations.[288,289] Emerging evidence, however, suggested a tumor suppressor function for *SOCS2*, whose expression is downregulated in several cancers, including breast, lung, hepatocellular and ovarian cancers.[290] In AMLs, instead, high *SOCS2* levels are associated with poor prognosis [288,291,292] and *SOCS2* is known to play a pro-leukemogenic function, contributing to the growth and maintenance of AML LSCs.[14,15] Oncogenic roles of *SOCS2* has been reported also in colon and prostate cancer.[293,294]

Sytl4 is an effector of Rab27a, a key regulator of exosome release.[295] Impaired exosome maturation and secretion has been associated to loss of HSCs quiescence, since HSCs release extracellular vesicles containing cytokines, such as TPO, able to maintain HSCs activity through autocrine signalings.[296] [23]In particular, AML exosomes favor the crosstalk between leukemic blasts and the microenvironment by inhibiting normal HSCs function and modulating immune response, angiogenesis and resistance to therapeutics.[297,298]

Notably, all these three genes are implicated in the regulation of AML growth though microenvironment-related mechanisms involving induction of niche-mediated quiescence and immune evasion. Indeed, we could show that downregulation of *Socs2*, *Stat1* or *Sytl4* in MA9 blasts prevented leukemia outgrowth *in vivo*, validating them as hits of our shRNA screening and establishing their critical role in AML growth. Then, we investigated mechanisms of the anti-leukemic effects exerted upon *Socs2* and *Stat1* interference, with particular reference to their effects on the establishment of quiescence.

Dedicated *in vivo* experiments displayed a progressive increase of G0/quiescent ($Ki67^-$) cells in mice injected with control MA9 blasts. *Socs2*- and *Stat1*-interfered blasts, instead, did not outgrow, and showed, over time, the same cell cycle distribution, with significant increase of cycling cells, marked reduction of quiescent cells and appearance of apoptotic cells, supporting a strong correlation between the ability of leukemic blasts to enter quiescence and their potential to grow *in vivo*. This is, to our knowledge, the first experimental model

clearly showing that quiescence is a feature of growing leukemia and it is not restricted to the small population of LSCs.

Analysis of the effect of *Socs2*- and *Stat1*-silencing on MA9 blasts *in vitro* showed a significant decrease in their clonogenic activity, that is consistent with the inhibition of LSCs regenerative potential, and with the strong growth reduction observed *in vivo*. However, more experiments are required to address this specific point.

Interestingly, *Socs2*- and *Stat1*-KD did not alter *in vitro* proliferation, cell cycle distribution and survival of bulk blasts, as instead observed *in vivo*. Thus, it appears that *Socs2* and *Stat1* interference, though capable of decreasing clonogenic potential of LSCs/progenitors blasts (likely through a cell-autonomous mechanism), does not affect *in vitro* growth of the bulk blast population, suggesting the presence, *in vivo*, of non cell-autonomous mechanisms.

scRNAseq analyses performed on *Socs2*-interfered BM-derived MA9 blasts allowed us to formulate some hypotheses regarding the impact of *Socs2* interference on blasts quiescence and its role in AML growth. In *Socs2*-interfered samples, indeed, we observed aberrant upregulation of genes related to the ISR, including UPR, ATF4 and autophagy, as well as apoptosis, and downregulation of some immune check-point molecules, involved in both innate (CD24a) and adaptive (galectin 9 and VISTA) immune response.

Taken together, these data suggest that AML blasts may need to enter into a transient quiescent state to resolve stress signals through the activation of ISR-related pathways.[265] Then, thanks to the activation of this pro-survival pathway, cells overcome the stress and re-enter into an actively proliferating cell phase. Quiescence, on its turn, may guarantee protection from immune clearance, due to the upregulation of several immune check-point molecules (as shown for normal stem cells[177]).[166,178,180,299] Notably, we showed that: 1) ISR is more active in proliferating MA9 blasts and LT-HSCs (as compared to cell cycle restricted MA9 blasts and LT-HSCs, respectively); 2) expression of immune check-point molecules is instead increased in cell cycle restricted MA9 blasts and LT-HSCs (as compared to proliferating MA9 blasts and HSCs, respectively); and 3) ISR and immune check-point molecules are aberrantly expressed in oncogene-expressing LT-HSCs and in MA9 blasts. Together, these data suggest that MA9 cells activate the ISR as a consequence of a conserved adaptive response to hyperproliferation, and that this response is exaggerated upon *Socs2* depletion. Most notably, regulation of ISR and immune check-point molecules were uncoupled following *Socs2* silencing, with ISR activation and concomitant downregulation of immune check-point molecules, suggesting that the inability to enter quiescence and to

resolve the accumulating stress leads to a switch of the ISR response, from pro-survival to apoptotic. The new genetic program may entail activation of immune-mediated cell death, as documented upon chemotherapy treatments, including down-regulation of immune check-point molecules.[271]

The mechanistic and hierarchical links among quiescence, ISR and expression of immune check-point molecules are not definitively ascertained. Upon *Socs2* and *Stat1* silencing *in vitro*, however, we did not observe any downregulation of Cd24a, galectin 9 and VISTA, suggesting that the downregulation of these immune check-point molecules likely correlates with the quiescent phenotype, and it is not directly caused by the reduction of *Socs2* expression in blasts.

To investigate if immune clearance played a role in the antileukemic effect observed upon *Socs2* and *Stat1* silencing, we evaluated the growth of *Socs2*-interfered and control MA9 blasts in immunodeficient animals (NSG), lacking B, T and NK cells.[254,255] In this case, although animals transplanted with *Socs2*-interferenced blasts still survived longer than control, disease latency was significantly reduced in comparison to that observed in immunocompetent syngeneic animals. More relevant, blasts recovered from *Socs2* moribund animal still contained a sizeable amount of TagRFP^{+} *Socs2*-interfered blasts, that have never been observed in the experiments performed in immunocompetent animals, suggesting a relieve of the selective pressure on *Socs2* interference in NSG mice. Remarkably, there was no difference in the fraction of quiescent cells (Ki67^{-}) in the BM of control and sh*Socs2* mice, and the percentage of quiescent cells in moribund NSG animals was significantly lower compared to the values observed in immunocompetent mice (14,57% ± 1,2% and 39,1% ± 9%, respectively). These data suggest that, in the absence of the adaptive immune system, there is a reduced "requirement" for growing blasts to enter quiescence and/or the equilibrium between cycling and quiescent blast is modified by the fact that cycling blasts are less exposed to the immune-mediated clearance.

We further performed two experiments to evaluate the role of macrophages-mediated innate immune response in our system. The results obtained in NSG animals suggested that the residual effect observed on mice survival and AML growth in these animals is independent by the residual innate response, which however is highly compromised in NSG mice,[254,255] and it may be due to overlapping molecular mechanisms: scRNAseq analysis of sh*Socs2* and control blasts in these animals will likely help us to dissect this complex phenotype. We then tested the role of macrophages in the immunocompetent context, by analyzing the effect of

their depletion in the immune clearance of *Socs2*-interfered blasts in syngeneic animals. Mice transplanted with sh*Socs2* blasts and treated with clodronate liposomes had an earlier disease onset compared to the ones treated with control liposomes, suggesting that also macrophages-mediated innate immune response play a role in the immune clearance of *Socs2*-interfered blasts in immunocompetent mice, while they did not seem to influence the cell cycle status of AML as we could observed in immunocompromised animals.

Overall, the data accumulated so far support the hypothesis that leukemic blasts are forced to enter a transient quiescent state to resolve stress that accumulates as a consequence of oncogene-induced hyperproliferation, as we have shown in our pre-leukemic HSCs model. However, we cannot exclude that the microenvironment, including the anti-tumor immune response, contributes to the observed stress accumulation. Regardless, growth of AML blasts appears as a fine equilibrium between proliferation, with consequent stress accumulation, and cell cycle restriction, needed to resolve the stress. Critical to this balance are the ER stress and UPR, which induce cell cycle exit as part of an adaptive pro-survival response to accumulating stress. The observed association of quiescence and upregulation of immune check-point molecules, may represent a mechanism of protection of normal cells to immune clearance during stress resolution and, in cancer cells, an adaptive mechanism of immune escape. The inability to enter quiescence might alter this equilibrium, since it prevents stress resolution and exacerbate stress accumulation, inducing a genetic reprogramming toward apoptosis, eventually activating ER stress-related immunogenic cell death (ICD).[271]

In AML, it has been previously shown that the ISR/UPR response is pivotal to the survival of both LSCs [277] and blast, [300] but there are no available data connecting the stress response to the cell cycle and mechanisms of tumor escape. In solid tumors, instead, it has been reported that disseminated tumor cells (DTCs) that have reached distant sites are subjected to new microenvironmental cues (e.g. different levels of oxygen, nutrients availability) that require a metabolic adaptation for their survival.[301] In these hostile microenvironments, UPR plays a pivotal role in favoring DTCs survival through the induction of dormancy.[154,170,185] Moreover, DTCs dormancy correlates with their ability to escape immune clearance all over the metastatic process and in particular in the blood stream. [148,302]

Interestingly, since AML blasts possess the innate ability of invasion and migration within other tissues, being able to survive in the bloodstream, home and colonize new tissues as

well as return into the circulation, we may insinuate that AML blasts exploit survival mechanisms similar to the ones observed for metastasizing DTCs.[75,76,303]

More in general, it is possible that tumor cells hijack mechanisms present in specific physiological settings. Agudo *et al*. showed that the machinery necessary for endogenous antigen presentation is downregulated in normal quiescent stem cells, whose immune privilege is associated to their proliferative state and is not a stable property. In particular, while fast cycling stem cells are eliminated by the immune system, slow cycling and dormant stem cells are protected from NK cells and T cells killing.[177] The fact that immune privilege is linked to the quiescent state and is not an intrinsic cell property was also demonstrated for quiescent DTCs in breast and lung cancer by the lab of Massagué.[166,180] In addition, pancreatic ductal carcinoma and lymphoma DTCs subjected to ER stress enter a state of quiescence and downregulate MHC I, evading T cell recognition.[178,299] Our data obtained on LT-HSCs further support a link between proliferation and stress response under physiological conditions, though, in this setting, the upregulation of immune check-point molecules is evident also in G2/M cells, suggesting its requirement to protect cycling HSCs. Of note, an overall increment of stress response is evident in pre-leukemic oncogene-expressing HSCs, as well as a parallel upregulation of immune check-point molecules, further supporting the ability of AML oncogenes to hijack physiological networks to promote survival, favoring AML development.

In AML, it has been demonstrated that the presence of T_{reg} cells in the LSC niche favors disease progression, promoting stemness and quiescence of LSCs.[304] Likewise, LSCs, but not the bulk AML blasts, lack the expression of NKG2D ligands, which protects them from NK cells clearance.[195] However, our data provide clear evidences that quiescence and immune privileges are not restricted to LSCs but are extended to a large part of the leukemic population, and are essential for AML growth. How quiescence is established and the role of a "niche-like" microenvironment (e.g. cells and soluble factors involved) is a critical issue that require further investigations. Indeed, this information will provide additional and crucial molecular targets to interfere with blast quiescence establishment, hopefully leading to AML eradication. In this regard, critical to our model, is the establishment of an inducible shRNA *in vivo* system to formally prove that blocking blasts quiescence in growing leukemia can result in AML regression.

Chapter 6: Future Plans

A set of experiments will be performed to test the key points of our working hypothesis (e.g. *Socs2*-depletion impedes quiescence entry of AML blasts, thus preventing ISR resolution and favoring apoptosis and/or immune-mediated cell death). Since many of the planned experiments are already ongoing, I am confident to be able to conclude the project and prepare a manuscript within the end of 2022.

1. Analysis of mechanisms underlying the anti-leukemic effect of other quiescence regulators (e.g. *Stat1*).

We are currently analyzing scRNAseq data of control and *Stat1*-interfered blasts, obtained from mice sacrificed at different time points post transplantation, to evaluate the occurrence of the same ISR phenotype as observed for *Socs2* (e.g. UPR activation and immune check-point molecules downregulation). Based on the results of these analyses, we will perform on *Stat1*-interfered blasts selected experiments as described for *Socs2*.

Additionally, we will perform a scRNAseq analysis on *Socs2*-interfered blasts grown in NSG animals to understand if they display UPR activation and immune check-point molecules downregulation in the absence of the adaptive immune response.

2. Formal demonstration that hyperactivation of the ISR is a critical step in the anti-leukemic effect of *Socs2*-depletion.

- ***In vivo* monitoring of ISR activation.** To this end, we will take advantage of a recently described lentiviral ATF4 reporter that constitutively expresses TagBFP, to mark transduced cells, and an ATF4-GFP cDNA under the control of two uORFs expressed upon UPR activation. [277] MA9 AML stably expressing the ATF4 reporter will be transduced with control, *Socs2*-shRNA and transplanted in C57BL/6J mice to evaluate ISR activation in Luc- or *Socs2*-interfered proliferating blasts. Moreover, the same experiment in NSG mice will investigate the role of B cells, T cells and NK cells in ISR activation.

- **Genetic or pharmacologic inhibition of the ISR *in vivo.*** To test whether the anti-leukemic effect of *Socs2*-interference is rescued by genetic or pharmacological inhibition of the ISR, we will use specific ATF4 shRNAs or ISR inhibitors, including ISRIB, LY-4 or

AMG-44 BCR-ABL inhibitors, the GSK2606414 inhibitor of PERK or specific inhibitors of IRE-1, a key component of the UPR.

3. Formal demonstration that *Socs2*-depletion switches ISR towards its apoptotic module, with activation of immunogenic cell death (ICD).

To this end, a number of ICD markers will be evaluated *in vivo*, including: 1) expression and/or intracellular localization of heat-shock protein (HSP)70, HSP90, calreticulin (CRT), HMGB proteins, type I IFNs, CXCL10 in *Socs2*-interfered blasts; and 2) engulfment of dying cancer cells by antigen presenting cells (dendritic cells and macrophages) and activation/maturation of $CD8^+$ and $CD4^+$ T-cells in BM and spleen of mice injected with *Socs2*-interefered blasts.

4. Formal demonstration that the anti-leukemic effect of *Socs2* depletion involves the immune clearance of leukemic cells.

To this purpose, we will challenge the anti-leukemic effect of *Socs2*-interference in syngeneic mice after depletion of macrophages (using anti-CD115 antibody, expanding data shown in section 4.10) and T-lymphocytes (using anti-CD8 and anti-CD4 antibodies).

For the last two points, we have recently generated inducible *Socs2*- and *Stat1*-shRNAs lentiviral vectors, which will be suitable to study the effects of acute *Socs2*- or *Stat1*-depletion in the *in vivo* log-growing leukemia and will provide evidence about the putative therapeutic opportunity of interfering with blasts quiescence to induce tumour regression.

References

1. Döhner, H., Weisdorf, D. J. & Bloomfield, C. D. Acute Myeloid Leukemia. *New England Journal of Medicine* **373**, 1136–1152 (2015).
2. Arber, D. A. The 2016 WHO classification of acute myeloid leukemia: What the practicing clinician needs to know. *Seminars in Hematology* vol. 56 90–95 (2019).
3. Kantarjian, H. *et al.* Acute myeloid leukemia: current progress and future directions. *Blood Cancer Journal* vol. 11 (2021).
4. Abdul, G. Acute Leukemia Clinical Presentation. in *Leukemia* (InTech, 2013). doi:10.5772/53531.
5. Yi, M. *et al.* The global burden and attributable risk factor analysis of acute myeloid leukemia in 195 countries and territories from 1990 to 2017: Estimates based on the global burden of disease study 2017. *Journal of Hematology and Oncology* **13**, (2020).
6. American Cancer Society. Key Statistics for Acute Myeloid Leukemia (AML) USA. (2020).
7. Thol, F. & Ganser, A. Treatment of Relapsed Acute Myeloid Leukemia. *Current Treatment Options in Oncology* vol. 21 (2020).
8. Stefan H. Faderl, Hagop M. Kantarjian & Elihu Estey. *Acute Leukemias*. (2021).
9. Daver, N. *et al.* New directions for emerging therapies in acute myeloid leukemia: the next chapter. *Blood Cancer Journal* vol. 10 (2020).
10. Voso, M. T., de Bellis, E. & Ottone, T. Diagnosis and Classification of AML: WHO 2016. in *Acute Myeloid Leukemia. Hematologic Malignancies* (eds. Röllig C. & Ossenkoppele G.J.) (Springer, 2021). doi:10.1007/978-3-030-72676-8_2.
11. Moarii, M. & Papaemmanuil, E. Classification and risk assessment in AML: integrating cytogenetics and molecular profiling. *Hematology Am Soc Hematol Educ Program* **1**, 37–44 (2017).
12. Estey, E. *et al.* Diagnosis and management of AML in adults: 2017 ELN recommendations from an international expert panel. *Blood* **129**, 424–447 (2017).
13. Morita, K. *et al.* Clonal evolution of acute myeloid leukemia revealed by high-throughput single-cell genomics. *Nature Communications* **11**, (2020).
14. Riva, L. *et al.* Acute promyelocytic leukemias share cooperative mutations with other myeloid-leukemia subgroups. *Blood Cancer Journal* vol. 3 (2013).
15. Miles, L. A. *et al.* Single-cell mutation analysis of clonal evolution in myeloid malignancies. *Nature* **587**, 477–482 (2020).
16. Welch, J. S. *et al.* The origin and evolution of mutations in acute myeloid leukemia. *Cell* **150**, 264–278 (2012).
17. Ding, L. *et al.* Clonal evolution in relapsed acute myeloid leukaemia revealed by whole-genome sequencing. *Nature* **481**, 506–510 (2012).
18. Qin, P. *et al.* Integrated decoding hematopoiesis and leukemogenesis using single-cell sequencing and its medical implication. *Cell Discovery* **7**, (2021).
19. Laurenti, E. & Göttgens, B. From haematopoietic stem cells to complex differentiation landscapes. *Nature* vol. 553 418–426 (2018).
20. Velten, L. *et al.* Human haematopoietic stem cell lineage commitment is a continuous process. *Nature Cell Biology* **19**, (2017).
21. Tusi, B. K. *et al.* Population snapshots predict early haematopoietic and erythroid hierarchies. *Nature* **555**, (2018).
22. Chao, M. P., Seita, J. & Weissman, I. L. Establishment of a Normal Hematopoietic and Leukemia Stem Cell Hierarchy. *Cold Spring Harbor Symposia on Quantitative Biology* **73**, (2008).
23. Yamashita, M., Dellorusso, P. v., Olson, O. C. & Passegué, E. Dysregulated haematopoietic stem cell behaviour in myeloid leukaemogenesis. *Nature Reviews Cancer* vol. 20 365–382 (2020).

24. Wei, C., Yu, P. & Cheng, L. Hematopoietic Reprogramming Entangles with Hematopoiesis. *Trends in Cell Biology* **30**, (2020).
25. Orkin, S. H. & Zon, L. I. Hematopoiesis: An Evolving Paradigm for Stem Cell Biology. *Cell* **132**, (2008).
26. Yamada, T., Park, C. S. & Lacorazza, H. D. Genetic control of quiescence in hematopoietic stem cells. *Cell Cycle* **12**, (2013).
27. Nakamura-Ishizu, A., Takizawa, H. & Suda, T. The analysis, roles and regulation of quiescence in hematopoietic stem cells. *Development* **141**, (2014).
28. O'Reilly, E., Zeinabad, H. A. & Szegezdi, E. Hematopoietic versus leukemic stem cell quiescence: Challenges and therapeutic opportunities. *Blood Reviews* (2021) doi:10.1016/j.blre.2021.100850.
29. Sun, S. *et al.* Chromatin remodeler Znhit1 preserves hematopoietic stem cell quiescence by determining the accessibility of distal enhancers. *Leukemia* **34**, (2020).
30. Pietras, E. M., Warr, M. R. & Passegué, E. Cell cycle regulation in hematopoietic stem cells. *Journal of Cell Biology* **195**, (2011).
31. Matthews, H. K., Bertoli, C. & de Bruin, R. A. M. Cell cycle control in cancer. *Nature Reviews Molecular Cell Biology* (2021) doi:10.1038/s41580-021-00404-3.
32. Cheng, T. *et al.* Hematopoietic Stem Cell Quiescence Maintained by p21cip1/waf1. *Science* **287**, (2000).
33. Matsumoto, A. *et al.* p57 Is Required for Quiescence and Maintenance of Adult Hematopoietic Stem Cells. *Cell Stem Cell* **9**, (2011).
34. Zou, P. *et al.* p57Kip2 and p27Kip1 Cooperate to Maintain Hematopoietic Stem Cell Quiescence through Interactions with Hsc70. *Cell Stem Cell* **9**, (2011).
35. Gao, Y. *et al.* Small-molecule inhibitors targeting INK4 protein p18INK4C enhance ex vivo expansion of haematopoietic stem cells. *Nature Communications* **6**, (2015).
36. Tesio, M. & Trumpp, A. Breaking the Cell Cycle of HSCs by p57 and Friends. *Cell Stem Cell* **9**, (2011).
37. Laurenti, E. *et al.* CDK6 Levels Regulate Quiescence Exit in Human Hematopoietic Stem Cells. *Cell Stem Cell* **16**, (2015).
38. Liu, Y. *et al.* p53 Regulates Hematopoietic Stem Cell Quiescence. *Cell Stem Cell* **4**, (2009).
39. Zhu, J. *et al.* Growth Factor Independent-1 Induced by IL-4 Regulates Th2 Cell Proliferation. *Immunity* **16**, (2002).
40. Taniura, H., Matsumoto, K. & Yoshikawa, K. Physical and Functional Interactions of Neuronal Growth Suppressor Necdin with p53. *Journal of Biological Chemistry* **274**, (1999).
41. Wang, Z., Li, G., Tse, W. & Bunting, K. D. Conditional deletion of STAT5 in adult mouse hematopoietic stem cells causes loss of quiescence and permits efficient nonablative stem cell replacement. *Blood* **113**, (2009).
42. Peng, S. L. Immune regulation by Foxo transcription factors. *Autoimmunity* **40**, (2007).
43. Zhang, J. *et al.* PTEN maintains haematopoietic stem cells and acts in lineage choice and leukaemia prevention. *Nature* **441**, (2006).
44. Lechman, E. R. *et al.* miR-126 Regulates Distinct Self-Renewal Outcomes in Normal and Malignant Hematopoietic Stem Cells. *Cancer Cell* **29**, (2016).
45. Perez-Roger, I. Cyclins D1 and D2 mediate Myc-induced proliferation via sequestration of p27Kip1 and p21Cip1. *The EMBO Journal* **18**, (1999).
46. Bradshaw, A. D. Regulation of cell behavior by extracellular proteins. in *Principles of Tissue Engineering* (Elsevier, 2020). doi:10.1016/B978-0-12-818422-6.00013-7.
47. Nilsson, S. K. *et al.* Osteopontin, a key component of the hematopoietic stem cell niche and regulator of primitive hematopoietic progenitor cells. *Blood* **106**, (2005).
48. Tzeng, Y.-S. *et al.* Loss of Cxcl12/Sdf-1 in adult mice decreases the quiescent state of hematopoietic stem/progenitor cells and alters the pattern of hematopoietic regeneration after myelosuppression. *Blood* **117**, (2011).
49. Nie, Y., Han, Y.-C. & Zou, Y.-R. CXCR4 is required for the quiescence of primitive hematopoietic cells. *Journal of Experimental Medicine* **205**, (2008).

50. Ramakrishnan, R. *et al.* CXCR4 Signaling Has a CXCL12-Independent Essential Role in Murine MLL-AF9-Driven Acute Myeloid Leukemia. *Cell Reports* **31**, (2020).
51. Sinclair, A. *et al.* CXCR2 and CXCL4 regulate survival and self-renewal of hematopoietic stem/progenitor cells. *Blood* **128**, (2016).
52. Bruns, I. *et al.* Megakaryocytes regulate hematopoietic stem cell quiescence through CXCL4 secretion. *Nature Medicine* **20**, (2014).
53. Zhao, M. *et al.* Megakaryocytes maintain homeostatic quiescence and promote post-injury regeneration of hematopoietic stem cells. *Nature Medicine* **20**, (2014).
54. Wang, X. *et al.* TGF-β1 Negatively Regulates the Number and Function of Hematopoietic Stem Cells. *Stem cell reports* **11**, (2018).
55. Jiang, L. *et al.* SHP-1 regulates hematopoietic stem cell quiescence by coordinating TGF-β signaling. *Journal of Experimental Medicine* **215**, (2018).
56. Katoh. Integrative genomic analyses of CXCR4: Transcriptional regulation of CXCR4 based on TGFβ, Nodal, Activin signaling and POU5F1, FOXA2, FOXC2, FOXH1, SOX17, and GFI1 transcription factors. *International Journal of Oncology* **36**, (2009).
57. Qian, H. *et al.* Critical Role of Thrombopoietin in Maintaining Adult Quiescent Hematopoietic Stem Cells. *Cell Stem Cell* **1**, (2007).
58. Gomei, Y. *et al.* Functional Difference of Two Tie2 Ligands, Angiopoietin-1 and -2, in the Regulation of the Adult Bone Marrow Hematopoietic Stem Cells. *Blood* **112**, (2008).
59. Arai, F., Ohneda, O., Miyamoto, T., Zhang, X. Q. & Suda, T. Mesenchymal Stem Cells in Perichondrium Express Activated Leukocyte Cell Adhesion Molecule and Participate in Bone Marrow Formation. *Journal of Experimental Medicine* **195**, (2002).
60. Saw, S., Weiss, A., Khokha, R. & Waterhouse, P. D. Metalloproteases: On the Watch in the Hematopoietic Niche. *Trends in Immunology* **40**, (2019).
61. Schönherr, E. & Hausser, H.-J. Extracellular Matrix and Cytokines: A Functional Unit. *Developmental Immunology* **7**, (2000).
62. Trumpp, A., Essers, M. & Wilson, A. Awakening dormant haematopoietic stem cells. *Nature Reviews Immunology* **10**, (2010).
63. Welch, J. S. *et al.* The origin and evolution of mutations in acute myeloid leukemia. *Cell* **150**, 264–278 (2012).
64. Valent, P. *et al.* Clonal Hematopoiesis with Oncogenic Potential (CHOP): Separation from CHIP and Roads to AML. *International Journal of Molecular Sciences* **20**, (2019).
65. Palomo, L. *et al.* Molecular landscape and clonal architecture of adult myelodysplastic/myeloproliferative neoplasms. *Blood* **136**, (2020).
66. Jaiswal, S. *et al.* Age-Related Clonal Hematopoiesis Associated with Adverse Outcomes. *New England Journal of Medicine* **371**, (2014).
67. Ferrando, A. A. & López-Otín, C. Clonal evolution in leukemia. *Nature Medicine* vol. 23 1135–1145 (2017).
68. Vetrie, D., Helgason, G. V. & Copland, M. The leukaemia stem cell: similarities, differences and clinical prospects in CML and AML. *Nature Reviews Cancer* vol. 20 158–173 (2020).
69. Corces, M. R. *et al.* Lineage-specific and single-cell chromatin accessibility charts human hematopoiesis and leukemia evolution. *Nature Genetics* **48**, (2016).
70. Mohrin, M. *et al.* Hematopoietic Stem Cell Quiescence Promotes Error-Prone DNA Repair and Mutagenesis. *Cell Stem Cell* **7**, (2010).
71. Zheng, R. & Small, D. Mutant FLT3 signaling contributes to a block in myeloid differentiation. *Leukemia & Lymphoma* **46**, (2005).
72. Viadana, E., Bross, I. D. J. & Pickren, J. W. An Autopsy Study of the Metastatic Patterns of Human Leukemias. *Oncology* **35**, (1978).
73. Laningham, F. H. *et al.* Childhood central nervous system leukemia: historical perspectives, current therapy, and acute neurological sequelae. *Neuroradiology* **49**, (2007).
74. Sipkins, D. A. *et al.* In vivo imaging of specialized bone marrow endothelial microdomains for tumour engraftment. *Nature* **435**, (2005).
75. Whiteley, A. E., Price, T. T., Cantelli, G. & Sipkins, D. A. Leukaemia: a model metastatic disease. *Nature Reviews Cancer* **21**, (2021).

76. Méndez-Ferrer, S. *et al.* Bone marrow niches in haematological malignancies. *Nature Reviews Cancer* vol. 20 285–298 (2020).
77. Ebinger, S. *et al.* Characterization of Rare, Dormant, and Therapy-Resistant Cells in Acute Lymphoblastic Leukemia. *Cancer Cell* **30**, (2016).
78. Ishikawa, F. *et al.* Chemotherapy-resistant human AML stem cells home to and engraft within the bone-marrow endosteal region. *Nature Biotechnology* **25**, (2007).
79. Hanoun, M. *et al.* Acute Myelogenous Leukemia-Induced Sympathetic Neuropathy Promotes Malignancy in an Altered Hematopoietic Stem Cell Niche. *Cell Stem Cell* **15**, (2014).
80. Bonnet, D. & Dick, J. E. Human acute myeloid leukemia is organized as a hierarchy that originates from a primitive hematopoietic cell. *Nature Medicine* **3**, (1997).
81. Essers, M. A. G. & Trumpp, A. Targeting leukemic stem cells by breaking their dormancy. *Molecular Oncology* vol. 4 443–450 (2010).
82. Arnone, M. *et al.* Acute myeloid leukemia stem cells: The challenges of phenotypic heterogeneity. *Cancers* vol. 12 1–21 (2020).
83. Karantanos, T. & Jones, R. J. Acute Myeloid Leukemia Stem Cell Heterogeneity and Its Clinical Relevance. in (2019). doi:10.1007/978-3-030-14366-4_9.
84. Gilliland, D. G. & Griffin, J. D. The roles of FLT3 in hematopoiesis and leukemia. *Blood* **100**, (2002).
85. Genomic and Epigenomic Landscapes of Adult De Novo Acute Myeloid Leukemia. *New England Journal of Medicine* **368**, (2013).
86. Thol, F. *et al.* Acute myeloid leukemia derived from lympho-myeloid clonal hematopoiesis. *Leukemia* **31**, (2017).
87. Shlush, L. I. *et al.* Identification of pre-leukaemic haematopoietic stem cells in acute leukaemia. *Nature* **506**, (2014).
88. Mer, A. S. *et al.* Biological and therapeutic implications of a unique subtype of NPM1 mutated AML. *Nature Communications* **12**, (2021).
89. Rau, R. & Brown, P. Nucleophosmin (NPM1) mutations in adult and childhood acute myeloid leukaemia: Towards definition of a new leukaemia entity. *Hematological Oncology* **27**, 171–181 (2009).
90. Brunetti, L., Gundry, M. C. & Goodell, M. A. New insights into the biology of acute myeloid leukemia with mutated NPM1. *International Journal of Hematology* vol. 110 150–160 (2019).
91. Heath, E. M. *et al.* Biological and clinical consequences of NPM1 mutations in AML. *Leukemia* vol. 31 798–807 (2017).
92. Metzeler, K. H. *et al.* Spectrum and prognostic relevance of driver gene mutations in acute myeloid leukemia. *Blood* **128**, (2016).
93. Borer, R. A., Lehner, C. F., Eppenberger, H. M. & Nigg, E. A. Major nucleolar proteins shuttle between nucleus and cytoplasm. *Cell* **56**, (1989).
94. Cheng, K. *et al.* The cytoplasmic NPM mutant induces myeloproliferation in a transgenic mouse model. *Blood* **115**, (2010).
95. Mallardo, M. *et al.* NPMc+ and FLT3_ITD mutations cooperate in inducing acute leukaemia in a novel mouse model. *Leukemia* **27**, (2013).
96. Vassiliou, G. S. *et al.* Mutant nucleophosmin and cooperating pathways drive leukemia initiation and progression in mice. *Nature Genetics* **43**, (2011).
97. Krönke, J. *et al.* Clonal evolution in relapsed NPM1-mutated acute myeloid leukemia. *Blood* **122**, (2013).
98. Jimenez, J. J., Chale, R. S., Abad, A. C., Schally, A. v & Frost, P. *Acute promyelocytic leukemia (APL): a review of the literature*. *Oncotarget* vol. 11 www.oncotarget.com (2020).
99. Ronchini, C. *et al.* PML-RARA-Associated cooperating mutations belong to a transcriptional network that is deregulated in myeloid leukemias. *Leukemia* **31**, 1975–1986 (2017).
100. Sirulnik, A., Melnick, A., Zelent, A., Licht, J. & Zelent, A. Molecular pathogenesis of acute promyelocytic leukaemia and APL variants. *BEST PRACTICE & RESEARCH CLINICAL HAEMATOLOGY* **16**, 387–408 (2003).

101. Redner, R. L., Chen, J. D., Rush, E. A., Li, H. & Pollock, S. L. The t(5;17) acute promyelocytic leukemia fusion protein NPM-RAR interacts with co-repressor and co-activator proteins and exhibits both positive and negative transcriptional properties. *Blood* **95**, (2000).
102. Nowak, D., Stewart, D. & Koeffler, H. P. Differentiation therapy of leukemia: 3 decades of development. (2009) doi:10.1182/blood-2009-01.
103. Yilmaz, M., Kantarjian, H. & Ravandi, F. Acute promyelocytic leukemia current treatment algorithms. *Blood Cancer Journal* vol. 11 (2021).
104. de Thé, H., Pandolfi, P. P. & Chen, Z. Acute Promyelocytic Leukemia: A Paradigm for Oncoprotein-Targeted Cure. *Cancer Cell* **32**, (2017).
105. Martelli, M. P. *et al.* Arsenic trioxide and all-trans retinoic acid target NPM1 mutant oncoprotein levels and induce apoptosis in NPM1-mutated AML cells. *Blood* **125**, (2015).
106. el Hajj, H. *et al.* Retinoic acid and arsenic trioxide trigger degradation of mutated NPM1, resulting in apoptosis of AML cells. *Blood* **125**, 3447–3454 (2015).
107. Hleihel, R. *et al.* A Pin1/PML/P53 axis activated by retinoic acid in NPM-1c-acute myeloid leukemia. *Haematologica* (2021) doi:10.3324/haematol.2020.274878.
108. Zou, Q. *et al.* NPM1 Mutant Mediated PML Delocalization and Stabilization Enhances Autophagy and Cell Survival in Leukemic Cells. *Theranostics* **7**, (2017).
109. Matsuo, H. *et al.* Fusion partner-specific mutation profiles and KRAS mutations as adverse prognostic factors in MLL-rearranged AML. *Blood Advances* **4**, 4623–4631 (2020).
110. Meyer, C. *et al.* The MLL recombinome of acute leukemias in 2017. *Leukemia* **32**, 273–284 (2018).
111. Milne, T. A. *et al.* MLL Targets SET Domain Methyltransferase Activity to Hox Gene Promoters. *Molecular Cell* **10**, 1107–1117 (2002).
112. Muntean, A. G. *et al.* The PAF Complex Synergizes with MLL Fusion Proteins at HOX Loci to Promote Leukemogenesis. *Cancer Cell* **17**, 609–621 (2010).
113. Alharbi, R. A., Pettengell, R., Pandha, H. S. & Morgan, R. The role of HOX genes in normal hematopoiesis and acute leukemia. *Leukemia* vol. 27 1000–1008 (2013).
114. Muntean, A. G. & Hess, J. L. The pathogenesis of mixed-lineage leukemia. *Annual Review of Pathology: Mechanisms of Disease* vol. 7 283–301 (2012).
115. Yokoyama, A. *et al.* The Menin Tumor Suppressor Protein Is an Essential Oncogenic Cofactor for MLL-Associated Leukemogenesis. *Cell* **123**, (2005).
116. Grembecka, J. *et al.* Menin-MLL inhibitors reverse oncogenic activity of MLL fusion proteins in leukemia. *Nature Chemical Biology* **8**, (2012).
117. Issa, G. C. *et al.* Therapeutic implications of menin inhibition in acute leukemias. *Leukemia* **35**, (2021).
118. Borkin, D. *et al.* Pharmacologic Inhibition of the Menin-MLL Interaction Blocks Progression of MLL Leukemia In Vivo. *Cancer Cell* **27**, (2015).
119. Klossowski, S. *et al.* Menin inhibitor MI-3454 induces remission in MLL1-rearranged and NPM1-mutated models of leukemia. *Journal of Clinical Investigation* **130**, (2020).
120. Bernt, K. M. *et al.* MLL-Rearranged Leukemia Is Dependent on Aberrant H3K79 Methylation by DOT1L. *Cancer Cell* **20**, (2011).
121. Stein, E. M. *et al.* The DOT1L inhibitor pinometostat reduces H3K79 methylation and has modest clinical activity in adult acute leukemia. *Blood* **131**, (2018).
122. Perner, F. *et al.* Novel inhibitors of the histone methyltransferase DOT1L show potent antileukemic activity in patient-derived xenografts. *Blood* **136**, (2020).
123. Alcalay, M. *et al.* Acute myeloid leukemia bearing cytoplasmic nucleophosmin (NPMc+ AML) shows a distinct gene expression profile characterized by up-regulation of genes involved in stem-cell maintenance. *Blood* **106**, (2005).
124. Hourigan, C. S. & Aplan, P. D. Accurate Medicine: Indirect Targeting of *NPM1* -Mutated AML. *Cancer Discovery* **6**, (2016).
125. Kühn, M. W. M. *et al.* Targeting Chromatin Regulators Inhibits Leukemogenic Gene Expression in *NPM1* Mutant Leukemia. *Cancer Discovery* **6**, (2016).
126. Vitale, I. *et al.* Mutational and Antigenic Landscape in Tumor Progression and Cancer Immunotherapy. *Trends in Cell Biology* **29**, (2019).

127. Wang, J. *et al.* Clonal evolution of glioblastoma under therapy. *Nature Genetics* **48**, (2016).
128. Vitale, I., Shema, E., Loi, S. & Galluzzi, L. Intratumoral heterogeneity in cancer progression and response to immunotherapy. *Nature Medicine* vol. 27 212–224 (2021).
129. van Galen, P. *et al.* Single-Cell RNA-Seq Reveals AML Hierarchies Relevant to Disease Progression and Immunity. *Cell* **176**, (2019).
130. Teixeira, V. H. *et al.* Deciphering the genomic, epigenomic, and transcriptomic landscapes of pre-invasive lung cancer lesions. *Nature Medicine* **25**, (2019).
131. Hinohara, K. & Polyak, K. Intratumoral Heterogeneity: More Than Just Mutations. *Trends in Cell Biology* vol. 29 569–579 (2019).
132. Azizi, E. *et al.* Single-Cell Map of Diverse Immune Phenotypes in the Breast Tumor Microenvironment. *Cell* **174**, (2018).
133. Costa, A. *et al.* Fibroblast Heterogeneity and Immunosuppressive Environment in Human Breast Cancer. *Cancer Cell* **33**, (2018).
134. Lawson, D. A., Kessenbrock, K., Davis, R. T., Pervolarakis, N. & Werb, Z. Tumour heterogeneity and metastasis at single-cell resolution. *Nature Cell Biology* vol. 20 1349–1360 (2018).
135. Schulz, W. L. *et al.* Impact of intra-tumoral heterogeneity detected by next-generation sequencing on acute myeloid leukemia survival. *Leukemia and Lymphoma* vol. 61 3269–3271 (2020).
136. Sandén, C. *et al.* Clonal competition within complex evolutionary hierarchies shapes AML over time. *Nature Communications* **11**, (2020).
137. Ramón y Cajal, S. *et al.* Clinical implications of intratumor heterogeneity: challenges and opportunities. *Journal of Molecular Medicine* vol. 98 161–177 (2020).
138. Marusyk, A., Janiszewska, M. & Polyak, K. Intratumor Heterogeneity: The Rosetta Stone of Therapy Resistance. *Cancer Cell* vol. 37 471–484 (2020).
139. Brocks, D. *et al.* Intratumor DNA Methylation Heterogeneity Reflects Clonal Evolution in Aggressive Prostate Cancer. *Cell Reports* **8**, (2014).
140. Silvera, D., Formenti, S. C. & Schneider, R. J. Translational control in cancer. *Nature Reviews Cancer* **10**, (2010).
141. Petti, A. A. *et al.* A general approach for detecting expressed mutations in AML cells using single cell RNA-sequencing. *Nature Communications* **10**, (2019).
142. Sharma, S. v. *et al.* A Chromatin-Mediated Reversible Drug-Tolerant State in Cancer Cell Subpopulations. *Cell* **141**, (2010).
143. de Angelis, M. L., Francescangeli, F., la Torre, F. & Zeuner, A. Stem Cell Plasticity and Dormancy in the Development of Cancer Therapy Resistance. *Frontiers in Oncology* **9**, (2019).
144. Tzamali, E., Tzedakis, G. & Sakkalis, V. Modeling How Heterogeneity in Cell Cycle Length Affects Cancer Cell Growth Dynamics in Response to Treatment. *Frontiers in Oncology* **10**, (2020).
145. Coller, H. A. The Essence of Quiescence. *Science* **334**, (2011).
146. Phan, T. G. & Croucher, P. I. The dormant cancer cell life cycle. *Nature Reviews Cancer* **20**, (2020).
147. Hadfield, G. The Dormant Cancer Cell. *BMJ* **2**, (1954).
148. Banys-Paluchowski, M., Reinhardt, F. & Fehm, T. Disseminated Tumor Cells and Dormancy in Breast Cancer Progression. in (2020). doi:10.1007/978-3-030-35805-1_3.
149. Owen, K. L. *et al.* Prostate cancer cell-intrinsic interferon signaling regulates dormancy and metastatic outgrowth in bone. *EMBO reports* **21**, (2020).
150. Parker, A. L. & Cox, T. R. The Role of the ECM in Lung Cancer Dormancy and Outgrowth. *Frontiers in Oncology* **10**, (2020).
151. Zhu, X. *et al.* FBX8 promotes metastatic dormancy of colorectal cancer in liver. *Cell Death & Disease* **11**, (2020).
152. Cole, A. J. *et al.* NFATC4 promotes quiescence and chemotherapy resistance in ovarian cancer. *JCI Insight* **5**, (2020).
153. Atkins, R. J. *et al.* Cell quiescence correlates with enhanced glioblastoma cell invasion and cytotoxic resistance. *Experimental Cell Research* **374**, (2019).

154. Ranganathan, A. C., Ojha, S., Kourtidis, A., Conklin, D. S. & Aguirre-Ghiso, J. A. Dual Function of Pancreatic Endoplasmic Reticulum Kinase in Tumor Cell Growth Arrest and Survival. *Cancer Research* **68**, (2008).
155. Santoni, M. *et al.* Circulating Tumor Cells in Renal Cell Carcinoma: Recent Findings and Future Challenges. *Frontiers in Oncology* **9**, (2019).
156. Khoo, W. H. *et al.* A niche-dependent myeloid transcriptome signature defines dormant myeloma cells. *Blood* **134**, (2019).
157. Senft, D. & Jeremias, I. A rare subgroup of leukemia stem cells harbors relapse-inducing potential in acute lymphoblastic leukemia. *Experimental Hematology* **69**, (2019).
158. Xi, Z. *et al.* Guttiferone K impedes cell cycle re-entry of quiescent prostate cancer cells via stabilization of FBXW7 and subsequent c-MYC degradation. *Cell Death & Disease* **7**, (2016).
159. Sobecki, M. *et al.* Cell-Cycle Regulation Accounts for Variability in Ki-67 Expression Levels. *Cancer Research* **77**, (2017).
160. Reya, T., Morrison, S. J., Clarke, M. F. & Weissman, I. L. Stem cells, cancer, and cancer stem cells. *Nature* **414**, (2001).
161. Sosa, M. S. *et al.* NR2F1 controls tumour cell dormancy via SOX9- and RARβ-driven quiescence programmes. *Nature Communications* **6**, (2015).
162. Lawson, M. A. *et al.* Osteoclasts control reactivation of dormant myeloma cells by remodelling the endosteal niche. *Nature Communications* **6**, (2015).
163. Pack, L. R., Daigh, L. H. & Meyer, T. Putting the brakes on the cell cycle: mechanisms of cellular growth arrest. *Current Opinion in Cell Biology* **60**, (2019).
164. Roesch, A. *et al.* A Temporarily Distinct Subpopulation of Slow-Cycling Melanoma Cells Is Required for Continuous Tumor Growth. *Cell* **141**, (2010).
165. Galvao, R. P. *et al.* Transformation of quiescent adult oligodendrocyte precursor cells into malignant glioma through a multistep reactivation process. *Proceedings of the National Academy of Sciences* **111**, (2014).
166. Malladi, S. *et al.* Metastatic Latency and Immune Evasion through Autocrine Inhibition of WNT. *Cell* **165**, (2016).
167. Sun, Y. *et al.* Single-cell landscape of the ecosystem in early-relapse hepatocellular carcinoma. *Cell* **184**, (2021).
168. Chen, J. *et al.* A restricted cell population propagates glioblastoma growth after chemotherapy. *Nature* **488**, (2012).
169. Meldi, K. *et al.* Specific molecular signatures predict decitabine response in chronic myelomonocytic leukemia. *Journal of Clinical Investigation* **125**, (2015).
170. Schewe, D. M. & Aguirre-Ghiso, J. A. ATF6 -Rheb-mTOR signaling promotes survival of dormant tumor cells in vivo. *Proceedings of the National Academy of Sciences* **105**, (2008).
171. Carlson, P. *et al.* Targeting the perivascular niche sensitizes disseminated tumour cells to chemotherapy. *Nature Cell Biology* **21**, (2019).
172. Aguirre-Ghiso, J. A. How dormant cancer persists and reawakens. *Science* **361**, (2018).
173. Naumov, G. N. *et al.* Ineffectiveness of Doxorubicin Treatment on Solitary Dormant Mammary Carcinoma Cells or Late-developing Metastases. *Breast Cancer Research and Treatment* **82**, (2003).
174. Dillekås, H., Rogers, M. S. & Straume, O. Are 90% of deaths from cancer caused by metastases? *Cancer Medicine* **8**, (2019).
175. Eyles, J. *et al.* Tumor cells disseminate early, but immunosurveillance limits metastatic outgrowth, in a mouse model of melanoma. *Journal of Clinical Investigation* **120**, (2010).
176. Merino, D. *et al.* Barcoding reveals complex clonal behavior in patient-derived xenografts of metastatic triple negative breast cancer. *Nature Communications* **10**, (2019).
177. Agudo, J. *et al.* Quiescent Tissue Stem Cells Evade Immune Surveillance. *Immunity* **48**, (2018).
178. Pommier, A. *et al.* Unresolved endoplasmic reticulum stress engenders immune-resistant, latent pancreatic cancer metastases. *Science* **360**, (2018).
179. Pantel, K. *et al.* Frequent down-regulation of major histocompatibility class I antigen expression on individual micrometastatic carcinoma cells. *Cancer research* **51**, (1991).

180. Laughney, A. M. *et al.* Regenerative lineages and immune-mediated pruning in lung cancer metastasis. *Nature Medicine* **26**, (2020).
181. Axelrod, M. L., Cook, R. S., Johnson, D. B. & Balko, J. M. Biological Consequences of MHC-II Expression by Tumor Cells in Cancer. *Clinical Cancer Research* **25**, (2019).
182. Fujisaki, J. *et al.* In vivo imaging of Treg cells providing immune privilege to the haematopoietic stem-cell niche. *Nature* **474**, (2011).
183. Cahu, X. *et al.* Bone marrow sites differently imprint dormancy and chemoresistance to T-cell acute lymphoblastic leukemia. *Blood Advances* **1**, (2017).
184. Brunton, L. L., Lazo, J. S., Parker, K., Buxton, I. & Blumenthal, D. Book Review: Goodman and Gilman's The Pharmacological Basis of Therapeutics: Digital Edition, 11th Edition. *Annals of Pharmacotherapy* **40**, (2006).
185. Ranganathan, A. C., Zhang, L., Adam, A. P. & Aguirre-Ghiso, J. A. Functional Coupling of p38-Induced Up-regulation of BiP and Activation of RNA-Dependent Protein Kinase–Like Endoplasmic Reticulum Kinase to Drug Resistance of Dormant Carcinoma Cells. *Cancer Research* **66**, (2006).
186. Pollyea, D. A. & Jordan, C. T. Therapeutic targeting of acute myeloid leukemia stem cells. (2017) doi:10.1182/blood-2016-10.
187. Lapidot, T. *et al.* A cell initiating human acute myeloid leukaemia after transplantation into SCID mice. *Nature* **367**, (1994).
188. Gerber, J. M. *et al.* Association of acute myeloid leukemias most immature phenotype with risk groups and outcomes. *Haematologica* **101**, (2016).
189. Sarry, J.-E. *et al.* Human acute myelogenous leukemia stem cells are rare and heterogeneous when assayed in NOD/SCID/IL2Rγc-deficient mice. *Journal of Clinical Investigation* **121**, (2011).
190. Lagadinou, E. D. *et al.* BCL-2 Inhibition Targets Oxidative Phosphorylation and Selectively Eradicates Quiescent Human Leukemia Stem Cells. *Cell Stem Cell* **12**, (2013).
191. Pietras, E. M. *et al.* Re-entry into quiescence protects hematopoietic stem cells from the killing effect of chronic exposure to type I interferons. *Journal of Experimental Medicine* **211**, (2014).
192. Pei, S. *et al.* AMPK/FIS1-Mediated Mitophagy Is Required for Self-Renewal of Human AML Stem Cells. *Cell Stem Cell* **23**, 86-100.e6 (2018).
193. Xu, Y. *et al.* Regulatory T cells promote the stemness of leukemia stem cells through IL10 cytokine-related signaling pathway. *Leukemia* (2021) doi:10.1038/s41375-021-01375-2.
194. Majeti, R. *et al.* CD47 Is an Adverse Prognostic Factor and Therapeutic Antibody Target on Human Acute Myeloid Leukemia Stem Cells. *Cell* **138**, (2009).
195. Paczulla, A. M. *et al.* Absence of NKG2D ligands defines leukaemia stem cells and mediates their immune evasion. *Nature* **572**, (2019).
196. Shlush, L. I. *et al.* Tracing the origins of relapse in acute myeloid leukaemia to stem cells. *Nature* **547**, (2017).
197. Goddard, E. T., Bozic, I., Riddell, S. R. & Ghajar, C. M. Dormant tumour cells, their niches and the influence of immunity. *Nature Cell Biology* **20**, (2018).
198. Jones, C. L. *et al.* Inhibition of Amino Acid Metabolism Selectively Targets Human Leukemia Stem Cells. *Cancer Cell* **34**, (2018).
199. Sheng, Y. *et al.* FOXM1 regulates leukemia stem cell quiescence and survival in MLL-rearranged AML. *Nature Communications* **11**, 928 (2020).
200. Silvestri, G. *et al.* Persistence of Drug-Resistant Leukemic Stem Cells and Impaired NK Cell Immunity in CML Patients Depend on *MIR300* Antiproliferative and PP2A-Activating Functions. *Blood Cancer Discovery* **1**, 48–67 (2020).
201. Schepers, K. *et al.* Myeloproliferative Neoplasia Remodels the Endosteal Bone Marrow Niche into a Self-Reinforcing Leukemic Niche. *Cell Stem Cell* **13**, 285–299 (2013).
202. Stauber, J., Greally, J. M. & Steidl, U. Preleukemic and leukemic evolution at the stem cell level. *Blood* **137**, (2021).
203. Morris, L. G. T. *et al.* Pan-cancer analysis of intratumor heterogeneity as a prognostic determinant of survival. *Oncotarget* **7**, (2016).

204. Sánchez-Corrales, Y. E., Pohle, R. V. C., Castellano, S. & Giustacchini, A. Taming Cell-to-Cell Heterogeneity in Acute Myeloid Leukaemia With Machine Learning. *Frontiers in Oncology* vol. 11 (2021).
205. Döhner, H., Wei, A. H. & Löwenberg, B. Towards precision medicine for AML. *Nature Reviews Clinical Oncology* vol. 18 577–590 (2021).
206. Bullinger, L., Döhner, K. & Döhner, H. Genomics of Acute Myeloid Leukemia Diagnosis and Pathways. *Journal of Clinical Oncology* **35**, (2017).
207. Smith, C. C. The growing landscape of FLT3 inhibition in AML. *Hematology* **2019**, (2019).
208. Molenaar, R. J. *et al. IDH1/2* Mutations Sensitize Acute Myeloid Leukemia to PARP Inhibition and This Is Reversed by IDH1/2-Mutant Inhibitors. *Clinical Cancer Research* **24**, (2018).
209. Stein, E. M. *et al.* Ivosidenib or enasidenib combined with intensive chemotherapy in patients with newly diagnosed AML: a phase 1 study. *Blood* **137**, (2021).
210. Cluzeau, T. *et al.* Eprenetapopt Plus Azacitidine in *TP53* -Mutated Myelodysplastic Syndromes and Acute Myeloid Leukemia: A Phase II Study by the Groupe Francophone des Myélodysplasies (GFM). *Journal of Clinical Oncology* **39**, (2021).
211. Wei, A. H. *et al.* Venetoclax plus LDAC for newly diagnosed AML ineligible for intensive chemotherapy: a phase 3 randomized placebo-controlled trial. *Blood* **135**, (2020).
212. Pollyea, D. A. *et al.* Enasidenib, an inhibitor of mutant IDH2 proteins, induces durable remissions in older patients with newly diagnosed acute myeloid leukemia. *Leukemia* **33**, (2019).
213. Roboz, G. J. *et al.* Ivosidenib induces deep durable remissions in patients with newly diagnosed IDH1-mutant acute myeloid leukemia. *Blood* **135**, (2020).
214. Stein, E. M. *et al.* The DOT1L inhibitor pinometostat reduces H3K79 methylation and has modest clinical activity in adult acute leukemia. *Blood* **131**, (2018).
215. Christian, S. *et al.* The novel dihydroorotate dehydrogenase (DHODH) inhibitor BAY 2402234 triggers differentiation and is effective in the treatment of myeloid malignancies. *Leukemia* **33**, (2019).
216. Jianbiao Zhou *et al.* ASLAN003, a potent dihydroorotate dehydrogenase inhibitor for differentiation of acute myeloid leukemia. *Haematologica* **105**, (2019).
217. Teague, R. M. & Kline, J. Immune evasion in acute myeloid leukemia: current concepts and future directions. *Journal for ImmunoTherapy of Cancer* **1**, (2013).
218. Wang, M. *et al.* CD8 + T cells expressing both PD-1 and TIGIT but not CD226 are dysfunctional in acute myeloid leukemia (AML) patients. *Clinical Immunology* **190**, (2018).
219. Curran, E. K., Godfrey, J. & Kline, J. Mechanisms of Immune Tolerance in Leukemia and Lymphoma. *Trends in Immunology* **38**, (2017).
220. Nair, R., Salinas-Illarena, A. & Baldauf, H. M. New strategies to treat AML: novel insights into AML survival pathways and combination therapies. *Leukemia* vol. 35 299–311 (2021).
221. Taghiloo, S. & Asgarian-Omran, H. Immune evasion mechanisms in acute myeloid leukemia: A focus on immune checkpoint pathways. *Critical Reviews in Oncology/Hematology* **157**, (2021).
222. Ravandi, F. *et al.* Updated results from phase I dose-escalation study of AMG 330, a bispecific T-cell engager molecule, in patients with relapsed/refractory acute myeloid leukemia (R/R AML). *Journal of Clinical Oncology* **38**, (2020).
223. Lambert, J. *et al.* Gemtuzumab ozogamicin for de novo acute myeloid leukemia: final efficacy and safety updates from the open-label, phase III ALFA-0701 trial. *Haematologica* **104**, (2019).
224. Riether, C. *et al.* CD70/CD27 signaling promotes blast stemness and is a viable therapeutic target in acute myeloid leukemia. *Journal of Experimental Medicine* **214**, (2017).
225. Chao, M. P. *et al.* Therapeutic Targeting of the Macrophage Immune Checkpoint CD47 in Myeloid Malignancies. *Frontiers in Oncology* **9**, (2020).
226. Loff, S. *et al.* Rapidly Switchable Universal CAR-T Cells for Treatment of CD123-Positive Leukemia. *Molecular Therapy - Oncolytics* **17**, (2020).
227. Mardiana, S. & Gill, S. CAR T Cells for Acute Myeloid Leukemia: State of the Art and Future Directions. *Frontiers in Oncology* **10**, (2020).

228. Orleans-Lindsay, J. K., Barber, L. D., Prentice, H. G. & Lowdell, M. W. Acute myeloid leukaemia cells secrete a soluble factor that inhibits T and NK cell proliferation but not cytolytic function - implications for the adoptive immunotherapy of leukaemia. *Clinical & Experimental Immunology* **126**, 403–411 (2001).
229. Cummins, K. D. & Gill, S. Will CAR T cell therapy have a role in AML? Promises and pitfalls. *Seminars in Hematology* **56**, 155–163 (2019).
230. Li, A. M. *et al.* Checkpoint Inhibitors Augment CD19-Directed Chimeric Antigen Receptor (CAR) T Cell Therapy in Relapsed B-Cell Acute Lymphoblastic Leukemia. *Blood* **132**, 556–556 (2018).
231. Letai, A. Apoptosis and Cancer. *Annual Review of Cancer Biology* **1**, (2017).
232. Moujalled, D. M. *et al.* Combining BH3-mimetics to target both BCL-2 and MCL1 has potent activity in pre-clinical models of acute myeloid leukemia. *Leukemia* **33**, (2019).
233. Pollyea, D. A. *et al.* Venetoclax with azacitidine or decitabine in patients with newly diagnosed acute myeloid leukemia: Long term follow-up from a phase 1b study. *American Journal of Hematology* **96**, (2021).
234. Teh, T.-C. *et al.* Enhancing venetoclax activity in acute myeloid leukemia by co-targeting MCL1. *Leukemia* **32**, (2018).
235. Berenstein, R. Class III Receptor Tyrosine Kinases in Acute Leukemia – Biological Functions and Modern Laboratory Analysis. *Biomarker Insights* **10s3**, (2015).
236. Cioccio, J. & Claxton, D. Therapy of acute myeloid leukemia: therapeutic targeting of tyrosine kinases. *Expert Opinion on Investigational Drugs* **28**, (2019).
237. Huey, M., Minson, K., Earp, H., DeRyckere, D. & Graham, D. Targeting the TAM Receptors in Leukemia. *Cancers* **8**, (2016).
238. Queiroz, K. C. S. *et al.* Hedgehog signaling maintains chemoresistance in myeloid leukemic cells. *Oncogene* **29**, (2010).
239. Brondfield, S. *et al.* Direct and indirect targeting of MYC to treat acute myeloid leukemia. *Cancer Chemotherapy and Pharmacology* **76**, (2015).
240. Pilié, P. G., Tang, C., Mills, G. B. & Yap, T. A. State-of-the-art strategies for targeting the DNA damage response in cancer. *Nature Reviews Clinical Oncology* **16**, (2019).
241. Dombret, H. *et al.* International phase 3 study of azacitidine vs conventional care regimens in older patients with newly diagnosed AML with >30% blasts. *Blood* **126**, (2015).
242. Barbier, V. *et al.* Endothelial E-selectin inhibition improves acute myeloid leukaemia therapy by disrupting vascular niche-mediated chemoresistance. *Nature Communications* **11**, (2020).
243. Roboz, G. J. *et al.* Phase I trial of plerixafor combined with decitabine in newly diagnosed older patients with acute myeloid leukemia. *Haematologica* **103**, (2018).
244. Ho, T.-C. *et al.* Evolution of acute myelogenous leukemia stem cell properties after treatment and progression. *Blood* **128**, (2016).
245. Škrtić, M. *et al.* Inhibition of Mitochondrial Translation as a Therapeutic Strategy for Human Acute Myeloid Leukemia. *Cancer Cell* **20**, (2011).
246. Saito, Y. *et al.* Induction of cell cycle entry eliminates human leukemia stem cells in a mouse model of AML. *Nature Biotechnology* **28**, (2010).
247. Krug, U. *et al.* Increasing intensity of therapies assigned at diagnosis does not improve survival of adults with acute myeloid leukemia. *Leukemia* **30**, (2016).
248. Takeishi, S. *et al.* Ablation of Fbxw7 Eliminates Leukemia-Initiating Cells by Preventing Quiescence. *Cancer Cell* **23**, (2013).
249. Baquero, P. *et al.* Targeting quiescent leukemic stem cells using second generation autophagy inhibitors. *Leukemia* **33**, 981–994 (2019).
250. Fukushima, N. *et al.* Small-molecule Hedgehog inhibitor attenuates the leukemia-initiation potential of acute myeloid leukemia cells. *Cancer Science* **107**, (2016).
251. Cortes, J. E. *et al.* Randomized comparison of low dose cytarabine with or without glasdegib in patients with newly diagnosed acute myeloid leukemia or high-risk myelodysplastic syndrome. *Leukemia* **33**, (2019).
252. Zhang, L. *et al.* Targeting miR-126 in inv(16) acute myeloid leukemia inhibits leukemia development and leukemia stem cell maintenance. *Nature Communications* **12**, (2021).

253. Esposito, M. T. *et al.* Synthetic lethal targeting of oncogenic transcription factors in acute leukemia by PARP inhibitors. *Nature Medicine* **21**, (2015).
254. Coughlan, A. M. *et al.* Myeloid Engraftment in Humanized Mice: Impact of Granulocyte-Colony Stimulating Factor Treatment and Transgenic Mouse Strain. *Stem Cells and Development* **25**, (2016).
255. Shultz, L. D. *et al.* Human Lymphoid and Myeloid Cell Development in NOD/LtSz-scid IL2Rγ null Mice Engrafted with Mobilized Human Hemopoietic Stem Cells. *The Journal of Immunology* **174**, (2005).
256. Salmon, P. & Trono, D. Production and Titration of Lentiviral Vectors. *Current Protocols in Human Genetics* **54**, (2007).
257. Universal Probe Library Roche.
258. Ravà, M. *et al.* Mutual epithelium-macrophage dependency in liver carcinogenesis mediated by ST18. *Hepatology* **65**, 1708–1719 (2017).
259. Biewenga, J. *et al.* Macrophage depletion in the rat after intraperitoneal administration of liposome-encapsulated clodronate: Depletion kinetics and accelerated repopulation of peritoneal and omental macrophages by administration of freund's adjuvant. *Cell and Tissue Research* **280**, 189–196 (1995).
260. Chen, W. *et al.* Malignant Transformation Initiated by Mll-AF9: Gene Dosage and Critical Target Cells. *Cancer Cell* **13**, (2008).
261. Stuart, T. *et al.* Comprehensive Integration of Single-Cell Data. *Cell* **177**, 1888-1902.e21 (2019).
262. Cabezas-Wallscheid, N. *et al.* Vitamin A-Retinoic Acid Signaling Regulates Hematopoietic Stem Cell Dormancy. *Cell* **169**, 807-823.e19 (2017).
263. Fukushima, T. *et al.* Discrimination of Dormant and Active Hematopoietic Stem Cells by G0 Marker Reveals Dormancy Regulation by Cytoplasmic Calcium. *Cell Reports* **29**, 4144-4158.e7 (2019).
264. KEGG_Apoptosis .
265. Pakos-Zebrucka, K. *et al.* The integrated stress response. *EMBO reports* **17**, (2016).
266. Hart, L. S. *et al.* ER stress–mediated autophagy promotes Myc-dependent transformation and tumor growth. *Journal of Clinical Investigation* **122**, (2012).
267. Rzymski, T., Milani, M., Singleton, D. C. & Harris, A. L. Role of ATF4 in regulation of autophagy and resistance to drugs and hypoxia. *Cell Cycle* **8**, (2009).
268. Halllmark_Unfolded Protein Response.
269. Reactome_Autophagy.
270. García-Jiménez, C. & Goding, C. R. Starvation and Pseudo-Starvation as Drivers of Cancer Metastasis through Translation Reprogramming. *Cell Metabolism* **29**, 254–267 (2019).
271. Fucikova, J. *et al.* Detection of immunogenic cell death and its relevance for cancer therapy. *Cell Death & Disease* **11**, 1013 (2020).
272. Barkal, A. A. *et al.* CD24 signalling through macrophage Siglec-10 is a target for cancer immunotherapy. *Nature* **572**, 392–396 (2019).
273. Gonçalves Silva, I. *et al.* The Tim-3-galectin-9 Secretory Pathway is Involved in the Immune Escape of Human Acute Myeloid Leukemia Cells. *EBioMedicine* **22**, 44–57 (2017).
274. Yuan, L., Tatineni, J., Mahoney, K. M. & Freeman, G. J. VISTA: A Mediator of Quiescence and a Promising Target in Cancer Immunotherapy. *Trends in Immunology* **42**, (2021).
275. Yasinska, I. M. *et al.* Ligand-Receptor Interactions of Galectin-9 and VISTA Suppress Human T Lymphocyte Cytotoxic Activity. *Frontiers in Immunology* **11**, (2020).
276. Christensen, J. L. & Weissman, I. L. Flk-2 is a marker in hematopoietic stem cell differentiation: A simple method to isolate long-term stem cells. *Proceedings of the National Academy of Sciences* **98**, 14541–14546 (2001).
277. van Galen, P. *et al.* Integrated Stress Response Activity Marks Stem Cells in Normal Hematopoiesis and Leukemia. *Cell Reports* **25**, (2018).
278. Kim, H. S. & Lee, M.-S. STAT1 as a key modulator of cell death. *Cellular Signalling* **19**, 454–465 (2007).

279. Ramana, C. v, Chatterjee-Kishore, M., Nguyen, H. & Stark, G. R. Complex roles of Stat1 in regulating gene expression. *Oncogene* **19**, 2619–2627 (2000).
280. Essers, M. A. G. *et al.* IFNα activates dormant haematopoietic stem cells in vivo. *Nature* **458**, 904–908 (2009).
281. King, K. Y. *et al.* Irgm1 protects hematopoietic stem cells by negative regulation of IFN signaling. *Blood* **118**, 1525–1533 (2011).
282. Chin, Y. E. *et al.* Cell Growth Arrest and Induction of Cyclin-Dependent Kinase Inhibitor p21 $^{WAF1/CIP1}$ Mediated by STAT1. *Science* **272**, 719–722 (1996).
283. Zhang, Y. & Liu, Z. STAT1 in cancer: friend or foe? *Discovery medicine* **24**, 19–29 (2017).
284. Moon, J. W. *et al.* IFNγ induces PD-L1 overexpression by JAK2/STAT1/IRF-1 signaling in EBV-positive gastric carcinoma. *Scientific Reports* **7**, 17810 (2017).
285. Spiekermann, K., Biethahn, S., Wilde, S., Hiddemann, W. & Alves, F. Constitutive activation of STAT transcription factors in acute myelogenous leukemia. *European journal of haematology* **67**, 63–71 (2001).
286. Kovacic, B. *et al.* STAT1 acts as a tumor promoter for leukemia development. *Cancer Cell* **10**, 77–87 (2006).
287. Baker, S. J., Rane, S. G. & Reddy, E. P. Hematopoietic cytokine receptor signaling. *Oncogene* **26**, 6724–6737 (2007).
288. Vitali, C. *et al.* SOCS2 Controls Proliferation and Stemness of Hematopoietic Cells under Stress Conditions and Its Deregulation Marks Unfavorable Acute Leukemias. *Cancer Research* **75**, 2387–2399 (2015).
289. Georgantas, R. W. *et al.* Microarray and Serial Analysis of Gene Expression Analyses Identify Known and Novel Transcripts Overexpressed in Hematopoietic Stem Cells. *Cancer Research* **64**, 4434–4441 (2004).
290. Haan, S. SOCS2 physiological and pathological functions. *Frontiers in Bioscience* **8**, 760 (2016).
291. Nguyen, C. H. *et al.* SOCS2 is part of a highly prognostic 4-gene signature in AML and promotes disease aggressiveness. *Scientific Reports* **9**, 9139 (2019).
292. Schultheis, B. *et al.* Overexpression of SOCS-2 in advanced stages of chronic myeloid leukemia: possible inadequacy of a negative feedback mechanism. *Blood* **99**, 1766–1775 (2002).
293. Kim, J.-H. *et al.* Alterations in the p53-SOCS2 axis contribute to tumor growth in colon cancer. *Experimental & Molecular Medicine* **50**, 1–10 (2018).
294. Hoefer, J. *et al.* SOCS2 correlates with malignancy and exerts growth-promoting effects in prostate cancer. *Endocrine-Related Cancer* **21**, 175–187 (2014).
295. Ostrowski, M. *et al.* Rab27a and Rab27b control different steps of the exosome secretion pathway. *Nature Cell Biology* **12**, 19–30 (2010).
296. Gu, H. *et al.* Sorting protein VPS33B regulates exosomal autocrine signaling to mediate hematopoiesis and leukemogenesis. *Journal of Clinical Investigation* **126**, 4537–4553 (2016).
297. Deng, W., Wang, L., Pan, M. & Zheng, J. The regulatory role of exosomes in leukemia and their clinical significance. *Journal of International Medical Research* **48**, 030006052095013 (2020).
298. Zhou, J., Wang, S., Sun, K. & Chng, W.-J. The emerging roles of exosomes in leukemogeneis. *Oncotarget* **7**, 50698–50707 (2016).
299. Granados, D. P. *et al.* ER stress affects processing of MHC class I-associated peptides. *BMC Immunology* **10**, (2009).
300. Zhou, C. *et al.* JUN is a key transcriptional regulator of the unfolded protein response in acute myeloid leukemia. *Leukemia* **31**, (2017).
301. Chen, X. & Cubillos-Ruiz, J. R. Endoplasmic reticulum stress signals in the tumour and its microenvironment. *Nature Reviews Cancer* **21**, (2021).
302. Risson, E., Nobre, A. R., Maguer-Satta, V. & Aguirre-Ghiso, J. A. The current paradigm and challenges ahead for the dormancy of disseminated tumor cells. *Nature Cancer* **1**, (2020).

303. Wang, A. & Zhong, H. Roles of the bone marrow niche in hematopoiesis, leukemogenesis, and chemotherapy resistance in acute myeloid leukemia. *Hematology* **23**, 729–739 (2018).
304. Xu, Y. *et al.* Regulatory T cells promote the stemness of leukemia stem cells through IL10 cytokine-related signaling pathway. *Leukemia* (2021) doi:10.1038/s41375-021-01375-2.